Editors

Prof. Dr. Coşkun ÖZALP
Prof. Dr. Ertaç HÜRDOĞAN
Doç. Dr. Nurullah GÜLTEKİN

gece kitaplığı

International Research and Evaluations in the Field of Mechanical Engineering

October 2025

Genel Yayın Yönetmeni / Editor in Chief • Eda Altunel

Kapak & İç Tasarım / Cover & Interior Design • Gece Kitaplığı

Birinci Basım / First Edition • © Ekim 2025

ISBN • 978-625-388-819-0

Gece Kitaplığı / Gece Kitaplığı
Türkiye Adres / Turkey Address: Kızılay Mah. Fevzi Çakmak 1. Sokak
Ümit Apt No: 22/A Çankaya/ANKARA
Telefon / Phone: 0312 384 80 40

web: www.gecekitapligi.com
e-mail: gecekitapligi@gmail.com

Baskı & Cilt / Printing & Volume
Sertifika / Certificate No: 42488

INTERNATIONAL RESEARCH AND EVALUATIONS IN THE FIELD OF MECHANICAL ENGINEERING

EDITORS

PROF. DR. COŞKUN ÖZALP
PROF. DR. ERTAÇ HÜRDOĞAN
DOÇ. DR. NURULLAH GÜLTEKİN

gece kitaplığı

CONTENTS

Chapter 1

EFFECTS OF METAL NANOPARTICLE ADDITIVES IN DIESEL FUELS[1]

Mithat ŞİMŞEK[2]

1 Corresponding author.

Address: Faculty of Engineering and Architecture, Tokat Gaziosmanpaşa University, Tokat, 60250, Türkiye.
2 E-mail address: mithat.simsek@gop.edu.tr (Assistant Prof. Mithat Şimşek).

Orcid: https://orcid.org/0000-0002-0534-1133

Tel: +90 356 252 16 16, Fax: +90 356 252 17 29.

1. Introduction

Today, the need for energy is constantly increasing due to reasons such as population growth, development of industrialization, proliferation of technological devices and rising living standards, and as a result, air pollution, especially in big cities, is becoming a growing problem (Bilgin, 2025; Mayer, 1999). One of the primary causes of this issue is fossil fuels, which are widely used in many areas, from industrial activities and energy production to transportation and heating (Govorushko, 2013; Gültekin, Gülcan, & Ciniviz, 2023). The use of fossil fuels has serious and adverse effects on both the environment (global warming, acid rain, depletion of the ozone layer) and human health (respiratory diseases, cancer, cardiovascular disorders (Lak, Rezaei, & Rahimpour, 2024)). In contrast, diesel engines, particularly those used in the transportation sector, are an indispensable part of many energy applications, from heavy-duty transport to generators, due to their high thermal efficiency and low fuel consumption (Xin Wang, Ge, Yu, & Feng, 2013). Diesel engines are widely used as the main power source in areas such as commercial road vehicles, marine vessels, agricultural machinery, and industrial equipment (Lamaris & Hountalas, 2010; Yaşar, 2020; Yaşar & Şimşek, 2020). The extensive utilization of fossil fuels is a primary factor contributing to the persistent high demand for these resources, hence exacerbating the risk of swiftly diminishing global fossil fuel stocks (B. R. Singh & Singh, 2012). Simultaneously, deleterious emissions including unburned hydrocarbons (HC), carbon monoxide (CO), nitrogen oxides (NOx), and particulate matter (PM) emitted from these engines substantially exacerbate air pollution and environmental health degradation (Mohammad et al., 2022; Ogunkunle & Ahmed, 2021). Consequently, enhancing fuel efficiency and reducing exhaust emissions are key objectives for researchers and engineers focused on internal combustion engines (Şimşek et al 2016; Gültekin, 2024). To attain these objectives, diverse strategies including the advancement of alternative fuels, enhancement of combustion processes, and incorporation of cutting-edge exhaust aftertreatment systems are currently being investigated and executed (Alkemade & Schumann, 2006; Gültekin et al., 2023; Jin, Long, Xie, & Tian, 2025; Lott & Deutschmann, 2021; Yaşar, 2020; Özseven, 2019).

The current energy situation, pollution problems, and rising petroleum fuel prices have encouraged studies towards developing alternative fuels that are more efficient, less harmful to the environment, and reduce fuel consumption (BİLGİN, 2025; Sandaka & Kumar, 2023; Vishnuram et al., 2025). Biodiesel stands out as one of the most promising alternative fuels because it can be used in diesel engines without requiring significant design changes (Atabani et al., 2012; Demirbas, 2008; A. Murugesan,

Umarani, Subramanian, & Nedunchezhian, 2009). Many researchers have conducted engine performance tests using blends of different biodiesel feedstocks. Most of these studies reported a slight decrease in engine performance compared to diesel fuel; however, emissions such as HC, smoke, and CO decreased significantly, except for NOx (Gültekin, Gülcan, & Ciniviz, 2024). The main goal of researchers is to increase performance and reduce emissions simultaneously without any modifications to the engine design. Initial studies focused on improving fuel quality using additives. However, micro-scale additives can lead to problems such as sediment formation, deposits, and irregular size distribution.Advancements in technology have enabled the production of particles smaller than 100 nm, thereby resolving these issues and facilitating their application as additives in engines (Ampah et al., 2022; Basha et al., 2022; Kittelson, 1998).

Recent study has demonstrated that the incorporation of nanoscale metallic particles (nanoparticles) into fuels enhances their overall characteristics. The characteristics of diesel or biodiesel fuels can be altered by including nanoparticles with certain physical and chemical properties (Elkelawy, Mohamad, Abo-Samra, & Elshennawy, 2023; Mujtaba et al., 2020). The use of such fuels improves physical properties such as thermal conductivity, diffusion, and viscosity, which reduces ignition delay and thus enables more effective combustion (Khan, Dewang, Raghuwanshi, Shrivastava, & Sharma, 2022; Mujtaba et al., 2020). The high energy density of metallic particles increases the total energy value of the fuel, which positively affects engine performance. Furthermore, the addition of nanoparticles has positive effects on ignition delay and ignition temperature; it increases momentum density, accelerating the combustion process, and improves the fuel injection rate into the combustion chamber, thereby enhancing engine performance. Nanoparticles with a high surface area-to-volume ratio provide more contact opportunity between the fuel and the oxidizer, increasing combustion efficiency efficiency (Ahmed et al., 2024; Bilgin, Onal, Akansu, & Ilhak, 2023; Bitire, Nwanna, & Jen, 2023). This situation contributes to the reduction of emissions, as nanoparticles accelerate soot oxidation by generating hydroxyl radicals or directly react with carbon, lowering the oxidation temperature (Ahmed et al., 2024; S. Kumar, Dinesha, & Bran, 2019).

The particles used in studies can be reduced to a size of <100 nm through various chemical and physical processes (S. Kumar et al., 2019; Nohynek & Dufour, 2012). Materials such as cerium, aluminum, manganese, zinc, copper, iron, magnesium, silicon, titanium, and their oxides are used in nano-fuel studies. Many researchers have added these metals and metal oxides as nano-additives to neat diesel fuel or biodiesel in varying proportions and subjected them to engine tests. In these tests, they

investigated the effects of the used nanoparticles on engine performance, emissions, and combustion characteristics (Sarma et al., 2023).

2. Methodology

Improving fuel efficiency and reducing exhaust emissions are among the primary goals of internal combustion engine research (Gupta et al., 2024). Nanoparticles used as fuel additives are in the size range of <100 nanometers (Nagappan & Babu, 2023). The size and distribution of powdered nanoparticles are typically determined using scanning electron microscope (SEM) analysis. Figure 1 shows SEM images of some nanoparticles. These additives are primarily classified into two main categories: metal nanoparticles and non-metal nanoparticles. Metal nanoparticles are further subdivided into metal monomers, metal oxides, and other metal compounds (K. Singh, Maurya, & Malviya, 2024). The most frequently utilized forms among these categories are Cerium oxide (CeO_2), Aluminum oxide (Al_2O_3), Zinc oxide (ZnO), Magnesium oxide (MgO), Copper oxide (CuO), Titanium oxide (TiO_2), Iron oxide (Fe_2O_3), and Silver nanoparticles (K. Singh, Maurya, & Malviya, 2024). The category of non-metal nanoparticles include several carbon-based nanomaterials, including Carbon Nanoparticles (CNP), Graphene Nano Platelets (GNP), Multi-Walled Carbon Nanotubes (MWCNT), and Carbon Nanotubes (CNT) (Ahmed et al., 2024).

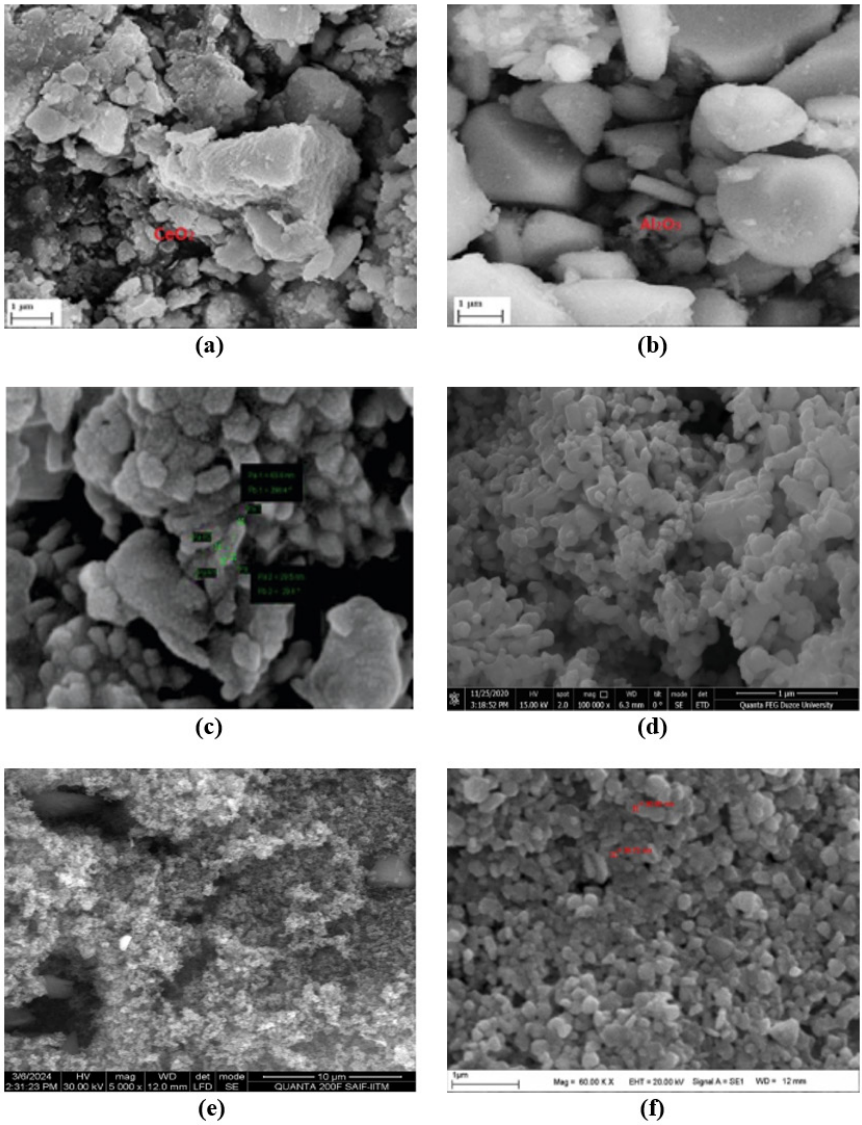

Figure 1. *SEM images of various nanoparticles* **(a)** *CeO_2 (Bhan, Gautam, & Singh, 2024)* **(b)** *Al_2O_3 (Bhan et al., 2024)* **(c)** *ZnO (Ganapathy, Jaikumar, Ramanathan, Hariram, & Sangeethkumar, 2025),* **(d)** *CuO (Ağbulut et al., 2021)* **(e)** *TiO_2 (Demir, Keskin, Özer, & Coskun, 2025)* **(f)** *Ag (Demir et al., 2025)*

2.1. Cerium Oxide Nanoparticles (CeO_2)

The application of cerium oxide (CeO_2) nanoparticles as an additive to diesel fuels stands out as a highly promising approach in terms of engine performance and emission control (Muruganantham & Pandiyan, 2021). These nanoparticles enhance combustion efficiency due to their oxygen storage capacity and reversible redox characteristics, resulting in improved thermal efficiency of the engine and decreased fuel consumption (Ahn, Jang, Shim, Jeon, & Roh, 2024). Experimental results indicate that CeO_2 nanoparticle additions substantially decrease emissions of CO, unburned HC, and particulate matter in diesel engines (Mei, Li, Wu, & Sun, 2016). Its most notable feature is its ability to catalytically reduce the increased NOx emissions, which are a characteristic problem of biodiesel fuels, through an oxygen release mechanism. A comprehensive examination of engineering characteristics, including the optimization of nanoparticle concentration, their dispersion stability in fuel, and their long-term impacts on engine components, is essential for the commercial feasibility of this technology.

2.2. Aluminum Oxide Nanoparticles (Al_2O_3)

Al_2O_3 nanoparticles are typically classified as non-energetic metal oxide additives, indicating their lack of direct involvement in the combustion reaction (Sateesh et al., 2022). Nonetheless, owing to their elevated specific surface area, thermal conductivity, and distinctive size-dependent characteristics, they elicit diverse physical and partial catalytic effects upon incorporation into diesel fuel. These nanoparticles enhance atomization by decreasing the fuel's viscosity and surface tension, facilitating the creation of smaller and more uniform fuel droplets. Moreover, their elevated thermal conductivity enhances heat transport within the cylinder, reducing ignition delay and facilitating more efficient and steady combustion (E. Murugesan, Dhairiyasamy, Dixit, & Singh, 2025). Their catalytic function, especially in facilitating the oxidation of carbon deposits (soot) generated post-combustion, results in substantial decreases in exhaust emissions, chiefly in HC and CO. Nonetheless, due to the restricted oxygen storage capacity of Al_2O_3 nanoparticles, their influence on NOx emissions is often indirect and may fluctuate, mostly reliant on the enhancement of combustion efficiency (E. Murugesan et al., 2025). In conclusion, Al_2O_3 nanoparticles stand out as an important additive for diesel engines, providing performance improvement and emission reduction. They are characterized primarily by their physical properties, but also exhibit partial catalytic activity (Kegl, Kralj, Kegl, & Kegl, 2021).

2.3. Zinc Oxide Nanoparticles (ZnO)

Zinc oxide (ZnO) nanoparticles are semiconductor materials that hold a significant place in the field of nanotechnology and are produced at sizes of <100 nanometers (Sani et al., 2023). These nanoparticles, which have a hexagonal crystal structure, stand out due to their high thermal conductivity, wide band gap (3.37 eV), and high absorption property against UV radiation (Ungula, 2015). Particularly within the scope of fuel technologies, they have been shown to be effective in increasing combustion efficiency and reducing harmful emissions when added to diesel and biodiesel fuels (Ganapathy et al., 2025). Experimental research demonstrates that, when suitable concentration and dispersion techniques are employed, ZnO nanoparticles provide substantial advantages in energy efficiency and emission regulation.

2.4. Copper Oxide Nanoparticles (CuO)

The use of copper oxide (CuO) nanoparticles as an additive in diesel fuels has been gaining increasing importance in recent research. The quest for energy efficiency and emission reduction highlights the unique properties of these nanoparticles, such as their high catalytic activity and thermal conductivity (Ağbulut et al., 2021). Laboratory tests show that diesel fuels containing CuO nanoparticles greatly increase brake thermal efficiency (BTE) and reduce brake specific fuel consumption (BSFC). In addition, CuO-doped fuels reduced CO, HC, and particulate matter emissions, but their influence on NOx emissions varied with engine state and nanoparticle concentration (Behera & Hotta, 2025)(Madhaiyan, Kandasamy, Raman, & Vellaiyan, 2025). However, nanoparticle dispersion stability, additive ratio, and long-term engine wear are significant issues requiring further research.

2.5. Titanium Dioxide Nanoparticles (TiO_2)

The use of titanium dioxide (TiO_2) nanoparticles as an additive in diesel fuels has become a notable research area in recent years due to their photocatalytic properties and high thermal stability (Ghanati, Doğan, & Yeşilyurt, 2024). Experimental studies show that diesel fuels modified with TiO_2 nanoparticles increase the engine's BTE and decrease its BSFC. The catalytic effect of the nanoparticles improves combustion efficiency, leading to significant reductions in CO, HC, and particulate matter emissions (Sarma et al., 2023). It is thought that their photocatalytic activity, especially when exposed to UV light, could provide an additional benefit in breaking down harmful emissions formed after combustion. However, the optimal concentration of TiO_2 nanoparticles, their dispersion stability within the fuel, and their effects on long-term engine performance

require more comprehensive investigation.

2.6. Iron Oxide Nanoparticles (Fe_2O_3)

The incorporation of iron oxide (Fe_2O_3) nanoparticles as an additive in diesel fuels has lately emerged as a significant research focus, notably because of their magnetic characteristics and elevated catalytic activity (Nouri, Isfahani, & Shirneshan, 2021). Experimental studies have shown that adding these nanoparticles to diesel fuel leads to an increase in BTE and a decrease in BSFC, which are key engine performance parameters (Valihesari, Pirouzfar, Ommi, & Zamankhan, 2019). Thanks to their magnetic properties, Fe_2O_3 nanoparticles achieve a homogeneous dispersion within the fuel and catalyze the combustion process, resulting in significant reductions in CO, HC, and particulate matter emissions (Mawlid, Abdelhady, & El-Deab, 2024). Moreover, their capacity for recovery from exhaust by magnetic separation offers an added benefit regarding environmental sustainability. The optimization of nanoparticle concentration, the long-term implications on engine wear, and a comprehensive examination of how magnetic characteristics affect combustion kinetics are critical areas for additional research.

2.7. Silver Nanoparticles (Ag)

The incorporation of silver oxide (Ag_2O) nanoparticles as an additive in diesel fuels is gaining attention as a viable study area due to its significant catalytic activity and thermal conductivity qualities (Bayindirli & Celik, 2024). Experimental results demonstrate that the incorporation of Ag_2O nanoparticles improves combustion efficiency in diesel engines, resulting in enhanced (BTE) and decreased BSFC. The elevated surface area and catalytic properties of the nanoparticles enhance the combustion process, leading to substantial decreases in CO, HC, and particulate matter emissions (Çelik, Mehregan, Bayındırlı, & Moghiman, 2025). On the other hand, factors such as the relatively high cost of silver oxide nanoparticles, their long-term stability in fuel, and their potential abrasive effects on engine components are considered major challenges to the widespread application of this technology.

3. Results and Discussions

Research on the incorporation of nanoparticles into diesel fuels has often yielded favorable results, indicating enhancements in engine performance and decreases in emissions. Nanoparticles improve fuel combustion efficiency owing to their elevated surface area, thermal conductivity, and catalytic characteristics, resulting in a more effective combustion process (Xiaorong Wang et al., 2020). This results in an increase in BTE

while reducing BSFC. Furthermore, the use of nanoparticle-doped diesel fuels leads to significant decreases in HC, CO, and Particulate Matter (PM) emissions (E. Murugesan et al., 2025). The principal reason for this is because nanoparticles enhance oxygen transport during combustion and encourage a more uniform combustion of the air-fuel mixture. The impact on NOx emissions remains ambiguous. Certain studies have indicated an increase, but others have noted a decline. This variance is contingent upon parameters including the type of nanoparticle employed, its dimensions, concentration, and the operational circumstances of the engine. The utilization of nanoparticle-doped diesel fuels is seen as a viable strategy for improving energy efficiency and minimizing environmental effect.

3.1. Cerium Oxide Nanoparticles

Investigations into the incorporation of cerium oxide (CeO_2) nanoparticles into diesel fuels have demonstrated significantly favorable outcomes for engine performance enhancement and emission reduction. Sajeevan and Sajith (Sajeevan & Sajith, 2013) utilized CeO_2 nanoparticles as a nano-additive in diesel fuel, resulting in a stable suspension. This suspension served as fuel in a four-stroke, single-cylinder, water-cooled compression ignition engine to assess performance and pollution metrics. The engine worked at a velocity of 1500 rpm, utilizing dodecenyl succinic anhydride as the surfactant. The incorporation of nanoparticles was noted to enhance viscosity, flash point, and fire point. The experiments were performed by altering the concentration of CeO_2 nanoparticles in the diesel fuel and the engine load.. The nanoparticle concentration in diesel was set at 5, 10, or 15 ppm. Experimental analyses showed that with the addition of CeO_2, a 6% increase in BTE and a 40-45% reduction in HC emissions were recorded, particularly at high loads. Furthermore, it was determined that with the addition of CeO_2, NOx emissions decreased by up to 30% at high load. In their experimental study, Muruganantham & Pandiyan (Muruganantham & Pandiyan, 2021) homogeneously dispersed 50-70 nm CeO_2 nanoparticles at concentrations of 25, 50, and 75 ppm into a 10% biodiesel-diesel blend (COB10) produced from corn oil via two-stage transesterification, using a magnetic stirrer and an ultrasonic probe. Engine tests conducted at a constant speed of 1500 rpm determined that the addition of nanoparticles increased the viscosity and density of the COB10 fuel, but also improved the calorific value due to the catalytic effect and high surface area. The reduction in BTE noted with pure COB10 relative to diesel fuel, attributed to its inferior calorific value, was mitigated by the incorporation of 50 ppm CeO_2, resulting in an increased BTE of 34.7%, surpassing that of diesel fuel (34.42%). The BSFC was optimized to a value of 0.242 kg/kW-h within the same mix. In emission analyses,

the COB10+50ppm blend attained a notable reduction of 83.3% in CO emissions and 20.8% in HC emissions, attributable to the supplementary oxygen from CeO_2 nanoparticles and enhanced combustion, although an increase in NOx emissions was noted due to elevated combustion temperatures. The study empirically validated that incorporating 50 ppm CeO_2 nanoparticles into the COB10 biodiesel mix enhances engine performance and markedly decreases detrimental emissions.

In their research, Alex et al. (Alex, Earnest, Raghavan, George Roy, & Koshy, 2022) sought to examine the performance and emission characteristics of a single-cylinder, four-stroke, air-cooled diesel engine by augmenting biodiesel derived from orange peel oil methyl ester (OPOME) with CeO_2 nanoparticles at concentrations of 15 and 25 ppm. Biodiesel was extracted from orange peel using steam distillation, while an ultrasonicator and magnetic stirrer facilitated the uniform dispersion of nanoparticles in the fuel. Experimental findings indicated that the biodiesel blend with 25 ppm CeO_2 (BC25) enhanced the BTE by as much as 12% and decreased the BSFC by 6.5% relative to pure diesel fuel. The identical blend was seen to decrease CO emissions by as much as 35%, NOx emissions by up to 80% at full capacity, and smoke opacity by up to 50%. The principal factors contributing to these enhancements include the nanoparticles' ability to improve fuel atomization, decrease ignition delay, optimize in-cylinder temperature distribution, and supply supplementary oxygen for more thorough combustion. In a separate study, Leo et al. (Leo et al., 2023) examined the impact of integrating waste cashew nut shell oil (CNSO) biodiesel, CeO_2 nanoparticles, and an acetylene aspiration system on the performance of an agricultural diesel engine. Experiments were performed using pure diesel, CNSO biodiesel, a B50 mix comprising 50% CNSO, and these fuels supplemented with 25 ppm CeO_2 nanoparticles in conjunction with 3-6 L/min acetylene aspiration. While pure CNSO, due to its lower calorific value, showed a 1.38% decrease in BTE and an increase in BSFC, the addition of CeO_2 increased BTE by 2.54% and reduced BSFC by 5.02%. Acetylene aspiration at 6 L/min resulted in a 3.18% increase in BTE and a 10.42% rise in maximum in-cylinder pressure. The high oxygen content of CNSO reduced CO (by 3.3%) and HC (by 21.44%) emissions but caused a 9.83% increase in NOx. In contrast, CeO_2 nanoparticles reduced NOx by 10.5%, HC by 44.45%, and smoke emissions significantly. Optimization via Response Surface Methodology (RSM) identified CNSO biodiesel with a CeO_2 addition as the ideal option, yielding a desirability value of 0.853, with model predictions corroborated by experimental data. The findings indicate that waste-derived CNSO biodiesel, enhanced with CeO_2 nanoparticles and acetylene, represents a sustainable alternative for agricultural diesel engines.

This experimental study by Uslu & Celik (Uslu & Celik, 2023) examined the performance and emission characteristics of a single-cylinder diesel engine under varying load conditions (8-25 Nm) by incorporating CeO_2 nanoparticles at concentrations of 25-100 ppm into diesel fuel, and conducted optimization using Response Surface Methodology (RSM). The results indicated that the incorporation of CeO_2 enhanced catalytic combustion, elevating the BTE by an average of 9.80% and yielding a marginal enhancement in specific fuel consumption. The enhanced combustion efficiency resulted in a 21.3% elevation in exhaust gas temperature and a 9.36% augmentation in NO_x emissions. However, the additional oxygen and catalytic effect provided by CeO_2 resulted in significant reductions of 11.93% in HC, 58.78% in CO, and 6.69% in smoke emissions. As a result of the RSM-based multi-objective optimization, a concentration of 100 ppm CeO_2 and an engine load of 12 Nm were determined to be the optimum parameters. Under these conditions, the predicted values were: BTE 23.125%, BSFC 429.766 g/kWh, EGT 335.143°C, CO 0.257%, HC 130.898 ppm, NO_x 786.309 ppm, and smoke 25.654%. The reliability of the RSM model was confirmed by a desirability value of 0.7115 and experimental error rates of less than 5%. It was proven that the CeO_2 nanoparticle additive provides effective improvements in all performance and emission parameters except for NO_x, and that RSM is an efficient optimization tool for such studies. Kesharvani et al. (Kesharvani, Chhabra, Dwivedi, Verma, & Pugazhendhi, 2023) included CeO_2 nanoparticles at concentrations of 40, 60, and 80 ppm into a diesel emulsion fuel comprising 15% water (E_{15}). The mixtures, homogenized with Span 80 and Tween 80 surfactants via ultrasonication and mechanical stirring, were evaluated in a multi-cylinder engine at a constant speed of 1650 rpm. Despite the increase in viscosity and flash point due to nanoparticle incorporation, the $E_{15}CeO_2(80)$ blend with the highest concentration demonstrated a 6.24% enhancement in BTE and a 4.53% reduction in specific fuel consumption relative to pure diesel fuel at full load. Significant reductions in emission values were achieved with the same blend: 40.27% in smoke opacity, 33.60% in NOx emissions, 30% in CO emissions, and 18.75% in HC emissions. The favorable outcomes were ascribed to the enhanced atomization facilitated by the micro-explosion effect of the emulsion fuel, together with the oxygen storage capability and catalytic characteristics of the CeO_2 nanoparticles, which boosted combustion efficiency. The decrease in combustion chamber temperature attributed to water content inhibited NOx generation, while the nanoparticles' capacity to diminish ignition delay and enhance heat transmission effectively reduced emissions.

Polat et al. (Polat, Sarıdemir, Gad, El-Shafay, & Ağbulut, 2024) examined the impact of incorporating 100 ppm CeO_2 nanoparticles into a 20% sunflower biodiesel-diesel blend (B20), alongside the infusion of 5 and 10 liters per minute (lpm) of hydrogen (H_2) into the intake manifold. The tests were performed at a consistent speed of 2000 rpm under different loads. It was observed that this combination improved the negative properties of biodiesel, such as its low calorific value and high viscosity. Compared to B20, the addition of CeO_2, 5 lpm H_2, and 10 lpm H_2 reduced BSFC by 1.77%, 4.71%, and 7.19%, respectively. Simultaneously, BTE rose by 1.39%, 4.04%, and 7.01%, while EGT declined by 2.62%, 4.77%, and 6.73%, respectively. Combustion investigations demonstrated that the introduction of 10 lpm H_2 elevated the in-cylinder pressure by 3% and the heat release rate by 3.52%, signifying a more efficient combustion process. The B20+CeO_2, B20+CeO_2+5 lpm H_2, and B20+CeO_2+10 lpm H_2 blends decreased CO emissions by 46.51%, 56.59%, and 63.57%, respectively, as compared to pure diesel. NOx emissions were reduced by 6.34%, 13.6%, and 20.71%, and HC emissions showed reductions of 12.09% and 28.57% with 5 and 10 lpm H_2, respectively. The study determined that the combination of CeO_2 nanoparticles and hydrogen mitigates the performance limitations of biodiesel while simultaneously improving emissions.

In their study, Hazar et al. (Hazar, Akcay, & Sevinc, 2025) evaluated the methods of preheating and CeO_2 nanoparticle additive together to improve the use of crude walnut oil (CWO) in diesel engines. Crude walnut oil, blended with diesel fuel at ratios of 10%, 20%, and 40%, was mixed with 50 ppm CeO_2, and all blends were preheated to 70°C to reduce viscosity. Tests conducted at a constant speed of 2000 rpm determined that the high viscosity and low calorific value of crude walnut oil increased CO, HC, smoke, BSFC, and EGT, while conversely reducing NO_x, vibration, and noise due to lower combustion temperatures. The preheating process reduced viscosity, thereby increasing combustion efficiency and improving CO, HC, and smoke emissions; however, it also caused a slight increase in NO_x and noise by raising the combustion temperature. The CeO_2 nanoparticle additive, with its oxygen storage capacity and catalytic effect, accelerated the combustion process, provided additional reductions in CO, HC, and smoke emissions, and improved BSFC, but this time led to an increase in NO_x, EGT, vibration, and noise. The most optimal results were achieved with the D90HW10N blend, which comprises 10% warmed walnut oil and 50 ppm CeO_2. This mixture preserved engine performance comparable to diesel while substantially diminishing hazardous emissions. The research indicated that the integration of preheating and nanoparticle additives effectively alleviates the negative impacts of crude vegetable oils on engine performance and emissions. In their

study, Çelik et al. (Çelik, Mehregan, Bayindirli, & Moghiman, 2025) performed a performance and emission analysis on a three-cylinder diesel engine at a constant speed of 1800 rpm and under variable loads (10-40 Nm) by adding CeO_2 nanoparticles at concentrations of 50 and 75 ppm to diesel and canola biodiesel fuels, determining the optimum operating conditions using the Grey-Taguchi method. It was determined that the nanoparticle additive reduced fuel viscosity and increased the calorific value. Canola biodiesel with a 75 ppm CeO_2 additive reduced BSFC by 5.2% and increased BTE by 4.8% at a 30 Nm load, while under the same conditions, diesel fuel provided a 7.4% improvement in BSFC and a 5.5% improvement in BTE. In terms of emission values, with 75 ppm canola biodiesel, CO decreased by 21.8% and smoke by 35.5%, while NO_x increased by 11.7%. For diesel fuel, CO decreased by 11% and smoke by 16.2%, while NO_x increased by 11.9%. Grey Relational Analysis and the Taguchi method determined that diesel fuel with a 75 ppm CeO_2 additive and a 10 Nm engine load provided the overall optimum performance. According to ANOVA results, the most influential parameter was the fuel type, followed by engine load and nanoparticle concentration. The study confirmed that the CeO_2 nanoparticle additive increases efficiency and reduces carbon-based emissions in both diesel and biodiesel; however, contrary to these positive results, an increase in NO_x emissions was observed. It was found that biodiesel-based nanofuels exhibited lower emissions, while diesel-based nanofuels demonstrated higher overall performance.

The consolidated experiments indicate that the incorporation of CeO_2 nanoparticles yields consistent and beneficial impacts on the performance and emission profiles of both diesel and diverse biodiesel fuels. In all investigations, the incorporation of CeO_2 was found to enhance BTE by 2-12%, augment BSFC by 4-20%, and result in substantial decreases of 20-80% in CO, HC, and smoke emissions. However, as a natural consequence of improved combustion efficiency, an increase of 10-30% in NO_x emissions was recorded. The optimum CeO_2 concentration was generally found to vary between 25-100 ppm, and it was determined that the nanoparticles' oxygen storage capacity, catalytic properties, and heat transfer enhancement effects contributed to these positive results. The research demonstrated that CeO_2 has synergistic effects when combined with hydrogen addition, preheating, and emulsion fuel systems. In conclusion, although CeO_2 nanoparticle-doped fuels enhance engine performance and diminish carbon emissions, prioritizing the regulation of NO_x emissions, addressing stability concerns, and examining the long-term impacts across various engine systems are essential research avenues for the commercialization of this technology.

3.2. Aluminum Oxide Nanoparticles (Al_2O_3)

This study synthesizes essential experimental data from numerous investigations examining the effects of alumina (Al_2O_3) nanoparticles on the performance, combustion, and emission characteristics of diverse diesel and biodiesel blends. The cumulative evidence indicates that Al_2O_3 nanoparticles reliably improve BTE, decrease specific fuel consumption, and markedly reduce carbon emissions, whereas their impact on NOx emissions is inconsistent, highlighting a crucial area for further refinement. Sadhik Basha and Anand (Sadhik Basha & Anand, 2013) examined the performance, emissions, and combustion characteristics of a single-cylinder diesel engine utilizing jatropha biodiesel modified with alumina (Al_2O_3), carbon nanotubes (CNT), and their composite nanoparticles at concentrations of 25 ppm and 50 ppm. The nanoparticles, analyzed via TEM and XRD, were uniformly disseminated in the fuel using an ultrasonic homogenizer. Experimental results indicated that all nanoparticle-doped fuels significantly enhanced BTE relative to pure biodiesel (JBD). The maximum BTE attained was 28.9% with the JBD25A25CNT combination, while the result for pure JBD was 24.9%. In the combustion analysis, nanoparticle-doped fuels exhibited a lower peak pressure (68.5 bar for JBD25A25CNT vs. 72.3 bar for JBD) and heat release rate (33.8 J/°CA for JBD25A25CNT vs. 40.1 J/°CA for JBD). Regarding emission values, the JBD25A25CNT fuel was found to reduce smoke opacity to 57% (compared to 67% in pure JBD) and also improved NOx emissions. Hot plate evaporation tests confirmed that the nanoparticles, due to their high surface area-to-volume ratio and thermal conductivity properties, shortened the evaporation time and reduced the ignition delay, demonstrating that nanoparticle additives have positive effects on the fuel's evaporation characteristics and combustion efficiency.

In their study, El-Seesy et al. (El-Seesy, Attia, & El-Batsh, 2018) investigated the effect of alumina nanoparticles (Al_2O_3) added in the range of 10-50 mg/l to a Jojoba biodiesel-diesel blend (JB20D) on engine performance and emissions. The experimental results showed that while JB20D exhibited lower engine performance than pure diesel, it improved emission values. The addition of Al_2O_3 nanoparticles had a positive effect on all performance parameters. At a concentration of 20 mg/l, a reduction of 70% in NOx, 80% in CO, 60% in unburned HC, and 35% in smoke opacity was achieved. At the 40 mg/l concentration, which yielded the best results in terms of engine performance, a 12% reduction in BSFC, an increase in cylinder peak pressure, a 4% rise in the maximum rate of pressure rise, and a 4% improvement in the maximum gross heat release rate were recorded. Based on the combined evaluation of engine performance and emission values, the recommended optimum Al_2O_3 concentration for

JB20D blends was determined to be 30 mg/l.

A study by Nour et al. (Nour, El-Seesy, Abdel-Rahman, & Bady, 2018) examined the performance, combustion, and emission characteristics of a single-cylinder diesel engine by incorporating Al_2O_3 nanoparticles at concentrations of 25, 50, 75, and 100 ppm into a Diesterol fuel blend consisting of 70% diesel, 20% ethanol, and 10% jojoba methyl ester. The results indicated that a 75 ppm Al_2O_3 concentration yielded an enhancement of almost 2% in BSFC and improved combustion efficiency, evidenced by a 1.5% rise in maximum in-cylinder pressure. Emission analyses demonstrated that the addition of Al_2O_3 at all concentration levels led to a reduction in pollutant emissions such as CO, HC, and particulate matter (PM). In their experimental study, Kaushik et al. (Kaushik et al., 2022) produced neem biodiesel from de-waxed neem oil via acid-catalyzed (sulfuric acid) followed by base-catalyzed (sodium hydroxide) transesterification processes. Al_2O_3 nanoparticles at concentrations of 25 ppm and 50 ppm were disseminated in 10-50% diesel-biodiesel blends utilizing an ultrasonic homogenizer for 30 minutes, followed by high-speed stirring at 2000 RPM. The studies were performed at compression ratios of 14:1, 16:1, and 18:1, under an 8 kg load, and at a constant speed of 1500 RPM, comparing performance metrics like BTE, BSFC, and engine emissions. Despite biodiesel exhibiting a lower BTE than pure diesel due to its diminished calorific value, the incorporation of Al_2O_3 nanoparticles enhanced fuel vaporization, expanded the surface area in contact with oxygen, and thereby partially mitigated this drawback by augmenting combustion efficiency. For example, the BTE loss for the B20 blend at CR 18, which was 7% compared to pure diesel, was reduced to 2% with the addition of 50 ppm nanoparticles. Furthermore, the increasing compression ratio and nanoparticle additive, thanks to the higher oxygen content, resulted in reductions of up to 12% in CO emissions for the 50 ppm blend at CR 18, and up to 25% in HC emissions compared to pure diesel. In conclusion, the B20A50 blend, containing 20% biodiesel and 50 ppm Al_2O_3 nanoparticles, was identified as the most suitable option in terms of optimum performance and emission values. Sateesh et al. (Sateesh et al., 2022) conducted an experimental study examining the combustion characteristics of a diesel engine functioning in dual-fuel mode, utilizing DiSOME biodiesel derived from dairy industry waste and producer gas (PG), with Al_2O_3 nanoparticle additives at concentrations between 10 and 40 ppm. The nanoparticles, analyzed using SEM, EDX, and XRD, measuring less than 100 nm, were uniformly disseminated in the fuel using an ultrasonic homogenizer. Tests performed within the 0-80% load spectrum revealed that the DiSOME-PG blend with 30 ppm Al_2O_3 additive yielded an 11.5% superior BTE relative to pure DiSOME-PG. A 23.2% decrease

in smoke opacity, a 21.4% reduction in HC emissions, and an 11.6% decline in CO emissions were noted, however a 36.8% rise in NOx emissions was documented as a result of elevated combustion temperatures. Concerning combustion properties, a reduction in ignition delay, an elevation in cylinder pressure and heat release rate, and a diminished combustion duration were attained. In evaluating the equilibrium between engine performance and emissions, a 30 ppm Al_2O_3 concentration was determined to be optimal, however a reduction in efficiency was noted at the 40 ppm concentration due to heightened viscosity. The study confirmed that Al_2O_3 nanoparticle additives increase combustion efficiency and reduce carbon-based emissions in biodiesel-producer gas dual-fuel systems, while also increasing NOx emissions.

Mostafa et al. (Mostafa, Mourad, Mustafa, & Youssef, 2023) conducted an experimental study examining the impact of incorporating 11 nm-sized Al_2O_3 nanoparticles at concentrations of 0, 50, and 100 ppm into diesel fuel on the emission and performance characteristics of a single-cylinder diesel generator, utilizing Response Surface Methodology (RSM). Tests performed at engine loads of 0.9, 1.8, and 2.7 kW revealed that the fuel containing a 50 ppm Al_2O_3 additive (D+50Al_2O_3) decreased NOx emissions by 32.28%, HC emissions by 21.74%, and CO emissions by 20% at a 2.7 kW load in comparison to pure diesel, while a marginal rise in CO_2 emissions, suggesting enhanced combustion efficiency, was noted. With the same blend, performance parameters showed an improvement in specific fuel consumption and a 4.91% increase in BTE, while the exhaust gas temperature was also found to decrease. The RSM models, confirmed by an $R^2 > 0.98$ coefficient of determination and statistical significance (p-value < 0.05), demonstrated high reliability. In the conducted economic analysis, despite the nanoparticle cost, a net gain of $0.0427 per liter was calculated due to the 4.3% reduction in fuel consumption. The study proved that 11 nm-sized Al_2O_3 nanoparticles at a 50 ppm concentration provide emission reduction and efficiency improvement in diesel fuels while also offering a technically and economically sustainable solution.

In their study, Murugesan et al. (E. Murugesan et al., 2025) conducted experiments by adding 50, 100, and 150 ppm (by weight) of Al_2O_3 nanoparticles to diesel fuel at an engine speed of 1500 rpm and under varying load conditions from 0% to 100%. At full load, a significant 4.5% reduction in BSFC was detected compared to pure diesel fuel, which was explained by increased combustion stability due to the high surface area and heat transfer capability of Al_2O_3. Under the same conditions, the Al_2O_3 blends showed an improvement in BTE of up to 5.8%. This increase was associated with improved fuel atomization and air-fuel mixture due

to the stable dispersion provided by the nanoparticles, a reduction in ignition delay, and the achievement of efficient combustion even at high loads. In terms of emissions, it was determined that the Al_2O_3 additive provided a reduction of approximately 12% in CO emissions and up to 18% in HC emissions at the 150 ppm concentration compared to pure diesel. The beneficial benefits were ascribed to the nanoparticles enhancing combustion efficiency and facilitating a more uniform mixture and stable flame propagation. Nevertheless, the enhanced combustion chamber temperature resulting from improved combustion led to a marginal increase of 2–3% in NOx emissions.

The studies indicate that the incorporation of Al_2O_3 nanoparticles consistently enhances performance and reduces emissions in both conventional diesel and diverse biodiesel mixes. In all experiments, the use of nanoparticles was found to enhance BTE by 2-12%, optimize specific fuel consumption by 2-20%, and achieve substantial reductions of 11-80% in CO, HC, and smoke emissions. However, as a natural consequence of improved combustion efficiency, increases in NOx emissions ranging from 2% to 37% were recorded. While the optimum concentration was determined to vary between 30-100 ppm, it was found that the nanoparticles' high surface area-to-volume ratio, thermal conductivity properties, and catalytic effects contributed to these positive results. Economic analyses showed that net gains can be achieved despite the nanoparticle cost, thanks to improvements in fuel consumption. In conclusion, while Al_2O_3 nanoparticle-doped fuels have the potential to enhance engine performance and environmental sustainability, controlling the increase in NOx emissions and resolving stability issues emerge as priority research areas for the commercialization of this technology.

3.3. Zinc Oxide Nanoparticles (ZnO)

Zinc oxide (ZnO) nanoparticles have proven to be an efficient fuel addition for improving the sustainability and performance of biodiesel in contemporary diesel engines. Recent experimental results indicate that ZnO nanoparticles, noted for their remarkable catalytic activity and elevated surface-area-to-volume ratio, substantially enhance combustion efficiency and diminish hazardous emissions across various biodiesel feedstocks. The incorporation of artificial intelligence and machine learning methodologies for modeling and optimization has significantly progressed the advancement of ZnO-nanoparticle-enhanced biofuels, facilitating accurate forecasting of engine performance and determination of ideal operational parameters. This synthesis evaluates the transformative potential of ZnO nanoparticles in biodiesel formulations, emphasizing their consistent capacity to enhance BTE, reduce specific fuel consump-

tion, and significantly diminish CO, HC, and smoke emissions, while also considering the complex effects on NOx emissions across various engine configurations and fuel blends.

Srinivasarao et al. (Srinivasarao et al., 2025) conducted an experimental study examining the impact of incorporating ZnO nanoparticles at concentrations of 40, 80, and 120 ppm with propanol-2 into a Calophyllum inophyllum biodiesel (CB20) and diesel blend on engine performance, combustion, and emission characteristics. Experiments involving five distinct blends (CB20, CB20P5, CB20P5ZnO40, CB20P5ZnO80, CB20P5ZnO120) revealed that the incorporation of ZnO nanoparticles enhanced BTE by as much as 3.91%, decreased specific fuel consumption by 11.53%, and in the blend containing 120 ppm ZnO, elevated the maximum cylinder pressure to 70.84 bar and the heat release rate to 36.65 J/°CA. Emission reductions of 38.7% for CO, 14.9% for HC, 4.8% for NOx, and 2.48% for smoke were documented. The research validated that forecasts generated by a Generalized Regression Neural Network (GRNN) model exhibited strong concordance with experimental data (R^2: 0.798-0.9995), and the minimal RMSE and MAPE values substantiated the model as a dependable predictive instrument. The findings indicated that the biodiesel-propanol-ZnO nanoparticle triad enhances engine performance and diminishes emissions, while the GRNN model serves as an efficient instrument for fuel formulation and engine optimization.

In their experimental study, Ganapathy et al. (Ganapathy et al., 2025) investigated the effect of ZnO nanoparticle additives on the performance, combustion, and emission characteristics of waste cooking oil (WCO)-based biodiesel (WCOB). The study used diesel, raw WCO, WCOB, and WCOB-ZnO blends with 25-100 ppm ZnO nanoparticle additives. Due to its high viscosity and density, raw WCO exhibited low BTE (22.84%) and high HC (51 ppm), CO (0.27% by volume), and smoke opacity (80%); however, due to its low combustion temperature, its NOx emissions were lower than diesel. Using WCOB increased the BTE to 25.15% and improved carbon-based emissions, but the oxygen content caused NOx emissions to rise to 843 ppm. The addition of ZnO nanoparticles provided significant improvement in all parameters. The WCOB-Z100 fuel, with a 100 ppm ZnO additive, attained the maximum BTE of 28.46%, concurrently producing the minimal emission levels for HC at 37 ppm, CO at 0.16% by volume, NOx at 740 ppm, and smoke opacity at 48%. Combustion analysis revealed that the ZnO additive elevated the peak in-cylinder pressure (63 bar) and heat release rate (73.123 J/° crank angle), reduced the ignition delay (10.4° crank angle), and facilitated more efficient combustion via catalytic effects, micro-explosions, and improved heat transfer.

In their experimental study, Soudagar et al. (Soudagar et al., 2025) investigated the effect of adding 3% ethanol and 40-100 ppm ZnO nanoparticles to cottonseed methyl ester (CSME) biodiesel on the performance and emissions of a Common Rail Direct Injection (CRDI) engine, performing optimization with Deep Neural Network (DNN) models and the Dragonfly Algorithm (DA). Experimental results showed that ZnO nanoparticles, due to their high surface area-to-volume ratio and catalytic activity, increased fuel atomization and combustion efficiency, raising the BTE to up to 38.89%, while also providing significant reductions in HC, CO, and smoke emissions. The DA and MODA algorithms, used for single and multi-objective optimization, determined the optimum values for engine load (20 kg), injection pressure (670-1180 bar), and nanoparticle concentration (>0.4%), and modeled the performance-emission balance using Pareto fronts. In the modeling section, it was found that while the single-layer Artificial Neural Network (ANN) model (R^2 ~0.7) provided insufficient predictions, the multi-layer ANN model achieved high accuracy (R^2 >0.95) and successfully captured the engine's complex behaviors. In their experimental study, Muniyappan & Krishnaiah (Muniyappan & Krishnaiah, 2025) investigated engine performance, combustion, and emission characteristics by adding ZnO nanoparticles at concentrations of 25, 50, and 75 mg/L to a diesel-Mahua biodiesel-ethanol blend (D60B25E15), performing optimization with ANN and Response Surface Methodology (RSM). In the study conducted using a Central Composite Design, it was determined that the blend with 50 mg/L ZnO additive (B25E15Zn50) provided a 7.6% and 8.8% increase in peak cylinder pressure, a 2.03% and 8.7% increase in heat release rate, and a 2.1% and 7.2% increase in BTE compared to pure diesel and the additive-free blend, respectively. It also achieved a 15.7% and 12.1% reduction in specific energy consumption. In terms of emission values, the same blend showed reductions of 35.7% and 29.3% in CO, 10.9% and 15.4% in HC, and 11.7% and 18.9% in smoke, respectively. However, due to the increased combustion temperature, NOx emissions increased by 5.4% compared to pure diesel and by 11.3% compared to the biodiesel blend. Optimization yielded optimal performance metrics at 71.04% engine load and 53.57 mg/L ZnO additive. While both models demonstrated high accuracy, the ANN model exhibited greater predictive capability with a reduced average error rate in comparison to RSM.

Comprehensive evaluation of the conducted tests indicates that the incorporation of ZnO nanoparticles consistently enhances the performance and emission characteristics of biodiesel fuels. In all experiments, the incorporation of ZnO was found to enhance BTE by 2-39%, improve specific fuel consumption by 4-12%, and result in substantial reductions of

10-39% in CO, HC, and smoke emissions. The favorable outcomes were attributed to the elevated surface area-to-volume ratio, catalytic efficacy, and enhanced heat transfer characteristics of ZnO nanoparticles. The concentration range of 50-100 ppm was determined to yield optimal outcomes, while artificial intelligence modeling techniques (ANN, DNN, GRNN) demonstrated great accuracy in optimizing these systems. The research indicated that ZnO has synergistic effects when combined with oxygenated additives like ethanol and propanol. In summary, although ZnO nanoparticle-doped biodiesel fuels enhance engine performance and diminish harmful emissions, prioritizing the optimization of NOx emission variability, improving nanoparticle stability, and examining long-term effects across various engine systems are essential research domains for the commercialization of this technology.

3.4. Copper Oxide Nanoparticles (CuO)

Ağbulut et al. (Ağbulut et al., 2021) examine the impact of incorporating large dosages (<77 nm) of copper oxide (CuO) nanoparticles into diesel fuel on the combustion, performance, and emission characteristics of a single-cylinder, air-cooled, direct injection diesel engine. Experiments were performed within the 2000-3000 rpm range with fuel blends formulated at concentrations of 1000 ppm (1000-CuO) and 2000 ppm (2000-CuO). The findings indicated that the nanoparticles expedited the combustion process by supplying oxygen molecules and functioning as a catalyst, enhanced thermal conductivity, and therefore lowered exhaust gas temperature (EGT). Emission reductions were noted for CO at 14.6% and 20.8%, for HC at 6.2% and 13.4%, and for NOx at 4% and 6.6% for the 1000-CuO and 2000-CuO fuels, respectively.. Regarding performance parameters, the BSFC decreased by 4.5% and 8%, while the BTE increased by 5.5% and 14.6% for the same fuels, respectively. Furthermore, it was determined that the CuO nanoparticles shortened the ignition delay (ID) by 3.03% and 5.45% for 1000-CuO and 2000-CuO, respectively, by increasing the cetane number and accelerating chemical reactions. Combustion analysis revealed that the maximum cylinder pressure (CP max) and heat release rate (HRR max) were higher for the nanoparticle-blended fuels than for pure diesel. The research highlighted that including up to 2000 ppm CuO nanoparticles did not lead to any obstruction in the fuel injection system and produced a tolerable rise in fuel viscosity. The experimental results demonstrate that the incorporation of high-dose CuO nanoparticles synergistically enhances diesel fuel, hence improving engine performance and diminishing hazardous emissions. In another study conducted, Yakut et al. (Yakut & Bilgiç Tüzemen, 2024) investigated the effect of adding CuO nanoparticles, produced via a green synthesis method using cherry laurel leaf extract, as an additive to diesel fuel on

engine performance and emission characteristics. The CuO nanoparticles, characterized and their successful synthesis confirmed by UV, XRD, SEM, EDS, and FT-IR analyses, were added to diesel fuel at concentrations of 10 ppm and 15 ppm and tested at a constant speed of 1500 rpm and a load range of 0-3000 W. According to the performance results, at a 3000 W load, the D100+15 ppm CuO blend provided a 1.80% improvement in specific fuel consumption compared to pure diesel. In terms of emission values, at a 2000 W load, the same blend was observed to provide significant reductions of 45.9% in CO emissions and 19.57% in HC emissions. However, it was determined that the CuO nanoparticle additive increased NOx and smoke emissions, with a 35.71% increase in smoke emission at 2000 W load and an 11.75% increase in NOx emission at 2500 W load. It was found that the rising combustion chamber temperature due to the increasing load caused an increase in CO2 emissions and a decrease in O2 emissions.

In their experimental study, Madhaiyan et al. . (Madhaiyan, Kandasamy, Raman, & Vellaiyan, 2025) investigated the synergistic effect of algal biodiesel (30% Chlorella emersonii methyl ester – CE), hydrated hydrazine (HH – 15% by volume), and CuO nanoparticles (100 ppm) on diesel engine performance and emissions. Based on test results of the blends prepared using algal biodiesel characterized by FTIR and CuO nanoparticles whose catalytic activity was confirmed by XRD/EDX analyses, pure CE biodiesel led to a 4.3% decrease in BTE and a 6.9% increase in BSFC, while it provided reductions of 9.3%, 11.7%, and 9.4% in HC, CO, and smoke emissions, respectively, but increased NOx emissions by 13.1%. The addition of HH further reduced BTE by 8.9% and increased BSHC, BSCO, and smoke emissions; however, it provided a 14.3% reduction in BSNOx. In contrast, the CuO nanoparticle additive led to a 7.6% improvement in BTE, a 7.3% decrease in BSFC, a 5.3% increase in in-cylinder pressure, and a 4.3% increase in net heat release rate. It also achieved comprehensive emission improvement by reducing BSHC by 9.8%, BSCO by 14.9%, smoke opacity by 7.7%, and BSNOx by 5.6%. In their experimental study, Raj et al. (Raj, Madhu, Dhanalakshmi, & Prakash, 2025) conducted a performance and emission analysis on a single-cylinder diesel engine by adding CuO nanoparticles at concentrations of 20-80 ppm to a ternary blend (B20: 80% Diesel + 10% WCOME + 10% PSOME) composed of waste cooking oil and pumpkin seed oil biodiesels. According to the results, it was determined that the CuO nanoparticle additive reduced the fuel's ignition delay, improved vaporization, and increased combustion efficiency. The B20C60 blend with 60 ppm CuO additive achieved the highest BTE value (35.78%), which represented a 13.02% improvement compared to pure B20 and a 6.6% improvement compared to pure diesel.

In the same blend, the BSFC decreased by 23.53% compared to B20 and by 7.14% compared to diesel. Significant reductions in CO and HC emissions were noted due to the catalytic influence of CuO; the B20C80 blend with 80 ppm CuO exhibited HC emissions that were 16% lower than those of pure diesel. It was determined that NOx emissions rose in all biofuel blends relative to pure diesel, attributable to the oxygen content of biodiesel and the nanoparticles elevating the combustion temperature. The research indicated that a 60 ppm CuO nanoparticle ingredient enhances the efficacy of waste-derived biodiesel blends and decreases carbon emissions, while simultaneously emphasizing the need for supplementary strategies for NOx regulation.

Behera and Hotta (Behera & Hotta, 2025) conducted an experimental study examining the influence of 100 ppm CuO nanoparticles on the performance, emissions, and combustion characteristics of blends of palm biodiesel, diesel, and N-butanol, utilizing an artificial neural network and genetic algorithm-based neuro-genetic model.Tests conducted on a Variable Compression Ratio engine at a constant 1500 rpm and an 18:1 compression ratio revealed that the BA10CuO blend, containing 10% Palm biodiesel, 10% N-butanol, 80% diesel, and 100 ppm CuO, achieved a BTE of 44.32% at a 16 N load, which was 6-8% higher than that of pure diesel. Due to the catalytic effect and oxygen-providing property of CuO nanoparticles, fuel atomization, vaporization, and air-fuel mixture improved, resulting in a decrease in BSFC and brake specific energy consumption. Emission investigations indicated substantial decreases in CO and HC emissions with the CuO addition, although a marginal rise in NOx emissions was seen attributable to the oxygen content of the biodiesel. Combustion analysis verified that the addition of CuO elevated cylinder pressure and heat release rate, while the ANN-GA model effectively improved engine parameters, with the error rate between experimental data and predictions ranging from 0.49% to 10%. Prabhahar et al. .(Prabhahar et al., 2025) conducted an experimental study to optimize the influence of algal oil methyl ester (AOME) biodiesel and CuO nanoparticle additives on the performance and emission characteristics of a diesel engine, utilizing both a thermal barrier coated (YSZ coated) piston and a standard (uncoated) piston, employing Response Surface Methodology (RSM).. In experiments investigating the parameters of AOME blend ratios (10-30%), load variations (0-100 kg), and CuO concentrations (50-100 ppm), it was determined that the YSZ-coated pistons provided higher BTE (31.1%) and lower BSFC (0.21 kg/kWh) compared to standard pistons, along with observed improvements n CO, HC, and smoke emissions. However, due to the YSZ coating increasing the combustion temperature, NOx emissions were recorded to rise from 385 ppm to 560 ppm. It was also determined

that the CuO nanoparticles reduced CO and HC emissions by increasing combustion efficiency but had no significant effect on NOx. The optimum conditions determined by RSM for AOME yield (0.5% KOH, 45°C, 8:1 molar ratio, 180 minutes) resulted in a 96.32% yield. In the engine tests, the best performance was observed with the combination of 60% AOME, 75 ppm CuO, and a 50 kg load.

When all of the investigations that have been carried out are taken into consideration, it is discovered that the addition of CuO nanoparticles has a good and consistent impact on the performance and emission characteristics of diesel fuel as well as a variety of biodiesel fuels. It was observed that the addition of CuO led to significant reductions in CO and HC emissions, with the range being between 9.3 and 45.9%. Additionally, the addition of CuO was found to increase BTE by 1.8-44.3%, improve BSFC by 1.8-23.5%, and lead to an increase in BTE. The qualities of CuO nanoparticles that were identified as contributing to these favorable outcomes were found to be their catalytic properties, oxygen-providing action, and fuel atomization enhancing characteristics among others. The increased combustion temperature, on the other hand, was responsible for the reported increases in NOx emissions, which ranged from 5.6% to 13.1%. On the other hand, the results for smoke emissions were observed to be very varied. It was usually determined that the optimal concentration of CuO should be somewhere in the range of 60-100 ppm, and it was demonstrated that artificial intelligence-based modeling techniques (ANN, GA, RSM) are effective for optimizing systems of this kind. Additionally, the research indicated that CuO demonstrates synergistic effects with additives such as ethanol, N-butanol, and hydrated hydrazine, and that it produces more efficient outcomes in engines that have thermal barrier coatings. CuO nanoparticle-doped fuels have been shown to improve engine performance and reduce carbon-based emissions. However, there are a number of priority research areas that need to be addressed before this technology can be commercialized. These include addressing issues of toxicity and stability, controlling the increase in NOx emissions, and investigating the long-term effects of this technology in a variety of engine systems.

3.5. Titanium Dioxide Nanoparticles (TiO_2)

The application of titanium dioxide (TiO_2) nanoparticles as fuel additives has become a significant approach in mechanical engineering to improve the performance, combustion properties, and emission profiles of diesel and biodiesel mixtures. Experimental research indicates that the elevated surface-area-to-volume ratio, intrinsic oxygen content, and catalytic characteristics of TiO_2 nanoparticles markedly enhance fuel atomi-

zation, oxidation rates, and heat transfer in combustion processes. These methods combined result in enhanced BTE and significant decreases in harmful emissions, including CO, HC, and smoke opacity. This study consolidates information from previous studies to critically assess the effectiveness and sustainability of TiO_2-enriched fuels as feasible options for internal combustion engines.

The experimental study by A. M. Kumar et al. (A. M. Kumar et al., 2025) examined the performance, combustion, and emission characteristics of M20 fuel (a mixture of 20% Madhuca oil and 80% diesel) augmented with 50 ppm and 100 ppm TiO_2 nanoparticles under dual-fuel conditions with a constant hydrogen flow of 10 LPM. The M20 blend with a 100 ppm TiO_2 additive demonstrated a 6.76% enhancement in BTE and a 4.46% decrease in BSFC relative to pure M20, alongside reductions of 2.63% in HC emissions and 8.53% in CO emissions. The incorporation of hydrogen into the M20 and 100 ppm TiO_2 mixture resulted in a BTE of 24.23%, an 8.32% reduction in specific fuel consumption, and notable decreases of 13.16% in HC emissions, 19.02% in CO emissions, and 4.04% in smoke opacity. Nevertheless, an increase in in-cylinder temperatures resulted in a 12.67% rise in NOx emissions with the M20 blend. In their experimental work, Hemtanon et al. (Hemtanon, Thawornprasert, & Somnuk, 2025) investigated diesel-biodiesel-ethanol-TiO_2 nanoparticle mixes (DxByEzTi) and determined the D20B70E10Ti blend to be optimum based on phase behavior and stability assessments. This particular blend exhibited a 1.23% superior BTE compared to pure diesel at 50% load and 2300 rpm, an enhancement ascribed to the high surface area-to-volume ratio and oxygen content of the TiO_2 nanoparticles, which improved fuel oxidation rates and heat transmission. The mixture produced significant emission reductions: 7.44% for CO, 37.12% for carbon dioxide, 66.29% for NOx, and 69.43% for smoke opacity. The researchers determined that the interplay between biodiesel's oxygen content and TiO_2's catalytic properties facilitated more thorough combustion, hence decreasing CO and smoke emissions, while ethanol's cooling action, coupled with enhanced heat transfer, lowered combustion temperature, resulting in a significant reduction in NO_2 levels. The research validates that the D20B70E10Ti mixture improves engine efficiency and significantly diminishes environmental effects, presenting a feasible alternative fuel for unaltered diesel engines.

Hemtanon et al. (Hemtanon et al., 2025; Vignesh & Sekar, 2025) examined the synergistic effects of n-butanol, diesel, and TiO_2 nanoparticles on performance, emissions, and combustion behavior in a Reactivity Controlled Compression Ignition (RCCI) engine. Among the evaluated blends under different engine loads (20-80%) and speeds up to 1500

rpm, the mixture comprising 40% n-butanol, 60% diesel, and 100 ppm TiO_2 demonstrated the most favorable outcomes. This blend achieved an in-cylinder pressure of 72 bar at 60% load, with TiO_2 nanoparticles increasing the heat release rate and diminishing ignition delay through better heat transmission and fuel-air mixing. Performance analyses revealed that the identical blend attained a brake power of 5.2 KW, a decrease in BSFC, and an enhancement in BTE to 35% at full load. Emission measurements indicated that, due to the elevated oxygen content of n-butanol and the catalytic influence of TiO_2, CO emissions diminished to 0.15%, CO_2 emissions to 0.13%, NOx emissions to 0.12 ppm, and smoke emissions to 4%. In their research, Jayaseelan et al. . (Jayaseelan, Musthafa, Anderson, Abishek, & Bhuvaneshwaran, 2025) assessed candle nut oil biodiesel-diesel blends (B20, B40, B60) using TiO_2 nanoparticle additions in a single-cylinder diesel engine. The B20 blend containing 100 ppm TiO_2 was recognized as the most promising, demonstrating specific fuel consumption equivalent to diesel and other blends. The TiO_2 nanoparticles, owing to their elevated surface-area-to-mass ratio, enhanced fuel vaporization and combustion efficiency, consequently augmenting BTE. Because biodiesel is more viscous and less volatile than diesel, combustion analysis found a lower maximum in-cylinder pressure for biodiesel mixes. The B20+TiO_2 mixture significantly reduced CO, HC, smoke opacity, and CO_2 emissions by utilizing biodiesel's oxygen content and TiO_2's catalytic capabilities. Despite an overall rise in NO_x emissions attributed to elevated combustion temperatures and fuel-bound oxygen, the TiO_2 addition mitigated this increase, particularly in the B20 blend. The research determined that the B20 blend with 100 ppm TiO_2 significantly decreases hazardous emissions while preserving satisfactory engine performance.

Babu et al. (Babu, Kumar, Basha, & Rao, 2025) conducted an experimental investigation examining the performance and emission characteristics of a CRDI diesel engine by incorporating TiO_2 nanoparticles at concentrations of 25, 50, and 100 ppm into a B20 blend derived from Jatropha oil methyl ester (JOME) biodiesel. The findings indicated that TiO_2 nanoparticles augment combustion efficiency owing to their catalytic characteristics, oxygen retention capability, and proficiency in enhancing fuel atomization. The B20+T50 blend, specifically with a 50 ppm TiO_2 content, demonstrated optimal performance, achieving the maximum BTE and the lowest BSFC. The catalytic oxidation capability of TiO_2 resulted in substantial decreases in CO and HC emissions for all nanoparticle-blended fuels when compared to both pure B20 and pure diesel. Smoke opacity increased significantly due to biodiesel's oxygen content and TiO_2's soot-oxidizing capabilities. The high oxygen content

in biodiesel increased NO_x emissions in all blends. The TiO_2 nanoparticle addition improved combustion uniformity, reducing this issue.

A thorough study shows that adding TiO_2 nanoparticles improves the performance and emissions of diesel and biodiesel fuels. TiO_2 improved BTE by 1.23-24.23%, optimized fuel utilization by 0.87-8.32%, and significantly reduced CO, HC, and smoke emissions by 2.63% to 69.43% in all trials. The positive results were attributed to TiO_2 nanoparticles' increased surface-area-to-volume ratio, catalytic properties, and heat transfer enhancement. The optimal concentration range was 50-100 ppm, with RCCI engine systems and hydrogen-enriched applications showing greater benefits. Concerning emissions, NO_x levels demonstrated variability; a reduction (5.50-66.29%) was noted in certain tests, whilst an increase (12.67%) was documented in others. Economically, it was established that sub-micron TiO_2 particles generated using ultrasonication exhibited equivalent performance at a cost seven times cheaper than that of commercial nanoparticles. In conclusion, although TiO_2 nanoparticle-enhanced fuels have demonstrated enhancements in engine performance and reductions in carbon emissions, specific areas necessitate more improvement for effective commercial implementation. Primary research priorities are the optimization of NO_x emissions variability, the enhancement of particle stability, the refinement of ultrasonication parameters, and the examination of long-term effects across various engine systems.

3.6. Iron Oxide Nanoparticles (Fe_2O_3)

The incorporation of nanoparticles as fuel additives has emerged as an effective approach to alleviate the performance constraints and environmental repercussions of biodiesel-diesel mixtures. Although titanium dioxide (TiO_2) has been thoroughly examined, recent investigations have progressively concentrated on the capability of ferric oxide (Fe_2O_3) nanoparticles to enhance combustion efficiency and diminish emissions. Experimental studies indicate that incorporating Fe_2O_3 nanoparticles into various biodiesel-diesel blends consistently enhances critical performance indicators, such as BTE and specific fuel consumption. Moreover, these tests indicate substantial decreases in CO and unburned HC. Nonetheless, akin to other metal oxide nanoparticles, a prevalent issue with Fe_2O_3 additions is their tendency to elevate NOx emissions as a result of heightened combustion temperatures. This work emphasizes the dual function of Fe_2O_3 in improving engine performance and modifying emission profiles, underscoring the necessity for meticulous optimization to fully leverage its advantages as a sustainable fuel catalyst.

Kishore & Gugulothu (Kishore & Gugulothu, 2022) conducted an ex-

perimental investigation examining the incorporation of Fe_2O_3 nanoparticles at several concentrations (40, 80, 120 ppm) into a Mahua methyl ester (MME) biodiesel and diesel blend (MME20). The nano-fuels, synthesized with a CTAB surfactant and ultrasonication, were evaluated in a Common Rail Direct Injection engine. The 80 ppm combination (MME20+IONP80) demonstrated superior performance. This optimal mixture resulted in an 8.8% enhancement in BTE, alongside considerable decreases in emission metrics: 5.38% in smoke density, 6.39% in HC, and 10.24% in CO. Nonetheless, despite enhancements in in-cylinder pressure and heat release rate attributable to elevated combustion efficiency, a notable increase in NOx emissions was observed, stemming from the high oxygen concentration and catalytic influence. Poudel, Gautam, and Adhikari (Poudel, Gautam, & Adhikari, 2023) conducted an experimental investigation examining the incorporation of Fe_2O_3 nanoparticles (90 ppm) into a pine oil and diesel blend (B20). Marked enhancements in the physicochemical characteristics of the nano-fuel blend produced through ultrasonication were noted in comparison to conventional diesel, with significant increases in kinematic viscosity (2.057 cSt), cetane number (55), and especially in calorific value (48,000 kJ/kg). Engine tests performed at compression ratios of 15 and 16 demonstrated that this nano-fuel mixture, in comparison to pure diesel, yielded a 9.92% enhancement in indicated power, a 4.39% improvement in brake power, a 4.64% rise in BTE, a 13.49% increase in indicated thermal efficiency, and a 2.89% boost in volumetric efficiency, while simultaneously decreasing specific fuel consumption by 17.14%. Notwithstanding a 12.83% reduction in mechanical efficiency, these findings indicate that the Fe_2O_3 nanoparticle-enhanced pine oil-diesel blend markedly enhances engine performance and offers a viable alternative for diminishing fossil fuel usage. In their study, Şener, Uslu, and Savaş (Şener, Uslu, & Savaş, 2025) revealed that the incorporation of magnetic maghemite (Fe_2O_3) nanoparticles into a jojoba biodiesel/diesel blend (J10) substantially improves engine performance and modifies emission profiles. Their findings indicated that a nanoparticle concentration of 100 ppm (100J10) significantly decreased CO emissions by 49.84% and HC emissions by 66.88%, while enhancing BTE by 4.21% and lowering brake-specific fuel consumption by 4.02%. Nonetheless, this improved combustion led to elevated CO_2 (26.33%) and NOx (24.04%) emissions. The study, utilizing Response Surface Methodology (RSM) optimization, determined that an engine load of 1.46 kW and a Fe_2O_3 concentration of 59.09 ppm are the optimal values, providing an ideal equilibrium between performance and emissions. The statistically significant findings ($R^2 > 90\%$) validate the role of Fe_2O_3 in enhancing combustion efficiency and diminishing specific emissions, while also underscoring the trade-off of elevated NOx and CO_2 levels, thus offering a

sophisticated strategy for optimizing biodiesel fuels doped with nanoparticles.

A comprehensive assessment of the studies indicates that the incorporation of iron oxide (Fe_2O_3) nanoparticles into various biodiesel/diesel blends (jojoba, pine oil, mahua) improves engine performance and combustion efficiency, resulting in enhanced BTE and decreased BSFC. Concurrently, notable decreases in CO, HC, and smoke emissions have been recorded, ascribed to the catalytic action and enhanced oxygen levels. Consequently, due to enhanced combustion efficiency, elevated cylinder temperatures have resulted in a persistent rise in NOx emissions in all tests, underscoring the imperative for NOx mitigation techniques when employing nanoparticles. The equilibrium between performance and emissions fluctuated with nanoparticle concentration, and an optimal concentration range (about 60-100 ppm) was determined for each fuel combination. In conclusion, Fe_2O_3 nanoparticle additions are a highly effective and promising approach for enhancing engine performance and reducing carbon-based emissions in biodiesel fuels. Nonetheless, the rise in NOx and the possible environmental repercussions of exhaust nanoparticle emissions continue to pose significant issues that necessitate additional research for the commercial feasibility of this technology.

3.7. Silver Nanoparticles (Ag)

The effects of adding silver nanoparticles (200, 400, and 600 ppm) to waste cooking oil-based biodiesel using commercial techniques and environmentally friendly methods using the Humulus lupulus L. plant were compared experimentally in a single-cylinder diesel engine running at partial loads (1-4 kW) by Demir et al. (Demir et al., 2025). Because of their improved dispersion and smaller particle size (30.60–36.72 nm), the green-synthesised nanoparticles (HL-AgNPs) were found to improve engine performance more effectively than the commercial versions. The enhancement in the 600 ppm green additive blend (B_G600) elevated the in-cylinder pressure to 44.62 bar and the heat release rate to 41.4 J/°CA, increasing thermal efficiency to 26.17% and decreasing specific fuel consumption to around 553 g/kWh. More efficient combustion led to substantial reductions in CO (71.42% in B_G600), HC (48.88% in B_G600), and particulate matter emissions in the green-synthesized blends. Increases in CO_2 (2.59% in B_G600) indicate complete combustion, whereas NO_x emissions (237 ppm in B_G400) and exhaust gas temperature (583 °C in B_G600) reflect enhanced combustion temperatures.

In their experimental study, Çelik, Mehregan, Bayındırlı, et al. (Çelik, Mehregan, Bayındırlı, et al., 2025) examined the impact of silver

nanoparticles—stabilized with sorbitan monooleate surfactant and incorporated into pure diesel fuel at concentrations of 10, 20, and 40 ppm (D10, D20, D40)—on engine performance and emissions in a low-heat-rejection (LHR) diesel engine across seven distinct speed modes (1330-1900 rpm). Experiments performed subsequent to thermally insulating the engine components (valves, piston, cylinder head) with a NiCrAl bond coat and a PSZ+TiO_2 ceramic composite top coat demonstrated that the nanoparticle additive enhanced fuel distribution, minimized ignition delay, and improved physical fuel characteristics, resulting in an approximate 1-3% reduction in fuel consumption and a 1.1% to 7.3% augmentation in brake power. Emission data demonstrated notable reductions of up to 20.5% in CO, 28% in HC, and 13% in NOx, attributed to enhanced combustion efficiency, although an increase in CO_2 emissions was noted as a sign of more complete combustion. The analysis revealed that the most advantageous enhancements were predominantly attained at the 20 ppm concentration (D20), whereas at 40 ppm, the rates of improvement either plateaued or diminished, highlighting the necessity of identifying the optimal nanoparticle concentration. In their experimental study, Samuelraj, Venkatesh, Premnath, Pradeep, and Vignesh (Samuelraj, Venkatesh, Premnath, Pradeep, & Vignesh, 2025) examined the impact of silver nanoparticles, stabilized with sorbitan monooleate surfactant and incorporated into diesel fuel at concentrations of 10, 20, and 40 ppm, on engine performance and emissions in a low-heat-rejection (LHR) diesel engine. Experiments on thermally insulated engine components (piston, cylinder head, valves) with a NiCrAl bond coat and a PSZ+TiO_2 ceramic composite top coat showed that the nanoparticle additive improved combustion efficiency by optimizing the fuel-air mixture, ignition properties, and fuel distribution.. Consequently, substantial reductions of up to 20.5% in CO emissions, 28% in HC emissions, and 13% in NOx emissions were documented in comparison to pure diesel fuel, alongside an increase in CO_2 emissions, signifying enhanced combustion efficiency. An enhancement in engine performance resulted in a brake power gain of up to 7.3% and a fuel consumption decrease of up to 3%. The study found that optimal results were achieved at a 20 ppm concentration, while higher concentrations, like 40 ppm, did not yield a substantial enhancement in performance and emission reductions.

Experimental studies consistently demonstrate that the incorporation of silver nanoparticles (AgNPs) boosts engine performance and decreases emission levels by optimizing combustion efficiency in both conventional and low-heat-rejection (LHR) diesel engines. Nanoparticles synthesized by green methods were determined to be more efficacious owing to their diminutive size and enhanced dispersion. These additives resulted

in substantial decreases in CO (up to 71.42%), HC (up to 48.88%), and NOx (up to 13%) emissions, concurrently enhancing performance with an increase in brake power (up to 7.3%) and a reduction in fuel consumption (up to 3%). Nonetheless, an escalation in CO_2 emissions due to more complete combustion, along with a reported rise in NOx levels in certain experiments, underscores the necessity for optimization. All studies underscore the paramount significance of identifying the optimal nanoparticle concentration (between 20-60 ppm) to achieve a balance between performance and emissions, and illustrate that silver nanoparticles are a superior additive in the formulation of sustainable fuel solutions for diesel engines.

4. Conclusions and Recommendations

This study provides a comprehensive review of various research that experimentally investigates the effects of metal nanoparticle additives on engine performance, combustion characteristics, and emissions in diesel and biodiesel-fueled engines. Due to concerns about the depletion risk of fossil fuels and increasing environmental pollution, interest in alternative fuels like biodiesel has grown. However, biodiesel has been observed to have disadvantages such as lower engine performance and higher NOx emissions compared to pure diesel fuel.

To overcome these problems, the use of metal and metal oxide nanoparticles (such as cerium oxide, aluminum, zinc oxide, copper oxide, titanium dioxide, iron oxide, and silver) as additives in diesel and biodiesel fuels has been investigated. Experimental studies have shown that nanoparticle additives, thanks to their high surface area-to-volume ratios and thermal conductivity, increase the fuel's BTE (BTE), reduce BSFC, and decrease HC, CO, and smoke emissions. Although NOx emissions generally increase with biodiesel use, it has been determined that some nanoparticles, like CeO_2, can reduce NOx emissions through their oxygen-providing catalytic effect.

However, it has been emphasized that factors such as nanoparticle type, concentration, size, and the properties of the base fuel are decisive on the results. The reviewed literature reveals that there are still significant research gaps in this field: the impact of variable engine operating conditions such as injection timing, injection pressure, and compression ratio; the effect of nanoparticle size on the fuel-air mixture; the potential for nanoparticles to be expelled with exhaust, leading to environmental pollution; the possibility of recovering magnetic nanoparticles; determining the optimum nanoparticle concentration; and issues such as agglomeration, stability problems, and their effects on injection characteristics

require further investigation.

In conclusion, it can be suggested that nanoparticle additives are a promising option for improving diesel engine performance and reducing emissions, provided the mentioned challenges are addressed. This could thereby reduce fossil fuel consumption and mitigate air pollution.

REFERENCES

Ağbulut, Ü., Sarıdemir, S., Rajak, U., Polat, F., Afzal, A., & Verma, T. N. (2021). Effects of high-dosage copper oxide nanoparticles addition in diesel fuel on engine characteristics. *Energy, 229*, 120611.

Ahmed, S. F., Ahmed, B., Mehnaz, T., Mehejabin, F., Shome, S., Almomani, F., . . . Kamangar, S. (2024). Impact of nanoparticle-based fuel additives on biodiesel combustion: An analysis of fuel properties, engine performance, emissions, and combustion characteristics.

Ahn, S.-Y., Jang, W.-J., Shim, J.-O., Jeon, B.-H., & Roh, H.-S. (2024). CeO2-based oxygen storage capacity materials in environmental and energy catalysis for carbon neutrality: extended application and key catalytic properties. *Catalysis Reviews, 66*(4), 1316-1399.

Alex, Y., Earnest, J., Raghavan, A., George Roy, R., & Koshy, C. (2022). Study of engine performance and emission characteristics of diesel engine using cerium oxide nanoparticles blended orange peel oil methyl ester. Energy Nexus. 2022; 8.

Alkemade, U. G., & Schumann, B. (2006). Engines and exhaust after treatment systems for future automotive applications. *Solid State Ionics, 177*(26-32), 2291-2296.

Ampah, J. D., Yusuf, A. A., Agyekum, E. B., Afrane, S., Jin, C., Liu, H., . . . Habil, M. (2022). Progress and recent trends in the application of nanoparticles as low carbon fuel additives—a state of the art review. *Nanomaterials, 12*(9), 1515.

Atabani, A. E., Silitonga, A. S., Badruddin, I. A., Mahlia, T., Masjuki, H., & Mekhilef, S. (2012). A comprehensive review on biodiesel as an alternative energy resource and its characteristics. *Renewable and sustainable energy reviews, 16*(4), 2070-2093.

Babu, S. R., Kumar, P. P., Basha, S. A., & Rao, M. M. (2025). Effect of titanium dioxide nanoparticle concentration on the performance and emissions of a common rail direct injection engine with jute oil mahua ester biodiesel. *Ecological Engineering & Environmental Technology (EEET), 26*(6).

Basha, J. S., Al Balushi, M., Soudagar, M. E. M., Safaei, M. R., Mujtaba, M., Khan, T. Y., . . . Elfasakhany, A. (2022). Applications of nano-additives in internal combustion engines: a critical review. *Journal of Thermal Analysis and Calorimetry, 147*(17), 9383-9403.

Bayindirli, C., & Celik, M. (2024). STUDYING HOW DIESEL ENGINE ADDITIVES USING SILVER OXIDE (Ag2O) NANOPARTICLES AFFECT THE ENVIRONMENT. *Journal of Engineering Studies and Research, 30*(1), 7-14.

Behera, B. N., & Hotta, T. K. (2025). Influence of copper oxide nano-particles on the performance, emission, and combustion measures of a VCR engine using palm biodiesel blended with N-butanol: A combined experimental and ANN-GA-based study. *Fuel, 381*, 133504.

Bhan, S., Gautam, R., & Singh, P. (2024). Analyzing the impact of adding

aluminum oxide and cerium oxide nanoparticles to waste cooking biodiesel on engine performance, combustion and emissions characteristics. *Petroleum Science and Technology, 42*(6), 706-734.

Bilgin, S. (2025). Thermal energy storage systems: current technologies and future trends *Research And Evaluations In The Field Of Mechanical Engineering* (Vol. 4, pp. 71).

Bilgin, S. Akansu, S. O., İlhak, M. İ. (2022). Carbonization, Activation and Investigation of Different Uses ofses of Wastewater Treatment Sludge *16th International Combustion Symposium*.

Bilgin, S., Onal, Y., Akansu, S. O., & Ilhak, M. I. (2023). The effect of using activated carbon obtained from sewage sludge as a fuel additive on engine performance and emissions. *Thermal Science, 27*(4 Part B), 3313-3322.

Bitire, S. O., Nwanna, E. C., & Jen, T.-C. (2023). The impact of CuO nanoparticles as fuel additives in biodiesel-blend fuelled diesel engine: A review. *Energy & Environment, 34*(7), 2259-2289.

Çelik, M., Mehregan, M., Bayindirli, C., & Moghiman, M. (2025). Thermal Efficiency Boost in Diesel Engines Using Cerium Oxide Nano-additives in Rapeseed and Diesel Fuels and Taguchi Optimization. *International Journal of Automotive Technology*, 1-8.

Çelik, M., Mehregan, M., Bayındırlı, C., & Moghiman, M. (2025). Optimization analysis of a compression ignition engine running with silver oxide and titanium dioxide nanoparticles blended into canola biodiesel and pure diesel using Taguchi technique. *Journal of Chemical and Petroleum Engineering, 59*(1), 65-80.

Demir, U., Keskin, M., Özer, S., & Coskun, G. (2025). The effect of adding green synthesized and commercial silver nanoparticles to biodiesel on diesel engine performance and emissions. *Case Studies in Thermal Engineering, 67*, 105797.

Demirbas, A. (2008). *Biodiesel: a realistic fuel alternative for diesel engines*: Springer.

El-Seesy, A. I., Attia, A. M., & El-Batsh, H. M. (2018). The effect of Aluminum oxide nanoparticles addition with Jojoba methyl ester-diesel fuel blend on a diesel engine performance, combustion and emission characteristics. *Fuel, 224*, 147-166.

Elkelawy, M., Mohamad, H. A. E., Abo-Samra, S., & Elshennawy, I. A.-E. (2023). Nanoparticles additives for diesel/biodiesel fuel blends as a performance and emissions enhancer in the applications of direct injection diesel engines: A comparative review. *Journal of Engineering Research, 7*(1), 112-121.

Ganapathy, S. A., Jaikumar, M., Ramanathan, V., Hariram, V., & Sangeethkumar, E. (2025). Assessing the Engine Behaviour when Fuelled with Zinc Oxide Nano-particle Infused Waste Cooking Biodiesel. *International Journal of Vehicle Structures & Systems, 17*(2), 263-272.

Ghanati, S. G., Doğan, B., & Yeşilyurt, M. K. (2024). The effects of the usage

of silicon dioxide (SiO2) and titanium dioxide (TiO2) as nano-sized fuel additives on the engine characteristics in diesel engines: a review. *Biofuels, 15*(2), 229-243.

Govorushko, S. (2013). Environmental problems of extraction, transportation, and use of fossil fuels. *Fossil fuels: sources, environmental concerns and waste management practices*, 1-84.

Gupta, A., Kumar, R., Maurya, A., Ahmadi, M. H., Ongar, B., Yegzekova, A., . . . Shelare, S. (2024). A comparative study of the impact on combustion and emission characteristics of nanoparticle-based fuel additives in the internal combustion engine. *Energy Science & Engineering, 12*(1), 284-303.

Gültekin, N. (2024). The hydrogen injection strategy's influence on the performance and emissions (exhaust, vibration, and noise) of a dual-fuel engine. *International Journal of Automotive Engineering and Technologies, 13*(4), 217-229.

Gültekin, N., Gülcan, H. E., & Ciniviz, M. (2023). Determination of effects of some alcohol blends on performance, emission, mechanical vibration and noise in diesel engines. *European Mechanical Science, 7*(4), 259-267.

Gültekin, N., Gülcan, H. E., & Ciniviz, M. (2024). Investigation of the effects of hydrogen energy ratio and valve lift amount on performance and emissions in a hydrogen-diesel dual-fuel compression ignition engine. *International Journal of Hydrogen Energy, 49*, 352-366.

Hazar, H., Akcay, C., & Sevinc, H. (2025). Impact of CeO2 nanoparticles and crude walnut oil–diesel blends on combustion, performance, and emission characteristics of a diesel engine. *Applied Thermal Engineering*, 128082.

Hemtanon, K., Thawornprasert, J., & Somnuk, K. (2025). Effects of Diesel–Biodiesel–Ethanol–TiO2 Nanoparticle Blended Fuels on the Performance and Emissions of a Direct Injection Diesel Engine. *ACS Omega, 10*(17), 17337-17352.

Jayaseelan, G. A. C., Musthafa, B., Anderson, A., Abishek, J. A., & Bhuvaneshwaran, K. (2025). Exploring the Impact of Titanium Dioxide Nanoparticles as Fuel Additives in Candlenut Biodiesel–diesel Blends in a CI Engine. *J. Environ. Nanotechnol, 14*(1), 84-90.

Jin, N., Long, W., Xie, C., & Tian, H. (2025). After-Treatment Technologies for Emissions of Low-Carbon Fuel Internal Combustion Engines: Current Status and Prospects. *Energies, 18*(15), 4063.

Kaushik, Y., Verma, V., Saxena, K. K., Prakash, C., Gupta, L. R., & Dixit, S. (2022). Effect of Al2O3 nanoparticles on performance and emission characteristics of diesel engine fuelled with diesel–neem biodiesel blends. *Sustainability, 14*(13), 7913.

Kegl, T., Kralj, A. K., Kegl, B., & Kegl, M. (2021). Nanomaterials as fuel additives in diesel engines: A review of current state, opportunities, and challenges. *Progress in Energy and Combustion Science, 83*, 100897.

Kesharvani, S., Chhabra, M., Dwivedi, G., Verma, T. N., & Pugazhendhi, A.

(2023). Execution and emission characteristics of automotive compression ignition engine powered by cerium oxide nanoparticles doped water diesel emulsion fuel. *Fuel, 349*, 128670.

Khan, S., Dewang, Y., Raghuwanshi, J., Shrivastava, A., & Sharma, V. (2022). Nanoparticles as fuel additive for improving performance and reducing exhaust emissions of internal combustion engines. *International Journal of Environmental Analytical Chemistry, 102*(2), 319-341.

Kishore, N. P., & Gugulothu, S. (2022). Effect of iron oxide nanoparticles blended concentration on performance, combustion and emission characteristics of crdi diesel engine running on mahua methyl ester biodiesel. *Journal of The Institution of Engineers (India): Series C, 103*(2), 167-180.

Kittelson, D. B. (1998). Engines and nanoparticles: a review. *Journal of aerosol science, 29*(5-6), 575-588.

Kumar, A. M., Nathan, K. S., Manickam, S., Gupta, D., Vikneswaran, M., Dhamodaran, G., . . . Al-Ansari, M. M. (2025). Effect of TiO2 nanoparticles and hydrogen on the combustion, performance, and emissions of madhuca biodiesel in a diesel engine. *International Journal of Hydrogen Energy.*

Kumar, S., Dinesha, P., & Bran, I. (2019). Experimental investigation of the effects of nanoparticles as an additive in diesel and biodiesel fuelled engines: a review. *Biofuels, 10*(5), 615-622.

Lak, S. Z., Rezaei, J., & Rahimpour, M. R. (2024). Health and pollution challenges of fossil fuels utilization. *Encycl. Renew. Energy Sustain. Environ, 8*, 155.

Lamaris, V., & Hountalas, D. (2010). A general purpose diagnostic technique for marine diesel engines–Application on the main propulsion and auxiliary diesel units of a marine vessel. *Energy conversion and management, 51*(4), 740-753.

Leo, G. L., Murugapoopathi, S., Thodda, G., Baligidad, S. M., Jayabal, R., Nedunchezhiyan, M., & Devarajan, Y. (2023). Optimisation and environmental analysis of waste cashew nut shell oil biodiesel/cerium oxide nanoparticles blends and acetylene fumigation in agricultural diesel engine. *Sustainable Energy Technologies and Assessments, 58*, 103375.

Lott, P., & Deutschmann, O. (2021). Lean-burn natural gas engines: Challenges and concepts for an efficient exhaust gas aftertreatment system. *Emission Control Science and Technology, 7*(1), 1-6.

Madhaiyan, R., Kandasamy, K. T. P. P., Raman, M., & Vellaiyan, S. (2025). Synergistic effect of copper oxide nanocatalysts and hydrous hydrazine in developing a sustainable diesel fuel blend for enhanced combustion and emission control. *Fuel, 402*, 135959.

Mawlid, O. A., Abdelhady, H. H., & El-Deab, M. S. (2024). Recent advances in magnetic nanoparticle-based heterogeneous catalysts for efficient biodiesel production: A review. *Energy & Fuels, 38*(21), 20169-20195.

Mayer, H. (1999). Air pollution in cities. *Atmospheric environment, 33*(24-25), 4029-4037.

Mei, D., Li, X., Wu, Q., & Sun, P. (2016). Role of cerium oxide nanoparticles

as diesel additives in combustion efficiency improvements and emission reduction. *Journal of Energy Engineering, 142*(4), 04015050.

Mohammad, N., Mansor, W. N. W., Abdullah, S., Wan, C., Othman, A., SHEIKH, A. A., . . . Jalaludin, J. (2022). Effects of exhaust emissions from diesel engine applications on environment and health: A review. *Journal of Sustainability Science and Management, 17*(1), 281-301.

Mostafa, A., Mourad, M., Mustafa, A., & Youssef, I. (2023). Influence of aluminum oxide nanoparticles addition with diesel fuel on emissions and performance of engine generator set using response surface methodology. *Energy Conversion and Management: X, 19*, 100389.

Mujtaba, M., Kalam, M., Masjuki, H., Gul, M., Soudagar, M. E. M., Ong, H. C., . . . Yusoff, M. (2020). Comparative study of nanoparticles and alcoholic fuel additives-biodiesel-diesel blend for performance and emission improvements. *Fuel, 279*, 118434.

Muniyappan, S., & Krishnaiah, R. (2025). Investigation on the Effects of the ZnO Combustion Enhancer to Ascertain the Blend Ratio Using Artificial Intelligence and a Statistical Approach for a Diesel–Biodiesel–Ethanol-Fueled CI Engine. *ACS Omega*.

Muruganantham, P., & Pandiyan, P. (2021). Analysis on performance and emission characteristics of corn oil methyl ester blended with diesel and cerium oxide nanoparticle. *Case Studies in Thermal Engineering, 26*, 101077.

Murugesan, A., Umarani, C., Subramanian, R., & Nedunchezhian, N. (2009). Bio-diesel as an alternative fuel for diesel engines—a review. *Renewable and sustainable energy reviews, 13*(3), 653-662.

Murugesan, E., Dhairiyasamy, R., Dixit, S., & Singh, S. (2025). The impact of nanoparticle-diesel blends on fuel properties, combustion efficiency, and emissions. *Case Studies in Thermal Engineering, 69*, 106070.

Nagappan, M., & Babu, J. (2023). In ternary blend fuelled diesel engines, nanoparticles are used as an additive in biofuel production and as a fuel additive: A review. *Materials Today: Proceedings*.

Nohynek, G. J., & Dufour, E. K. (2012). Nano-sized cosmetic formulations or solid nanoparticles in sunscreens: a risk to human health? *Archives of toxicology, 86*(7), 1063-1075.

Nour, M., El-Seesy, A. I., Abdel-Rahman, A. K., & Bady, M. (2018). Influence of adding aluminum oxide nanoparticles to diesterol blends on the combustion and exhaust emission characteristics of a diesel engine. *Experimental Thermal and Fluid Science, 98*, 634-644.

Nouri, M., Isfahani, A. H. M., & Shirneshan, A. (2021). Effects of Fe2O3 and Al2O3 nanoparticle-diesel fuel blends on the combustion, performance and emission characteristics of a diesel engine. *Clean Technologies and Environmental Policy, 23*(8), 2265-2284.

Ogunkunle, O., & Ahmed, N. A. (2021). Overview of biodiesel combustion in mitigating the adverse impacts of engine emissions on the sustainable human–environment scenario. *Sustainability, 13*(10), 5465.

Özseven, T., Erentürk, K., Yaşar, E., Düğenci, M., Ünal, A., Dumbadze, G., & Davitadze, Z. (2019). Innovative Approaches in Engineering, Mathematics and Natural Sciences, Ekin Publishing

Polat, F., Sarıdemir, S., Gad, M., El-Shafay, A., & Ağbulut, Ü. (2024). Enhancing diesel engine performance, combustion, and emissions reductions under the effect of cerium oxide nanoparticles with hydrogen addition to biodiesel fuel. *International Journal of Hydrogen Energy, 83*, 884-896.

Poudel, K., Gautam, R., & Adhikari, S. P. (2023). Performance Analysis and Testing of Diesel with Ferric Oxide (Fe2O3) Nanomaterial and Pine Oil in Internal Combustion Engine.

Prabhahar, M., Prakash, S., Dharsan, P., Elumalai, P., Xueyi, F., & Hasan, N. (2025). Optimization of thermal barrier coating with induced copper oxide nanoparticles in CI engine using algae methyl ester as fuel. *Scientific Reports, 15*(1), 21221.

Raj, R. S., Madhu, P., Dhanalakshmi, C. S., & Prakash, M. A. (2025). Application of CuO nanoparticles on performance and emission characteristics of ternary blends of diesel, waste cooking oil and pumpkin seed oil biodiesel in an IC engine. *Indian Journal of Chemical Technology (IJCT), 32*(1), 33-40.

Sadhik Basha, J., & Anand, R. (2013). The influence of nano additive blended biodiesel fuels on the working characteristics of a diesel engine. *Journal of the Brazilian Society of Mechanical Sciences and Engineering, 35*(3), 257-264.

Sajeevan, A. C., & Sajith, V. (2013). Diesel engine emission reduction using catalytic nanoparticles: an experimental investigation. *Journal of Engineering, 2013*(1), 589382.

Samuelraj, D., Venkatesh, R., Premnath, K., Pradeep, M., & Vignesh, K. (2025). Nanoparticle-Enabled Reduction of Emissions and Fuel Consumption in Compression Ignition LHR Engines. *J Mat Sci Eng Technol, 3*(3), 1-6.

Sandaka, B. P., & Kumar, J. (2023). Alternative vehicular fuels for environmental decarbonization: A critical review of challenges in using electricity, hydrogen, and biofuels as a sustainable vehicular fuel. *Chemical Engineering Journal Advances, 14*, 100442.

Sani, G. D., Yakubu, A., Saidu, A., Aati, R., Sahabi, S., & Abdullahi, S. (2023). A review on industrial applications of zinc oxide nanoparticles. *International Journal of Advances in Engineering and Management, 5*, 1031-1041.

Sarma, C. J., Sharma, P., Bora, B. J., Bora, D. K., Senthilkumar, N., Balakrishnan, D., & Ayesh, A. I. (2023). Improving the combustion and emission performance of a diesel engine powered with mahua biodiesel and TiO2 nanoparticles additive. *Alexandria Engineering Journal, 72*, 387-398.

Sateesh, K., Yaliwal, V., Soudagar, M. E. M., Banapurmath, N., Fayaz, H., Safaei, M. R., . . . EL-Seesy, A. I. (2022). Utilization of biodiesel/Al2O3 nanoparticles for combustion behavior enhancement of a diesel engine operated on dual fuel mode. *Journal of Thermal Analysis and Calorimetry, 147*(10), 5897-5911.

Singh, B. R., & Singh, O. (2012). Global trends of fossil fuel reserves and climate change in the 21st century. *Fossil fuel and the environment, 8*, 167-192.

Singh, K., Maurya, K. K., & Malviya, M. (2024). Review of electrochemical sensors and biosensors based on first-row transition metals, their oxides, and noble metals nanoparticles. *Journal of Analysis and Testing, 8*(2), 143-159.

Soudagar, M. E. M., Wei, H.-R., Afzal, A., Sundara, V., Fouad, Y., Almehmadi, F. A., . . . Bisht, Y. S. (2025). A Biofuel-Powered Study with Deep Learning Neural Networks and Dragonfly Algorithm: Optimizing CRDi Engine Performance with ZnO Nanoparticles and Cotton Seed Methyl Ester. *Energy*, 137031.

Srinivasarao, M., Srinivasarao, C., Kumari, A. S., Rao, B. J., Gandhi, P., PraveenKumar, S., . . . Elboughdiri, N. (2025). Combustion enhancement and emission reduction in an IC engine by adopting ZnO nanoparticles with calophyllum biodiesel/diesel/propanol blend: a case study of general regression neural network (GRNN) modelling. *Industrial Crops and Products, 227*, 120812.

Şener, R., Uslu, S., & Savaş, A. (2025). The role of magnetic maghemite (Fe2O3) nanoparticles for the improvement of 2nd generation biodiesel/diesel Blends: RSM based multi-objective optimization. *Renewable Energy*, 123211.

Simsek, M., Nteziyaremye, O., & Durak, E. (2016). Additive effects on wear and friction performance of micro-arc oxidative coated journal bearings. Journal of the Balkan Tribological Association, 22(1).

Ungula, J. (2015). *Growth and characterization of ZnO nanoparticles by sol-gel process.* University of the Free State (Qwaqwa Campus).

Uslu, S., & Celik, M. (2023). Response surface methodology-based optimization of the amount of cerium dioxide (CeO2) to increase the performance and reduce emissions of a diesel engine fueled by cerium dioxide/diesel blends. *Energy, 266*, 126403.

Valihesari, M., Pirouzfar, V., Ommi, F., & Zamankhan, F. (2019). Investigating the effect of Fe2O3 and TiO2 nanoparticle and engine variables on the gasoline engine performance through statistical analysis. *Fuel, 254*, 115618.

Vignesh, T., & Sekar, S. (2025). Experimental investigation of n-butanol diesel with titanium dioxide nanoparticles impact on performance, emissions and combustion behaviour in RCCI engines. *Combustion Theory and Modelling, 29*(2), 222-245.

Vishnuram, P., Alagarsamy, S., Bajaj, M., Alqahtani, M., Ahmed, I., & Khalid, M. (2025). A critical review on alternative fuels for road transportation: Pollution mitigation, environment and economic perspective. *Energy Strategy Reviews, 61*, 101894.

Wang, X., Ge, Y., Yu, L., & Feng, X. (2013). Comparison of combustion characteristics and brake thermal efficiency of a heavy-duty diesel engine fueled with diesel and biodiesel at high altitude. *Fuel, 107*, 852-858.

Wang, X., Zhang, J., Wang, G., Han, J., Dai, M., & Sun, Z. (2020). A comprehensive review on the properties of nanofluid fuel and its additive effects to compression ignition engines. *Applied Surface Science, 504*, 144581.

Yakut, Ş. M., & Bilgiç Tüzemen, G. (2024). Effects of green synthesized copper oxide nanoparticle additive on diesel engine performance and emission characteristics. *Energy Sources, Part A: Recovery, Utilization, and Environmental Effects, 46*(1), 5151-5167.

Yaşar, E. (2020). Sürü Robotların Hareket Planlamada Kullanılması. *Avrupa Bilim ve Teknoloji Dergisi*(20), 24-29.

Yaşar, E., & Şimşek, M. (2020). Resim İşleme İle Sprey Kalitesinin Belirlenmesi. *Gaziosmanpaşa Bilimsel Araştırma Dergisi, 9*(3), 60-74.

Chapter 2

BIOCHAR FOR SUSTAINABLE ENERGY STORAGE APPLICATIONS AND TURKIYE'S BIOCHAR POTENTIAL FROM WASTE

Serhat BİLGİN[1]

1 Corresponding author.

Address: Faculty of Engineering and Architecture, Tokat Gaziosmanpaşa University, Tokat, 60250, Türkiye.

E-mail address: serhat.bilgin@gop.edu.tr (Assistant Prof. Serhat Bilgin).

Orcid: https://orcid.org/0000-0002-6812-6641

Tel: +90 356 252 16 16, Fax: +90 356 252 17 29.

1. Introduction

The rapidly increasing global population, advancing technologies, and industrialization are causing a continuous rise in energy demand worldwide. Currently, a large portion of energy is derived from fossil fuels, whose reserves are rapidly depleting and which lead to serious environmental problems such as global warming and climate change. In this context, the development of low-carbon, clean, and renewable energy systems has become a vital necessity both for ensuring energy supply security and for reducing environmental degradation. For the sustainability of energy systems, focusing solely on renewable energy production is not sufficient; the efficient and long-term storage of the produced energy also holds critical importance (Shkatulov, Houben, Fischer, & Huinink, 2020; Shrivastava, Gill, Juyal, Lal, & Jain, 2025). The increase in global energy demand, climate change, and environmental pollution concerns are increasing the need for sustainable energy sources and efficient energy storage systems day by day (Kalla, Mayilswamy, Kandasubramanian, & Mahajan-Tatpate, 2024; Liu, Jiang, & Yu, 2019). Reducing dependence on fossil fuels and decreasing carbon emissions are among the priority objectives of the energy sector. In this pursuit, biochar, a carbon-rich material obtained from lignocellulosic biomass, emerges as a prominent candidate due to its potential applications in various sectors (adsorption, catalysis, and gas storage), including energy storage (Konwar, Boro, & Deka, 2014).

From a mechanical engineering perspective, the use of biochar in energy storage devices requires interdisciplinary approaches such as materials science, thermodynamics, electrochemistry, and system integration (Das, Pektezel, & Sımsek, 2025). This book chapter will examine in detail the production techniques of biochar, its physicochemical properties, its role in sustainable energy storage applications, and particularly the biochar production potential from Turkey's abundant biomass wastes. Furthermore, the challenges faced by biochar-based energy storage systems and future perspectives will also be addressed. This study aims to shed light on new research and development areas for a sustainable energy future by highlighting the potential of biochar in energy storage technologies.

2. Biochar: Structure, Properties, and Production Methods

Biochar is a carbon-rich, solid material obtained through the thermal decomposition (pyrolysis) of biomass in an oxygen-free or limited-oxygen environment (Ahmed et al., 2024; Simon, Harikumar, & Sreeja, 2025). This process enables the conversion of a wide range of organic materials, from wood to food waste, into a valuable resource for energy storage and various environmental applications. The unique physical and chemical

properties of biochar make it a promising candidate for sustainable technologies.

2.1. Biochar Feedstocks

The final properties of biochar are largely dependent on the type and composition of the feedstock used. Feedstocks can generally be classified as follows:

- **Woody Biomass:** Lignocellulosic materials such as forest residues, tree bark, sawdust, and pruning waste are widely used for high-quality biochar production due to their high carbon content and low ash ratio (Ahmed et al., 2024).
- **Agricultural Biomass:** Post-harvest residues such as corn stover, wheat straw, rice husks, hazelnut shells, and olive pits represent abundant and renewable feedstock sources. This category of biomass typically exhibits elevated ash and potassium content (Ahmed et al., 2024; Simon et al., 2025).
- **Urban Biomass:** The organic fraction of municipal solid waste, encompassing food waste, park and garden trimmings, and sewage sludge, offers a dual benefit by addressing waste management challenges while serving as a valuable biochar precursor (Ahmed et al., 2024).
- **Industrial Biomass:** Organic waste streams originating from food processing, paper manufacturing, and furniture industries are viable for biochar production. The inherent homogeneity of these waste materials can facilitate the standardization of the production process (Ahmed et al., 2024).
- **Specialized Biomass Sources:** Other organic materials, including animal manure and algae, also present significant potential for biochar generation. Algae, in particular, are noteworthy due to their rapid growth rates and minimal requirement for agricultural land (Simon et al., 2025).

2.2. Fundamental Charecteristics of Biochar

Biochar is characterized by a suite of distinctive properties, including a high carbon content, expansive surface area, substantial cation exchange capacity (CEC), and a robust structural integrity. These attributes are predominantly governed by the nature of the feedstock material and the specific processing parameters employed during its production. Consequently, the efficacy of biochar in energy storage applications is intrinsi-

cally linked to its optimized physical and chemical characteristics.

Physical Properties:

- **Surface Area and Porosity:** Biochar typically exhibits a hierarchical porous structure, comprising micropores, mesopores, and macropores. A high specific surface area (as determined by BET analysis) significantly enhances the interfacial contact between the electrode and electrolyte, thereby facilitating the efficient transfer of ions and electrons. This characteristic directly influences both the capacitance and the charge/discharge rates of energy storage devices (Kalla et al., 2024; Simon et al., 2025).
- **Density and Structure:** Its inherently low density coupled with a robust structural framework enables the development of lightweight energy storage devices. The carbonaceous matrix of biochar is commonly a composite of amorphous and graphitic domains, with the latter being crucial for augmenting electrical conductivity (Ahmed et al., 2024).
- **Electrical Conductivity:** The electrical conductivity of biochar is directly correlated with its degree of graphitization. Elevating the pyrolysis temperature to approximately 1000 °C is instrumental in producing highly graphitized biochar, which possesses superior electrical conductivity.

Table 1. Role of Biochar's Key Properties in Energy Storage

Property	**Definition**	**Significance for Energy Storage**
High Surface Area	Total surface area per unit mass.	Expands the electrode-electrolyte interface, thereby increasing ion storage capacity.
Porous Structure	Presence of pores of varying sizes.	Facilitates rapid diffusion of electrolyte ions, enhancing power density.
Electrical Conductivity	Ability of the material to conduct electric current.	Enables swift electron transfer and reduces internal resistance.
Surface Chemistry	Type and density of functional groups on the surface.	Improves wettability and provides additional storage through pseudocapacitance.

Chemical Properties:

- **Carbon Content and pH:** A high carbon content (typically 70-90%) forms the fundamental conductive backbone of the material. Biochar generally exhibits an alkaline pH, which can be advantageous for certain electrochemical reactions (Ahmed et al., 2024).
- **Chemical Composition and the Effect of Pyrolysis Temperature:** The elemental composition of biochar is not limited to C, H, and O; it can also incorporate heteroatoms such as S, N, and P, depending on the feedstock. Elevated pyrolysis temperatures lead to a reduction in oxygen (O) content and lower O/C and H/C molar ratios due to the decrease in carboxyl groups. This process enhances carbonization, thereby increasing the environmental stability of biochar. Biochar produced at higher temperatures typically possesses a more refractory (decomposition-resistant) structure.
- **Surface Functional Groups:** Oxygen-containing functional groups, such as carboxyl (-COOH), hydroxyl (-OH), and phenolic groups, present on the biochar surface, enhance the material's wettability and contribute additional energy storage capacity through pseudocapacitance mechanisms (Liu et al., 2019).
- **Inorganic Components (Ash):** Inorganic minerals (ash) originating from the feedstock and formed during production can influence biochar's conductivity and catalytic activity. In some instances, these minerals may function as active sites in lithium/sodium-ion batteries (Simon et al., 2025).

2.3. Production Technologies

Biochar is synthesized through the thermal decomposition (thermochemical conversion) of biomass in an oxygen-free or partially oxygenated environment. A diverse array of thermochemical conversion technologies exists for biochar production. The primary thermochemical methods include pyrolysis, gasification, and hydrothermal carbonization. Each technology influences the yield and characteristics of products such as biochar, bio-oil, and syngas under distinct operating conditions.

2.3.1. Pyrolysis

Pyrolysis stands as the most prevalent method for biochar production, involving the thermal degradation of biomass in an oxygen-deficient (inert gas) atmosphere within a temperature range of 350-1000°C. Product yields are modulated by parameters such as temperature, heating rate, and residence time. Three principal types of pyrolysis are recognized:

- **Slow Pyrolysis:** Characterized by low heating rates and extended reaction durations, slow pyrolysis primarily aims to maximize solid biochar yield (35-50%). Temperatures typically range from 300–900°C, employing very low heating rates (5-10 °C/min) and prolonged residence times (exceeding 1 hour or even days).
- **Fast Pyrolysis:** Designed to maximize liquid bio-oil production (up to 75%) through high heating rates and short reaction times. This process necessitates very high heating rates (>200 °C/min) and extremely brief reaction durations. While fast pyrolysis reduces biochar yield, the resulting biochar byproduct possesses high carbon content and stability.
- **Flash Pyrolysis:** Utilizes exceptionally high heating rates and ultra-short reaction times to optimize the yields of bio-oil and gaseous products (Kalla et al., 2024).

2.3.2. Gasification

Gasification involves the conversion of biomass into syngas at high temperatures, typically above 700°C, in the presence of a controlled amount of a gasifying agent such as oxygen, air, or steam. The primary output is syngas, which is rich in hydrogen and carbon monoxide. Biochar (char) is generated as a significant byproduct, albeit with lower yields, during this process. Biochar derived from gasification, produced at elevated temperatures (e.g., above 750 °C), exhibits a denser structure. Gasification with feedstock mixtures containing high ash content can lead to pore blockage, consequently reducing the surface area.

2.3.3. Hydrothermal Carbonization (HTC)

HTC is a thermochemical conversion process of biomass conducted in the presence of water, under moderate-to-high pressure, and at relatively low temperatures (180–250°C). This method is particularly well-suited for biomass with high moisture content (e.g., aquatic plants, algae, sewage sludge), as it obviates the need for pre-drying. The solid product obtained from HTC is termed hydrochar. Hydrochar generally possesses a greater abundance of surface functional groups (hydroxyl and carbonyl) and higher microporosity compared to pyrolysis biochar.

2.3.4. Torrefaction

Torrefaction is a mild pyrolysis pre-treatment performed at lower temperatures, typically within the 200-300°C range. This process effectively removes moisture from the biomass, enhances its energy density, and renders it more brittle and hydrophobic. The objective is to reduce the oxy-

gen and hydrogen content of the biomass, thereby increasing its carbon ratio and energy content. Torrefaction leads to the complete degradation of hemicellulose. The primary product is torrefied biomass, which is predominantly utilized as fuel rather than for energy storage applications (Ahmed et al., 2024).

2.3.5. Advanced Production Methods

- **Microwave-Assisted Carbonization:** This critical technology facilitates the conversion of biomass by enabling faster and more homogeneous heating through microwave energy, as opposed to conventional external heating. Microwave heating promotes internal-to-external heating, offering advantages such as high heating rates, uniform heating, and superior energy conversion efficiency. This method holds the potential to produce biochar with a higher surface area while consuming less energy (Shrivastava et al., 2025). The implementation of automated control systems and intelligent obstacle avoidance algorithms in robotic material handling systems (Yıldırım & Yaşar, 2015) can further optimize the microwave-assisted carbonization process by ensuring consistent feedstock positioning and minimizing operational interruptions.

- **Laser and Plasma-Assisted Carbonization:** High-energy laser-assisted methods can induce the formation of unique carbon structures (e.g., graphene-like layers) by providing extremely rapid heating rates, though they incur high energy costs (Peng et al., 2024). Plasma-assisted pyrolysis involves the conversion of biomass within a reactive plasma region, rich in electrons and ions generated by high-energy radiation. Plasma energy rapidly heats the feedstock, transforming it into hydrogen and light hydrocarbons. This technique can also serve as an activation/modification method to enhance biochar's surface properties and improve its performance in energy storage applications.

- **Catalytic Pyrolysis:** The incorporation of catalysts into the pyrolysis process can alter reaction pathways, allowing for the tailored development of biochar's pore structure, surface area, and functional groups to meet specific requirements (Ramos, Abdelkader-Fernández, Matos, Peixoto, & Fernandes, 2022).

Table 2. Effect of Pyrolysis Process Characteristics on Biochar

Production Method	**Temperature (°C)**	**Heating Rate**	**Main Product**	**Biochar Yield**
Slow Pyrolysis	350 - 650	Low	Biochar	High
Fast Pyrolysis	600 - 650	High	Bio-oil	Low
Gasification	> 700	High	Syngas	Very Low
Hydrothermal Carbonization HTC	180 - 250	Low	Hydrochar	Medium-High
Torrefaction	200 - 300	Low	Torrefied Biomass	Very High

Catalytic pyrolysis is a thermochemical conversion method that employs catalysts to enhance the yield and quality of specific products, such as fuels or high-value chemicals, during the pyrolysis process. These catalysts can also play a crucial role in the decomposition of tar compounds (tar cracking) formed during gasification. Furthermore, biochar itself can serve as a support material for catalytic reactions, such as the selective phenol hydrogenation of agricultural wastes (e.g., straw seed). To improve its catalytic performance, biochar can be transformed into engineered biochar through chemical or physical modifications, including doping with heteroatoms (N, S, P, B) or impregnation with metal/metal oxides (Fe, Co, Ni, Mn, Cu).

3. Sustainable Energy Applications

The intermittent and variable nature of renewable energy sources (e.g., solar, wind) necessitates the efficient storage of generated energy. Energy storage systems enhance grid stability by balancing energy supply and demand, thereby facilitating the broader integration of renewable energy. Sustainable energy storage technologies aim to minimize environmental impacts, ensure longevity, and maintain economic competitiveness. These technologies encompass electrochemical, thermal, mechanical, and chemical storage methods.

Biochar is emerging as a promising material, particularly within electrochemical energy storage systems (EES). EES devices are capable of directly converting chemical energy into electrical energy and storing it reversibly. The primary types of EES include:

- **Supercapacitors (Electrochemical Double-Layer Capacitors - EDLCs):** These devices offer high power density, rapid charge/discharge capabilities, and extended cycle life. They store energy through the physical accumulation of ions at the electrode-electrolyte interface, forming an electrochemical double layer (Kalla et al., 2024).

- **Batteries:** Characterized by high energy density, batteries store energy via chemical reactions (redox reactions) occurring at their electrodes. This category includes lithium-ion, sodium-ion, and metal-air batteries (Kalla et al., 2024; Liu et al., 2019).

- **Fuel Cells:** These systems continuously convert chemical energy (typically from a fuel like hydrogen) into electrical energy through electrochemical reactions, offering both storage and conversion functionalities (Liu et al., 2019).

Biochar's role in these systems typically involves its use as an active electrode material, a conductive additive, or a structural support. Its derivation from sustainable sources, low cost, and tunable properties render it an attractive alternative to fossil fuel-based carbon materials (e.g., activated carbon, carbon black) (Liu et al., 2019).

4. The Role of Biochar in Energy Storage Systems

As a sustainable and environmentally friendly material, biochar assumes diverse roles within energy storage systems. Its high surface area, tunable porous structure, favorable electrical conductivity, and chemical stability enable its application across a broad spectrum, ranging from supercapacitors to battery technologies, fuel cells, and gas storage systems (Kalla et al., 2024; Liu et al., 2019). With an increasing focus on sustainable and renewable energy sources, biochar-based materials have emerged as promising candidates for various energy-related applications (Chandrasekaran, Jadhav, Selvam, Krishnamoorthy, & Balasubramanian, 2024).

4.1. Supercapacitor Applications

Supercapacitors, also known as electrochemical double-layer capacitors (EDLCs), are energy storage devices characterized by high power density, rapid charge/discharge cycles, and extended cycle life. Biochar demonstrates significant potential as an active electrode material for these applications. The high surface area and optimized porous structure of biochar facilitate the swift adsorption and desorption of electrolyte ions onto the electrode surface, thereby enabling the achievement of high capacitance values (Kalla et al., 2024; Liu et al., 2019).

Research indicates that biochar derived from various biomass sources can exhibit electrochemical performance comparable to or even superior to that of activated carbon. For instance, biochars obtained from diverse biomass feedstocks have been successfully employed in supercapacitors, yielding capacitance values up to 1600 F/g and surface areas up to 340 m^2/g (Kalla et al., 2024). Further enhancements in supercapacitor performance can be achieved through heteroatom doping (e.g., with nitrogen or sulfur) and surface modifications, which improve biochar's wettability and conductivity (Liu et al., 2019).

4.2. Battery Technologies

Biochar-based materials are being investigated as both anode and cathode materials in various battery technologies. Its low cost, abundant availability, and inherent sustainability position it as an attractive alternative to conventional battery materials.

- **Sodium-Ion Batteries (SIBs):** Given the finite nature of lithium resources, sodium-ion batteries are considered a promising alternative. Biochar can provide a suitable carbon matrix for the storage of sodium ions. Optimized pore size distribution and surface functional groups support rapid sodium ion diffusion and stable cycling performance (Yu et al., 2023).
- **Lithium-Ion Batteries (LIBs):** Biochar can be utilized as an anode material in lithium-ion batteries. Specifically, biochars pyrolyzed at high temperatures can acquire graphite-like structural characteristics, making them suitable for lithium ion intercalation. The porous architecture of biochar can also contribute to extended cycle life by accommodating volume changes during cycling (Kalinke et al., 2021; Kalla et al., 2024).
- **Lithium-Sulfur Batteries (LSBs):** LSBs possess high theoretical energy density but face challenges such as the low conductivity of sulfur and the dissolution of polysulfides. Biochar can help overcome these issues by acting as a conductive matrix for sulfur and a scaffold capable of adsorbing polysulfides (Khandaker et al., 2025; Wang et al., 2023).
- **Solid-State Battery Applications:** Solid-state electrolytes offer safer and more stable batteries compared to their liquid counterparts. Biochar-based carbon materials can be employed as additives to enhance the conductivity of solid-state electrolytes or to stabilize the electrode/electrolyte interface (Raj, Perumal, Padhy, Rao, & Mohapatra, 2024).

4.3. Fuel Cell Applicaitons

Owing to its abundance and tunable surface chemistry, biochar is utilized as a catalyst or support material in fuel cells for electrochemical processes such as the oxygen reduction reaction (ORR) and hydrogen evolution reaction (HER), serving as a sustainable alternative to expensive commercial catalysts.

- **Microbial Fuel Cell (MFC) Electrode Development:** In MFCs, biochar can function as a bio-anode material, supporting microbial growth and facilitating electron transfer. The porous structure of biochar provides a large surface area for microorganisms and promotes biofilm formation (Logan, 2009).
- **Polymer Electrolyte Membrane Fuel Cell (PEMFC) Supports:** Platinum-based catalysts in PEMFCs are typically supported on carbon materials. Biochar can serve as a suitable support material for platinum nanoparticles. Its high surface area and corrosion resistance can enhance catalyst activity and longevity (Antolini, 2009).
- **Direct Carbon Fuel Cell (DCFC) Feedstock Applications:** DCFCs directly convert solid carbon fuels into electricity. Biochar can be used as a fuel in these cells, providing efficient energy conversion due to its high carbon content (Giddey, Badwal, Kulkarni, & Munnings, 2012).
- **Biochar-Based Electrocatalyst Synthesis:** Biochar can be employed as a precursor material in the synthesis of metal-free or metal-doped electrocatalysts for critical electrochemical reactions such as the oxygen reduction reaction (ORR) and oxygen evolution reaction (OER). Doping with heteroatoms like nitrogen and sulfur significantly enhances catalytic activity (Zhang & Dai, 2015).

4.4. Hyrogen and Gas Storage Systems

The high porosity and surface area of biochar render it a potential adsorbent for the storage of hydrogen (H_2) and other gases (e.g., CO_2). Particularly under high pressure and low temperatures, the micropores of biochar can effectively trap gas molecules. Surface modifications and the formation of composites with metal-organic frameworks (MOFs) can further augment storage capacity (J.-R. Li, Kuppler, & Zhou, 2009).

4.5. Thermal Energy Storage

Biochar can be utilized as a support matrix for phase change materials (PCMs) in thermal energy storage systems. PCMs are capable of storing or releasing substantial amounts of thermal energy during melting and freezing. Thermal energy storage systems are often supported by renewable energy sources such as solar energy concentrating systems (Mehmet, PEKTEZEL, SIMSEK, & AKPINAR, 2025). Biochar's high thermal conductivity and stable structure can enhance the thermal cycling stability and heat transfer rate of PCMs (Sharma, Tyagi, Chen, & Buddhi, 2009).

4.6. Advanced Energy Storage Systems

Beyond conventional systems, biochar is also actively being investigated in next-generation energy storage technologies.

4.6.1. Metal – Air Batteries

Metal-air batteries (e.g., zinc-air, lithium-air) have garnered significant interest due to their high theoretical energy densities. Biochar can serve as a catalyst support material for the air electrode in these batteries. Its porous structure and active surface areas can catalyze oxygen reduction and oxygen evolution reactions, thereby improving battery performance (Y. Li & Lu, 2017).

4.6.2. Redox Flow Batteries

Redox flow batteries are promising systems for large-scale energy storage. Biochar-based carbon felts or electrode materials can provide the active surface area where redox reactions occur in these batteries. Surface modification of biochar can enhance electrode kinetics and overall battery efficiency (Weber et al., 2011).

4.6.3. Hybrid Photo-Electrochemical Systems

Hydrid photo-electrochemical systems can convert solar energy into electrical energy while simultaneously storing it. Biochar can be employed as a conductive and catalytic component for photoelectrodes or counter electrodes in these systems. The tunable optical and electronic properties of biochar hold the potential to enhance the efficiency of these systems (Walter et al., 2010).

5. Turkey's Waste Status and Current Potential

Turkey possesses a significant biomass waste potential owing to its rich biodiversity and extensive agricultural lands. These waste materials, through appropriate management and conversion processes, constitute a

valuable resource for biochar production. The conversion of waste into biochar not only offers a sustainable solution to waste management challenges but also provides value-added materials for energy storage applications (Dursun, 2024).

Table 3. Turkey's Biomass Waste Resources and Biochar Production Potential

Waste Category	Total Waste Amount (ton/tear)	Energy Equivalent (TEP/year)	Biochar Potential (ton/year)
Agricultural Waste	46,990,000	19,260,200	11,747,500-16,446,500
Animal Waste	191,070,000	4,313,500	47,767,500-66,874,500
Municipal Organic Waste	32,170,975	3,373,011	8,042,744-11,259,841
Forest Waste	3,914,904 (stere)	859,899	978,726-1,370,216
TOTAL	**270,240,975**	**27,806,610**	**67,560,244-94,584,341**

5.1. Agricultural Wastes

Turkey, as a prominent nation in agricultural production, consequently generates substantial quantities of agricultural waste. These residues present a significant potential for biochar production.

Table 4. Biochar Potential from Agricultural Wastes in Turkey

Waste Category	Total Waste Amount (ton/year)	Energy Eşquivalent (TOE/year)	Biochar Potential (ton/year)
Agricultural Wastes	8,000 – 12,000	50,000 – 75,000	100,000 – 150,000
	2040	15,000,000 – 20,000,000	12,000 – 16,000

Figure 1. Waste amounts of the 12 agricultural products with the highest biochar potential in Turkey. Wheat straw (20 M ton/year) represents the largest potential by volume, while hazelnut shell (1.09 M ton/year) is the highest priority feedstock in terms of collectability and quality. Source: Republic of Turkey Ministry of Energy and Natural Resources, BEPA, 2024.

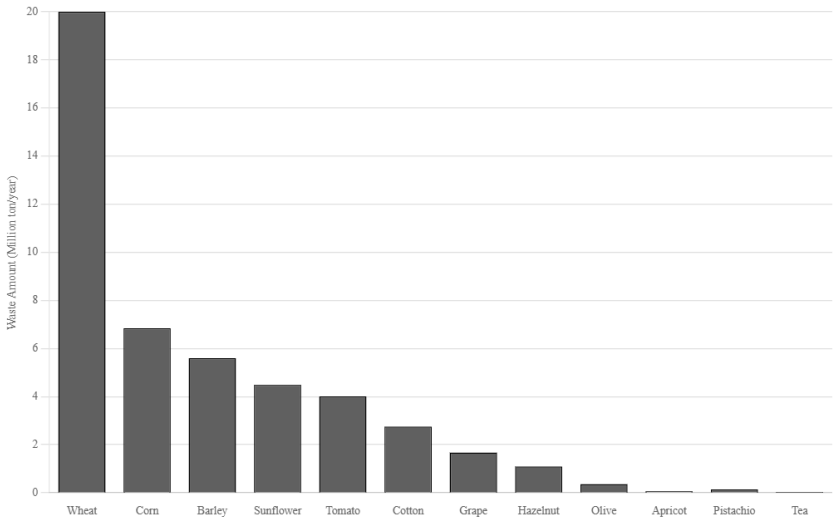

Figure 1. Agricultural Products with Highest Biochar Potential

5.1.1. Cereal Residues

Post-harvest stalks and stubble from cereals such as wheat, barley, and corn are abundantly available across Turkey's extensive agricultural lands. These residues, owing to their lignocellulosic composition, serve as suitable feedstocks for biochar production. According to the 2023 Agricultural Product Market Reports, cereal production in Turkey remains at high levels, signifying a substantial waste potential (Tarım ve Orman Bakanlığı, 2023).

5.1.2. Olive Processing Wastes

Turkey holds a significant position in global olive production. Olive pomace (pulp) and olive branches generated from olive processing facilities are ideal for biochar production due to their high organic matter content. Olive pomace, in particular, can also be utilized for energy recovery owing to its elevated oil content (Doymaz, 2011).

5.1.3. Hazelnut Processing Wastes

As Turkey accounts for a major portion of the world's hazelnut production, hazelnut shells constitute a significant agricultural waste stream. Hazelnut shells are highly suitable for producing high-quality biochar due to their high carbon content and rigid structure (TOPCU & DEMİRKESEN).

5.1.4. Tea Industry Wastes

Tea production, concentrated in the Black Sea Region, generates considerable amounts of tea stalks and leaf waste. These wastes can be valorized through biochar production, contributing to the regional economy (Müftüoğlu, Türkmen, & Kavdır, 2019).

5.1.5. Cotton Stalks

Cotton, extensively cultivated in the southern and southeastern regions of Turkey, leaves behind large quantities of stalk waste after harvest. Cotton stalks are viable for biochar production owing to their lignocellulosic nature (Bilek, Melikoğlu, & Cesur, 2019).

5.1.6. Garden and Vegetables Wastes

Widespread garden and vegetable farming across Turkey generates various wastes, including pruning residues, post-harvest plant remains, and spoiled vegetables. These wastes can be utilized for local-scale biochar production (Dursun, 2024; Erdem, İnce, Akyol, Özbayram, & İnce, 2015). A study by (Dursun, 2024) estimated the biochar potential from pruning wastes of fruit-bearing trees in Turkey to be 175 thousand tons for 2021. Apple trees were identified as having the highest biochar potential (41.5 thousand tons/year) (Dursun, 2024).

5.2. Forest and Wood Wastes

Turkey's extensive forested areas and robust timber industry provide a substantial feedstock source for biochar production.

5.2.1. Forest and Pruning Wastes

Branches, leaves, and other woody materials resulting from forest management, logging operations, and fire prevention efforts constitute forest wastes. These wastes can be utilized for biochar production while simultaneously mitigating the risk of forest fires (Ünlü, 2025).

5.2.2. Furniture and Timber Industry Wastes

Sawdust, wood chips, and cutting residues generated from furniture and timber production are ideal industrial wastes for biochar production due to their high carbon content and homogeneous composition (Şenkal, 2023).

5.3. Urban Solid Wastes and Organic Wastes

Organic wastes, which form a significant portion of the increasing urban solid waste stream due to urbanization, can be valorized through biochar technology.

5.3.1. Sewage Sludge

Sewage sludge from wastewater treatment plants contains substantial amounts of organic matter. Biochar produced from the pyrolysis of this sludge can both reduce sludge volume and immobilize heavy metals, thereby lowering environmental risks (Kabakcı & Koca, 2019).

5.3.2. Park, Garden and Landscape Wastes

Park, garden, and landscape wastes (e.g., grass clippings, pruned branches) collected by municipalities represent a sustainable urban biomass source for biochar production (Bilici & Karaer, 2024). Furthermore, the total biochar potential from pruning wastes of fruit-bearing trees in Turkey is estimated at 175 thousand tons for 2021 (Dursun, 2024).

- Apple trees: 41,5 thousand tons/year (highest potential)
- Apricot trees: 25,3 thousand tons/year
- Cherry trees: 32,1 thousand tons/year
- Peach trees: 27,2 thousand tons/year
- Plum trees: 66,0 thousand tons/yearıl
- Sour cherry trees: 30,4 thousand tons/year

5.3.3. Food Wastes

Household and commercial food wastes pose a significant waste management challenge in Turkey. Converting these wastes into biochar can help reduce methane emissions and contribute to a circular economy (Solak & Pekküçükşen, 2018).

5.4. Industrial Wastes

Organic wastes originating from various industrial processes can be utilized for biochar production.

5.4.1. Fruit Juice Factory Wastes

Pomace and peels remaining from fruit juice production are suitable feedstocks for biochar production due to their high organic matter con-

tent (Şener & Ünal, 2008).

5.4.2. Food Industry Wastes

Wastes from the general food industry (e.g., canning, baked goods) can be valorized through biochar production, thereby reducing waste management costs and yielding new products (Demirbaş, 2001).

5.4.3. Fish Factory Wastes

Wastes from fish processing facilities (e.g., bones, skin, offal) can be used to produce biochar rich in minerals such as phosphorus and calcium. This biochar can also be beneficial as an agricultural (Arvanitoyannis & Kassaveti, 2008).

5.4.4. Meat Industry Wastes

Wastes generated from meat processing facilities (e.g., bones, blood, fat) offer potential for producing specialized biochar types due to their high protein and mineral content (Jayathilakan, Sultana, Radhakrishna, & Bawa, 2012).

5.5. Animal Wastes

Turkey's developed livestock sector generates substantial amounts of animal manure waste. These wastes represent a valuable resource for biochar production. Animal wastes constitute the largest category of waste generated in Turkey.

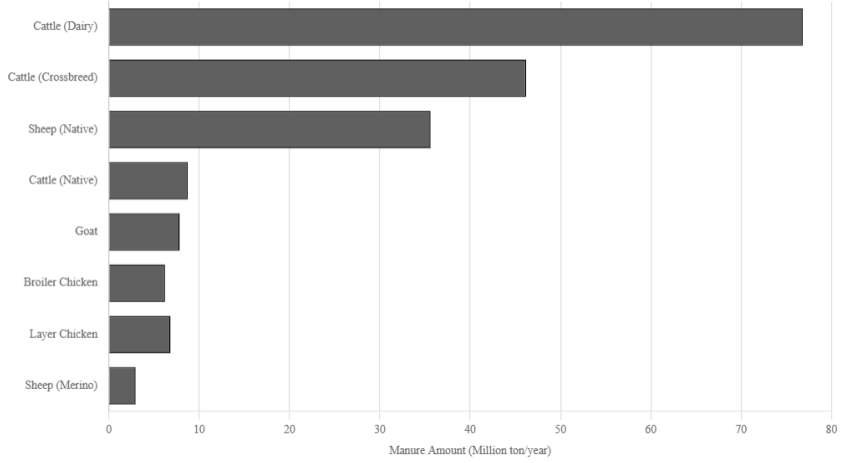

Figure 2. Biochar Potential from Animal Waste

Figure 2. Manure-based biochar potential of main livestock types in Turkey. Dairy cattle (76.8 M ton/year manure) represents the highest potential, while poultry (12.99 M ton/year) is particularly important for electrocatalyst applications due to high N-P content. Source: Republic of Turkey Ministry of Energy and Natural Resources, BEPA, 2024.

5.5.1. Poultry Manure

Poultry manure, characterized by its high nitrogen and phosphorus content, serves as a suitable feedstock for biochar production. The resulting biochar can also be effectively utilized as a soil amendment (Cantrell, Hunt, Uchimiya, Novak, & Ro, 2012).

5.5.2. Cattle and Small Ruminant Manure

Manure from cattle and small ruminants constitutes widely available biomass waste across Turkey. Converting these manures into biochar can contribute to reducing greenhouse gas emissions and recycling valuable nutrients (Dede,Dede, Dede, & Özdemir, 2018).

Turkey's rich waste potential presents a significant opportunity to support biochar production and, consequently, sustainable energy storage applications. The establishment of biochar production facilities optimized according to waste type and regional distribution will yield both environmental and economic benefits. If Turkey's total annual waste were directed towards biochar production, the estimated total biochar potential would be approximately 10.8 million tons (Kutlu & Kocar, 2017).

6. Biochar –Based Energy Storage Applications

Biochar's high carbon content, tunable porous structure, and natural abundance position it as a crucial raw material for sustainable energy storage solutions, particularly when compared to conventional fossil-based materials (Lonappan, Liu, Rouissi, Brar, & Surampalli, 2020). Turkey's substantial waste potential, in this context, offers significant opportunities.

6.1. Global Biochar Applications

Globally, biochar is extensively researched, especially in electrochemical energy storage systems such as supercapacitors and batteries. Studies indicate that biochar produced from diverse biomass sources (e.g., bamboo, rice husks, wood waste) exhibits promising electrochemical performance due to its high surface area and optimized porous structure (Kalla et al., 2024; Liu et al., 2019). For instance, some research has reported that biochar-based electrodes can achieve capacitance and energy density

values comparable to, or even exceeding, those of commercial activated carbon electrodes (Khandaker et al., 2025).

Furthermore, the utilization of biochar as an anode or cathode material in lithium-ion, sodium-ion, and zinc-air batteries is becoming increasingly prevalent. Biochar's function as a conductive carbon matrix and its provision of active sites for ion storage enhance the performance of these batteries (Kalla et al., 2024; Liu et al., 2019). Additionally, innovative applications include the use of biochar as a support matrix for phase change materials in thermal energy storage systems and as a catalyst support in fuel cells (Kalla et al., 2024; Liu et al., 2019).

6.2. Turkey's Potential

Turkey possesses a rich potential in agricultural waste, forest waste, urban organic waste, and industrial biomass. The valorization of this potential for biochar production and its subsequent application in energy storage technologies holds immense environmental and economic significance.

- **Domestic and Sustainable Electrode Production:** Turkey's abundant waste resources enable the production of domestic and sustainable electrode materials for energy storage devices. This can reduce external dependency and contribute to national energy security.
- **Waste Management and Circular Economy:** Converting waste into biochar alleviates the burden on landfills, reduces greenhouse gas emissions, and offers a waste management model consistent with circular economy principles.
- **Regional Development:** The establishment of biochar production facilities, particularly in regions with intensive agriculture and forestry, can create local employment and foster regional development.
- **R&D and Innovation:** urkish universities and research institutions can conduct R&D activities focused on producing biochar with optimized properties from different waste types and enhancing its performance in energy storage systems. This will contribute to Turkey's technological advancement and competitiveness in this field internationally.

A study by (Dursun, 2024) highlights the substantial biochar potential derivable solely from pruning wastes. Fully evaluating this potential, including other waste types, will play a crucial role in Turkey's achievement

of its sustainable energy goals.

Despite Turkey's high renewable energy potential, the capacity utilization rate for biomass energy remains low at 0.68% (Akusta & Cergibozan, 2020). This indicates an inadequacy in facilities and technologies required for converting biomass resources into energy (Akusta & Cergibozan, 2020). In this context, channeling idle biomass potential into biochar production will both mitigate waste management issues and provide domestic input for the energy storage sector (Gün & Balbay, 2025).

7. Future Outlook

The future of biochar in sustainable energy storage will be shaped by innovative research in materials science, engineering, and economics. Key areas expected to be the focus of future research include:

- **Customized Biochar Production:** The production of biochars with optimized porous structures, surface areas, and chemical properties from diverse biomass sources for specific energy storage applications (e.g., supercapacitors requiring high power or batteries demanding high energy density) is critically important. Precise control over production parameters (temperature, heating rate, catalyst usage) will be pivotal in achieving this objective.
- **Advanced Composite Materials:** Combining biochar with other functional materials such as graphene, carbon nanotubes, metal oxides, or conductive polymers to develop hybrid composite electrodes holds the potential to simultaneously increase energy and power density. These composites can offer superior performance by leveraging the synergistic effects of each component.
- **3D Printing and Flexible Devices:** The development of biochar-based inks could enable the fabrication of complex and customized electrode structures using 3D printing technology. Furthermore, integrating biochar into flexible polymer matrices will pave the way for the development of flexible supercapacitors and batteries for wearable electronic devices.
- **Life Cycle Analysis (LCA) and Economic Evaluation:** Comprehensive life cycle analyses (LCA) and techno-economic assessments are necessary to fully understand the environmental impacts and economic feasibility of biochar-based energy storage systems. These analyses will provide roadmaps for the commercialization of the technology.
- **Integration and System Optimization:** The integration of bio-

char-based energy storage units with renewable energy systems (solar panels, wind turbines) and the optimization of these integrated systems using mechanical engineering principles (e.g., thermal management, power electronics) will enhance efficiency and reliability. Advanced motion planning and path optimization algorithms, such as swarm robotics approaches (Yaşar, 2020), can be integrated into automated biochar production and material handling systems to improve operational efficiency and reduce energy consumption.

8. Conclusion and Recommendations

This book chapter has elucidated the multifaceted role and potential of biochar as a sustainable resource in energy storage applications. Biochar is an environmentally friendly, low-cost, and tunable carbon material that can be produced from abundant and diverse biomass wastes. It offers promising results across a wide range of applications, including supercapacitors, batteries, fuel cells, and thermal energy storage systems.

Turkey, with its rich agricultural, forest, and urban waste potential, is strategically positioned for biochar production and its utilization in energy storage technologies. Harnessing this potential will significantly contribute to the country's sustainable energy goals, address waste management challenges, and facilitate a transition to a circular economy model.

To accelerate progress in this field, the following recommendations are put forth:

1. **Development of a National Biochar Strategy:** A comprehensive national biochar strategy should be formulated, mapping Turkey's waste potential, identifying priority regions and waste types, and promoting R&D activities and commercial production.

2. **Support for R&D and Innovation:** Projects focusing on the production of high-performance biochar from different waste types and its application in energy storage devices should be supported through collaboration among universities, research centers, and the private sector.

3. **Establishment of Pilot Facilities:** Pilot-scale biochar production and energy storage system integration facilities, based on local waste resources, should be established in various regions to demonstrate the technology's feasibility and scalability.

4. **Interdisciplinary Collaboration:** Interdisciplinary collaboration among mechanical engineers, chemical engineers, materials

scientists, and environmental scientists should be encouraged to address all processes, from the design to the production and optimization of biochar-based energy storage systems, with a holistic approach.

5. **Technology Transfer and Localization:** Internalizing biomass conversion technologies (pyrolysis, gasification) within Turkey and supporting the use of domestic components are crucial for reducing foreign dependency in the energy sector and building export capacity.

In conclusion, biochar stands as an exciting and transformative material with significant potential at the intersection of mechanical engineering and sustainable energy. Realizing this potential will be a crucial step towards a cleaner, safer, and more sustainable energy future.

References

Ahmed, S. F., Mehejabin, F., Chowdhury, A. A., Almomani, F., Khan, N. A., Badruddin, I. A., & Kamangar, S. (2024). Biochar produced from waste-based feedstocks: Mechanisms, affecting factors, economy, utilization, challenges, and prospects. GCB Bioenergy, 16(8), e13175.

Akusta, E., & Cergibozan, R. (2020). Yenilenebilir enerji ve ekonomik büyümenin çevre üzerinde etkisi: Türkiye örneği. Öneri Dergisi, 15(54), 431-462.

Antolini, E. (2009). Carbon supports for low-temperature fuel cell catalysts. Applied Catalysis B: Environmental, 88(1-2), 1-24.

Arvanitoyannis, I. S., & Kassaveti, A. (2008). Fish industry waste: treatments, environmental impacts, current and potential uses. International Journal of Food Science and Technology, 43(4), 726-745.

Bilek, S., Melikoğlu, A. Y., & Cesur, S. (2019). Tarımsal atıklardan selüloz nanokristallerinin eldesi, karakteristik özellikleri ve uygulama alanları. Akademik Gıda, 17(1), 140-148.

Bilici, G., & Karaer, M. (2024). Büyükşehir Belediyelerinin Atık Yönetim Sistemlerinin Tüik Verileri Açısından Değerlendirilmesi. SOCIAL MENTALITY AND RESEARCHER THINKERS JOURNAL (SMART JOURNAL), 9(78), 5458-5465.

Cantrell, K. B., Hunt, P. G., Uchimiya, M., Novak, J. M., & Ro, K. S. (2012). Impact of pyrolysis temperature and manure source on physicochemical characteristics of biochar. Bioresource technology, 107, 419-428.

Chandrasekaran, S., Jadhav, S., Selvam, S. M., Krishnamoorthy, N., & Balasubramanian, P. (2024). Biochar-based materials for sustainable energy applications: a comprehensive review. Journal of Environmental Chemical Engineering, 12(6), 114553.

Das, M., Pektezel, O., & Sımsek, M. (2025). Solar energy for greenhouse drying: Performance evaluation of parabolic trough solar collector with two-axis tracking system. Solar Energy, 299, 113716.

Dede, Ö. H., Dede, G., Dede, C., & Özdemir, S. (2018). Hayvansal atıklardan biyogaz üretimi için küçük ölçekli reaktör modeli geliştirilmesi. Karaelmas Fen ve Mühendislik Dergisi, 8(1), 138-146.

Demirbaş, A. (2001). Biomass resource facilities and biomass conversion processing for fuels and chemicals. Energy conversion and Management, 42(11), 1357-1378.

Doymaz, İ. (2011). Experimental study on drying characteristics of pomegranate peels. Food Science and Biotechnology, 20(4), 965-970.

Dursun, N. (2024). Estimation of pruning wastes and biochar production potential of Turkey. BioResources, 19(2), 2503.

Erdem, E. I., İnce, O., Akyol, Ç., Özbayram, E. G., & İnce, B. (2015). Bahçe Atıkları Kompostunun Yasal Düzenlemeler Çerçevesinde Toprak Şartlandırıcısı Olarak Kullanımının İncelenmesi. Çanakkale Onsekiz Mart Üniversitesi Fen Bilimleri Enstitüsü Dergisi, 1(1), 65-80.

Giddey, S., Badwal, S., Kulkarni, A., & Munnings, C. (2012). A comprehensive review of direct carbon fuel cell technology. Progress in Energy and Combustion Science, 38(3), 360-399.

Gün, B. Ş., & Balbay, Ş. (2025). TÜRKİYE'DE SANAYİ ATIKLARI VE KARAKTERİZASYON YÖNTEMLERİ. Çevre Şehir ve İklim Dergisi(7), 82-105.

Jayathilakan, K., Sultana, K., Radhakrishna, K., & Bawa, A. (2012). Utilization of byproducts and waste materials from meat, poultry and fish processing industries: a review. Journal of food science and technology, 49(3), 278-293.

Kabakcı, S. B., & Koca, D. (2019). Enerji geri kazanımı için arıtma çamurunun hidrotermal karbonizasyonu. Dicle Üniversitesi Mühendislik Fakültesi Mühendislik Dergisi, 10(3), 1061-1072.

Kalinke, C., de Oliveira, P. R., Bonacin, J. A., Janegitz, B. C., Mangrich, A. S., Marcolino-Junior, L. H., & Bergamini, M. F. (2021). State-of-the-art and perspectives in the use of biochar for electrochemical and electroanalytical applications. Green chemistry, 23(15), 5272-5301.

Kalla, A., Mayilswamy, N., Kandasubramanian, B., & Mahajan-Tatpate, P. (2024). Biochar: a sustainable and an eco-friendly material for energy storage applications. International Journal of Green Energy, 21(7), 1695-1709.

Khandaker, T., Islam, T., Nandi, A., Anik, M. A. A. M., Hossain, M. S., Hasan, M. K., & Hossain, M. S. (2025). Biomass-derived carbon materials for sustainable energy applications: a comprehensive review. Sustainable Energy & Fuels, 9(3), 693-723.

Konwar, L. J., Boro, J., & Deka, D. (2014). Review on latest developments in biodiesel production using carbon-based catalysts. Renewable and Sustainable Energy Reviews, 29, 546-564.

Kutlu, O., & Kocar, G. (2017). Biochar from residual biomass in Turkey, and possibility of return to the soil: an estimation of the supply and demand. Polish Journal of Agronomy(30), 10-24.

Li, J.-R., Kuppler, R. J., & Zhou, H.-C. (2009). Selective gas adsorption and separation in metal–organic frameworks. Chemical Society Reviews, 38(5), 1477-1504.

Li, Y., & Lu, J. (2017). Metal–air batteries: will they be the future electrochemical energy storage device of choice? ACS Energy Letters, 2(6), 1370-1377.

Liu, W.-J., Jiang, H., & Yu, H.-Q. (2019). Emerging applications of biochar-based materials for energy storage and conversion. Energy & environmental science, 12(6), 1751-1779.

Logan, B. E. (2009). Exoelectrogenic bacteria that power microbial fuel cells. Nature Reviews Microbiology, 7(5), 375-381.

Lonappan, L., Liu, Y., Rouissi, T., Brar, S. K., & Surampalli, R. Y. (2020). Development of biochar-based green functional materials using organic acids for environmental applications. Journal of Cleaner Production, 244, 118841.

Mehmet, D., PEKTEZEL, O., SIMSEK, M., & AKPINAR, E. (2025). Thermodynamic and Artificial Intelligence-Based Performance Analysis of Parabolic Vacuum Tube Solar Collector Assisted Greenhouse Drying System. Case Studies in Thermal Engineering, 107129.

Müftüoğlu, N. M., Türkmen, C., & Kavdır, Y. (2019). Çay çöpünden kompost yapımı ve oluşan kompostun bazı özellikleri. Mediterranean Agricultural Sciences, 32, 109-114.

Peng, S., Zou, J., Pu, T., Wang, H., Wang, R., Tian, X., . . . Cao, Q. (2024). Femtosecond laser-induced plasma-assisted backward deposition of robustly adherent porous carbon films on glass substrates. Surfaces and Interfaces, 55, 105304.

Raj, B., Perumal, P., Padhy, A. K., Rao, D., & Mohapatra, M. (2024). Physicochemical dependency of biochar-based nano-phase composites derived through ball milling for visionary energy storage applications Nanofabrication (pp. 194-208): CRC Press.

Ramos, R., Abdelkader-Fernández, V. K., Matos, R., Peixoto, A. F., & Fernandes, D. M. (2022). Metal-supported biochar catalysts for sustainable biorefinery, electrocatalysis, and energy storage applications: a review. Catalysts, 12(2), 207.

Sharma, A., Tyagi, V. V., Chen, C. R., & Buddhi, D. (2009). Review on thermal energy storage with phase change materials and applications. Renewable and Sustainable Energy Reviews, 13(2), 318-345.

Shkatulov, A., Houben, J., Fischer, H., & Huinink, H. (2020). Stabilization of K2CO3 in vermiculite for thermochemical energy storage. Renewable Energy, 150, 990-1000.

Shrivastava, K., Gill, F. S., Juyal, S., Lal, M., & Jain, A. (2025). Green Carbon for Clean Energy: Biomass-Derived Hierarchical Structures in Energy Storage. Wiley Interdisciplinary Reviews: Energy and Environment, 14(2), e70007.

Simon, S., Harikumar, P., & Sreeja, P. (2025). Green Power: The Role of Plant-Based Biochar in Advanced Energy Storage. ChemPhysChem, 26(1), e202400569.

Solak, S. G., & Pekküçükşen, S. (2018). Türkiye'de kentsel katı atık yönetimi: karşılaştırmalı bir analiz. MANAS Sosyal Araştırmalar Dergisi, 7(3).

Şener, A., & Ünal, M. Ü. (2008). Gıda sanayii atıklarının biyoteknolojik yöntemlerle değerlendirilmesi. Türkiye, 10, 21-23.

Şenkal, H. (2023). Mobilya endüstrisinde döngüsel ekonomiye geçiş: Değerlendirme yaklaşımı. Mobilya ve Ahşap Malzeme Araştırmaları Dergisi, 6(2), 146-161.

Tarım ve Orman Bakanlığı. (2023). Tarım Ürünleri Piyasa Raporları. TEPGE.

T.C. Enerji ve Tabii Kaynaklar Bakanlığı Enerji İşleri Genel Müdürlüğü. (2024). Biyokütle Enerji Potansiyeli Atlası. T.C. Enerji ve Tabii Kaynaklar Bakanlığı Enerji İşleri Genel Müdürlüğü. Erişim Tarihi 16 Aralık 2024, https://bepa.enerji.gov.tr/

Topcu, Y., & Demirkesen, B. 15-Fındık Zurufundan Hidrotermal Karbonizasyon Yöntemiyle Aktif Karbon Üretimi. Kimya Sanayiinde Proses İyileştirme Ve Yenilikçi, 15.

Ünlü, M. (2025). Orman varlığı ve orman yangınlarının etkisi. International Journal of Geography and Geography Education(55), 212-229.

Walter, M. G., Warren, E. L., McKone, J. R., Boettcher, S. W., Mi, Q., Santori, E. A., & Lewis, N. S. (2010). Solar water splitting cells. Chemical reviews, 110(11), 6446-6473.

Wang, Z., Ma, Y., Song, J., Xu, X., Wu, Y., Wang, X., . . . Lei, W. (2023). Multiple heterostructures of Co and derivatives decorated high N-doped biochar host accelerating polysulfide redox kinetics for lithium sulfur batteries. Journal of Alloys and Compounds, 968, 171920.

Weber, A. Z., Mench, M. M., Meyers, J. P., Ross, P. N., Gostick, J. T., & Liu, Q. (2011). Redox flow batteries: a review. Journal of applied electrochemistry, 41(10), 1137-1164.

Yaşar, E. (2020). Sürü Robotların Hareket Planlamada Kullanılması. European Journal of Science and Technology, (20), 24-29.

Yıldırım, Ş., & Yaşar, E. (2015). Development of an obstacle avoidance algorithm for snake like robots. Measurement, 68-73.

Yu, T., Li, G., Duan, Y., Wu, Y., Zhang, T., Zhao, X., . . . Liu, Y. (2023). The research and industrialization progress and prospects of sodium ion battery. Journal of Alloys and Compounds, 958, 170486.

Zhang, J., & Dai, L. (2015). Heteroatom-doped graphitic carbon catalysts for efficient electrocatalysis of oxygen reduction reaction. Acs Catalysis, 5(12), 7244-7253.

Chapter 3

MECHANICAL AND TRIBOLOGICAL CHARACTERIZATION OF TUNGSTEN CARBIDE-REINFORCED METAL MATRIX COMPOSITE COATINGS

İbrahim Savaş DALMIŞ[1]

1 İbrahim Savaş DALMIŞ, Doç.Dr., Tekirdağ Namık Kemal Üniversitesi, Çorlu Mühendislik Fakültesi, Makine Mühendisliği Bölümü, ORCID: 0000-0002-4401-9155, idalmis@nku.edu.tr

1. INTRODUCTION

The degradation of engineering components due to abrasion and wear remains one of the most persistent challenges in mechanical systems exposed to particulate or high-friction environments. In industries such as mining, construction, and manufacturing, abrasive wear mechanisms drastically shorten the operational life of machinery, leading to frequent maintenance cycles and substantial economic losses. Developing durable, wear-resistant surfaces is therefore a key technological objective to improve reliability and efficiency in such demanding applications. Within this context, metal matrix composite (MMC) coatings reinforced with hard ceramic particles such as tungsten carbide (WC) have gained notable attention for their superior hardness, wear resistance, and thermal stability compared with conventional metallic coatings [1–4].

Among particle-reinforced systems, WC–Fe-based MMC coatings offer a compelling combination of cost-effectiveness and mechanical robustness. The Fe-based matrix provides ductility and toughness, while the WC reinforcement imparts high hardness and abrasion resistance. Recent advances in laser wire cladding and hardfacing have further enhanced the fabrication of these coatings by enabling precise control over dilution, carbide dissolution, and microstructural integrity [5–10]. For instance, optimization of wire transfer modes—such as wire stubbing, wire plunging, and liquid spreading—can significantly influence WC particle retention and the resulting microstructure. Figure 1 to Figure 3 and Table 1 in the present study provide representative compositional and microstructural data, confirming the presence of WC as the principal reinforcing phase within an Fe–C–Cr–Si matrix.

Furthermore, prior investigations have revealed that although WC particles generally improve wear performance, excessive content or improper heat input may lead to undesirable particle cracking or weak interfacial bonding, reducing coating performance [7–9]. Hence, controlling the degree of WC dissolution and maintaining strong metallurgical bonding are crucial to the overall coating integrity [11–14]. Partial dissolution of WC can lead to the formation of beneficial secondary carbides, such as faceted M_6C or eutectic M_6W_3C, enhancing both hardness and adhesion [15–17]. Similarly, post-processing techniques like thermal spraying, microwave

post-treatment, or energy-controlled laser cladding can refine the coating microstructure, minimize porosity, and improve hardness and wear resistance [17, 18]. Altogether, existing literature emphasizes that achieving optimal microstructural integrity and wear performance in WC–Fe MMC coatings requires the integration of appropriate heat control, particle retention, and matrix design [19–24].

Given these developments, it is evident that WC–Fe MMC coatings represent a promising approach for surface protection under severe tribological conditions. Nevertheless, there remains a need for comprehensive understanding of the microstructure–property relationship, especially for coatings produced via industrial-scale hardfacing processes. The present chapter addresses this gap by conducting a systematic mechanical and tribological characterization of WC–Fe MMC coatings fabricated through the hardfacing technique. The study correlates microstructural features (as shown in Figures 1–5) with hardness (Tables 2–3) and wear behavior (Tables 4–6 and Figures 6–8), thereby establishing a robust foundation for practical applications in wear-critical components.

In conclusion, this research contributes to advancing the knowledge of WC-reinforced MMC coatings by elucidating how microstructural design, reinforcement distribution, and interfacial bonding collectively dictate mechanical and tribological performance. The outcomes are anticipated to support further optimization of coating processes for industrial implementation, enhancing durability and operational efficiency in abrasive service environments.

2. EXPERIMENTAL PROCEDURE

A systematic experimental framework was established to investigate the microstructural, mechanical, and tribological properties of the tungsten carbide (WC)–reinforced Fe-based metal matrix composite (MMC) coatings. This section details the substrate material, coating composition, and characterization techniques used to evaluate the coating's performance. A clear understanding of the materials and methods is essential to ensure the reproducibility and reliability of the results presented in later sections.

2.1. Base Material and Coating Composition

The WC–Fe composite coatings were deposited onto a structural steel substrate chosen for its favorable combination of toughness and machin-

ability. Energy Dispersive X-ray Spectroscopy (EDX) analysis of the substrate (Figure 1) confirmed a composition of 98.13 wt% Fe and 1.87 wt% Mn, characteristic of a low-to-medium carbon manganese steel. The base metal thus provides sufficient bulk strength and ductility to support the hard overlay during tribological loading.

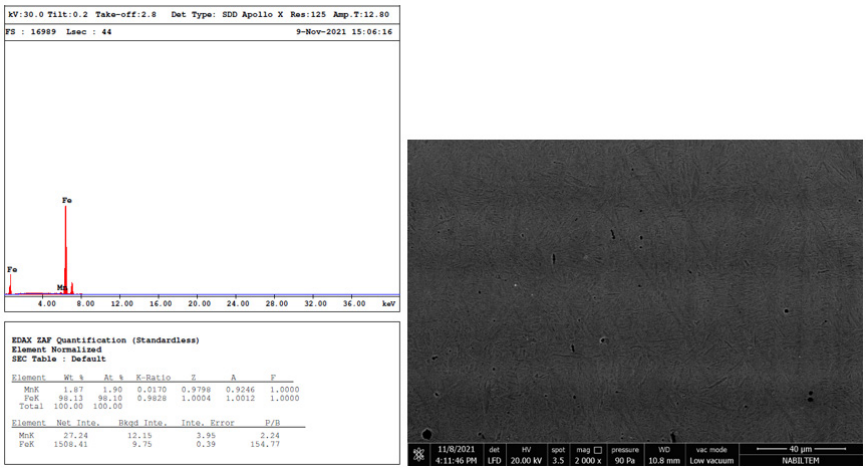

Figure 1. Base material elemental analysis and SEM micrograph

The binder matrix, serving as the metallic phase for the MMC coating, was an Fe-based hardfacing alloy enriched with carbon, chromium, and silicon. EDX analysis (Figure 2) revealed approximately 31.22 wt% C, 9.29 wt% Cr, and 8.71 wt% Si. These alloying elements are known to form high-hardness carbides (such as Fe_3C and Cr_7C_3), thereby strengthening the metallic binder and promoting metallurgical bonding between WC particles and the substrate.

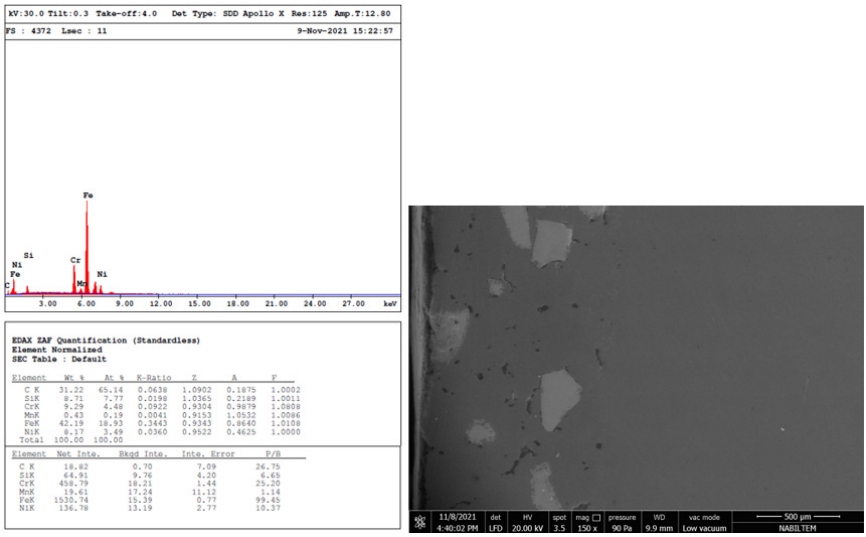

Figure 2. Binder matrix elemental analysis and SEM micrograph

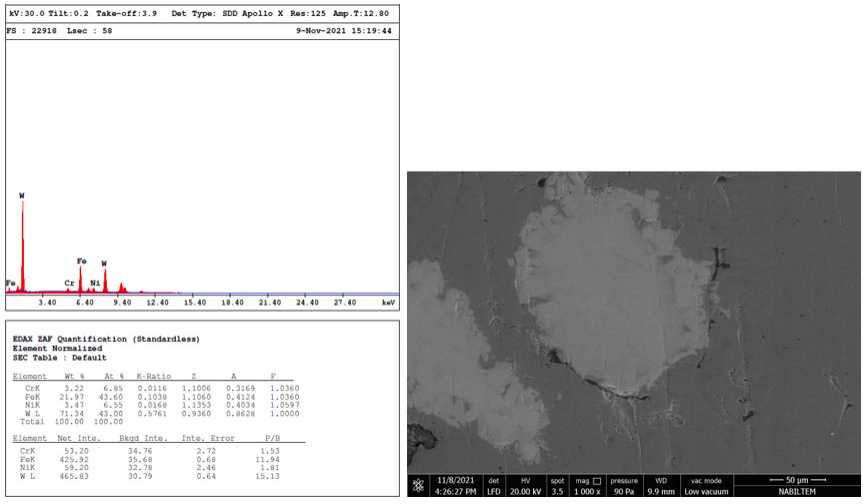

Figure 3. Reinforcing phase elemental analysis and SEM micrograph

The reinforcing phase consisted primarily of tungsten carbide (WC) particles uniformly distributed within the binder. EDX mapping of individual particles (Figure 3) confirmed a high tungsten concentration of 71.34 wt%, with partial Fe mixing (21.97 wt%), verifying that the reinforcement phase maintained its WC integrity during deposition. The summarized elemental compositions of all regions are provided in Table

1, highlighting the distinct chemical contributions of the substrate, binder, and reinforcement to the coating system.

Table 1: Representative Elemental Composition of the Substrate, Binder Matrix, and Reinforcing Phase (Weight %)

Region	**Key Elements (Wt %)**	**Representative Function / Material**
Base Material (Substrate)	Fe: 98.13, Mn: 1.87	Structural Steel for Bulk Toughness
Coating Matrix (Binder)	C: 31.22, Fe: 47.90, Cr: 9.29, Si: 8.71	Hardfacing Alloy (Fe-C-Cr-Si-Ni)
Reinforcing Phase (WC)	W: 71.34, Fe: 21.97 (Partial Mixing)	Primary Abrasion Resistance (WC)

Figure 1–3 and Table 1 collectively establish the chemical and microstructural foundation of the composite, confirming successful WC incorporation within a stable Fe–C–Cr–Si matrix.

2.2. Coating Deposition and Characterization Methods

The coatings were fabricated using an industrial hardfacing process, a technique widely utilized for producing wear-resistant overlays due to its robust metallurgical bonding and adaptability to large-scale operations. The controlled heat input during deposition was optimized to prevent excessive dilution and WC dissolution, ensuring strong particle retention within the Fe-based binder.

After deposition, cross-sectional specimens were prepared using standard metallographic procedures involving grinding, polishing, and etching. Optical microscopy and scanning electron microscopy (SEM) analyses (Figure 4–5) were employed to examine coating uniformity, interfacial integrity, and the dispersion of WC particles. The EDX line scans confirmed a consistent transition between the substrate and the overlay, indicating strong adhesion and minimal porosity. The microstructural observations served as the basis for correlating the mechanical and tribological results discussed in the following sections.

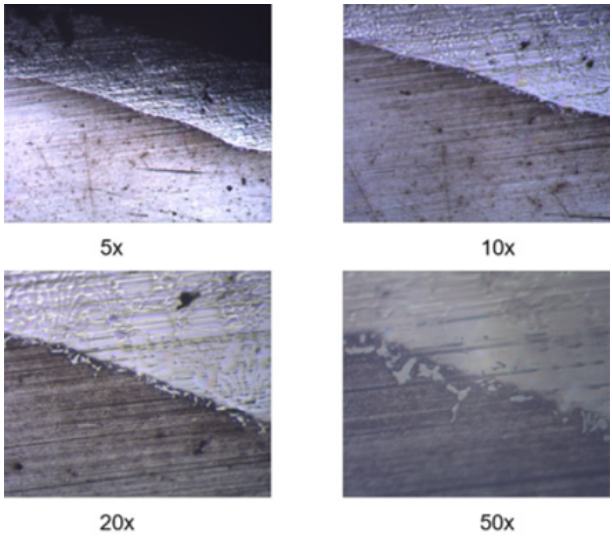

Figure 4. The optical microscope images showing the coating

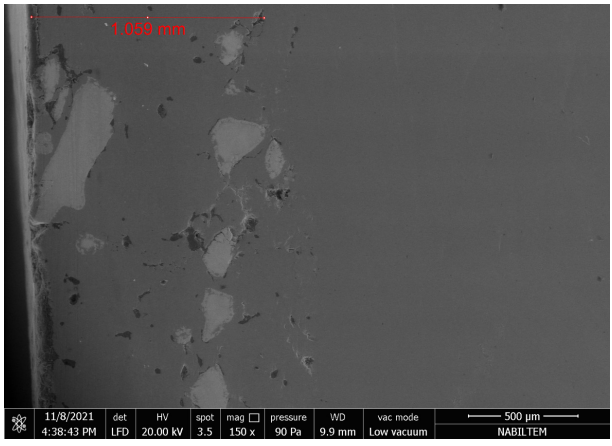

Figure 5. The SEM micrograph showing the coating

2.3. Mechanical and Tribological Testing

Mechanical and wear evaluations were conducted to quantify the performance improvement achieved through WC reinforcement.

Hardness measurements were carried out at both macro and micro scales. The macrohardness was determined using the Rockwell C (HRC) method, while the microhardness of the surface layer and substrate was evaluated using Vickers indentation ($HV_{0.025}$). The results, summarized in Tables 2 and 3, demonstrate the consistency and reproducibility of the

hardness profiles across multiple test points.

Wear resistance was assessed through abrasive wear tests, in which both coated and uncoated samples were subjected to controlled normal loads ranging from 5 N to 20 N. The resulting weight losses were recorded (Tables 4 and 5) and plotted against applied load (Figure 5) to quantify the relationship between load intensity and wear behavior. This experimental design enables a direct comparison between the coating and the substrate, isolating the effect of WC reinforcement on the tribological response.

The use of multiple characterization and testing methods ensures a comprehensive understanding of the material's behavior. Figures 1–6 and Tables 1–5 together provide a complete depiction of the experimental framework, from elemental composition to mechanical and wear evaluation.

In summary, the experimental procedure was structured to provide a clear linkage between processing parameters, resulting microstructure, and measurable performance metrics. This methodological rigor forms the basis for interpreting the findings in the Results and Discussion section, where mechanical, microstructural, and tribological correlations are analyzed in depth.

3. RESULTS AND DISCUSSION

3.1. Overview

The mechanical and tribological performance of the WC–Fe-based metal matrix composite (MMC) coatings were systematically evaluated to establish correlations between the coating microstructure, hardness enhancement, and wear mechanisms. This section integrates the microstructural evidence presented in Figures 1–4 and the quantitative data in Tables 1–5 and Figures 6–8 to explain the strengthening and wear-resistant behavior of the developed coatings. Understanding these interrelations is vital for optimizing process parameters and tailoring coatings for industrial use in high-friction environments such as mining, drilling, and earth-moving equipment.

The application of WC–Fe coatings significantly improved surface hardness and wear performance compared to the uncoated steel substrate. Microstructural analyses confirmed a uniform distribution of WC particles with limited dissolution, while hardness testing revealed an increase exceeding 40%. These results are consistent with previous studies reporting that moderate WC additions enhance grain refinement and load-bearing capability [14, 20]. The coating exhibited stable wear behavior under

increasing loads, reflecting the reinforcing role of WC in transforming the wear mechanism from severe micro-cutting to micro-scratching [10, 13]. This performance aligns with comparative findings from laser cladding and microwave-treated coatings, demonstrating the critical influence of WC particle retention and post-processing on tribological stability [17, 15].

3.2. Microstructural Integrity and Phase Distribution

Microstructural characterization (Figures 1–4) confirmed successful incorporation of tungsten carbide within the Fe–C–Cr–Si matrix, as supported by compositional data in Table 1. The homogeneous dispersion of WC particles, observed in the SEM micrographs of Figure 3 and the cross-sectional image in Figure 4, demonstrates minimal particle agglomeration and strong metallurgical bonding at the particle–matrix interfaces. This uniform distribution ensures even load transfer during contact and suppresses localized stress concentrations—key factors contributing to the mechanical stability of the coating.

Additionally, the EDX results reveal partial Fe diffusion into the WC regions, indicating controlled carbide dissolution. This limited dissolution contributes to the formation of fine secondary carbides such as Fe_3W_3C or Cr_7C_3, which further reinforce the metallic matrix. Similar secondary phase formation has been correlated with improved microhardness and wear resistance in comparable Fe- and Ni-based coatings [5, 9, 13]. The optimized process parameters thus maintained a beneficial balance between particle integrity and carbide precipitation, ensuring both toughness and hardness within the surface layer.

3.3. Mechanical Properties: Hardness Enhancement

The hardness data presented in Tables 2 and 3 confirm a significant improvement in the surface mechanical properties of the coated specimens compared to the uncoated substrate. The average Rockwell hardness increased from 33.47 HRC for the substrate to 46.95 HRC for the coating—an enhancement of approximately 40%. On the micro-scale, the coating achieved an average Vickers hardness of 1553.4 $HV_{0.025}$, compared to 446.2 $HV_{0.025}$ for the base steel.

Table 2: Rockwell C (HRC) Hardness Results

Measurement	Coating Hardness (HRC)	Substrate Hardness (HRC)
1	45.1	36.1
2	46.6	30.1
3	47.1	32.8
4	49.0	34.9
AVERAGE	46.95	33.47

Table 3: Vickers ($HV_{0.025}$) hardness results

Measurement	Coating Hardness ($HV_{0.025}$)	Substrate Hardness ($HV_{0.025}$)
1	1589.8	437.0
2	1287.8	428.6
3	1782.5	473.0
AVERAGE	1553.4	446.2

This high hardness level, far exceeding that of conventional Fe-based hardfacing alloys (typically ≤ 900 HV), can be attributed to the synergistic reinforcement provided by the WC phase and the Cr- and Si-enriched Fe matrix. The fine-grained microstructure, along with the presence of secondary carbides observed in Figure 4, restricts dislocation mobility and resists plastic deformation under load. Similar findings were reported by Zhang et al. [5] and Zhao et al. [7], where controlled WC retention led to optimized hardness gradients across the coating thickness. The consistent hardness distribution also suggests uniform energy input and effective metallurgical bonding during deposition, which are critical for maintaining structural integrity under cyclic loading conditions.

3.4. Tribological Performance and Wear Factor Analysis

The abrasive wear test results (Tables 4 and 5; Figure 6) reveal the substantial tribological advantage of the WC-reinforced coatings. Under increasing applied loads from 5 N to 20 N, the coated surfaces exhibited negligible increases in weight loss, maintaining values between 0.092 g and 0.110 g, while the uncoated substrate showed a progressive rise from 0.5559 g to 1.9870 g. At 15 N, the coating reduced wear by a factor of approximately 22, confirming superior load-bearing capability and structural resilience.

Table 4: Uncoated Substrate Wear Results (Weight Loss)

Sample	Applied Load (N)	Weight Loss (g)
1	5	0.5559
2	10	1.1307
3	15	1.5160
4	20	1.9870

Table 5: Coated Specimen Wear Results (Weight Loss)

Sample	Applied Load (N)	Weight Loss (g)
1	5	0.1014
2	10	0.1103
3	15	0.0950
4	20	0.0920

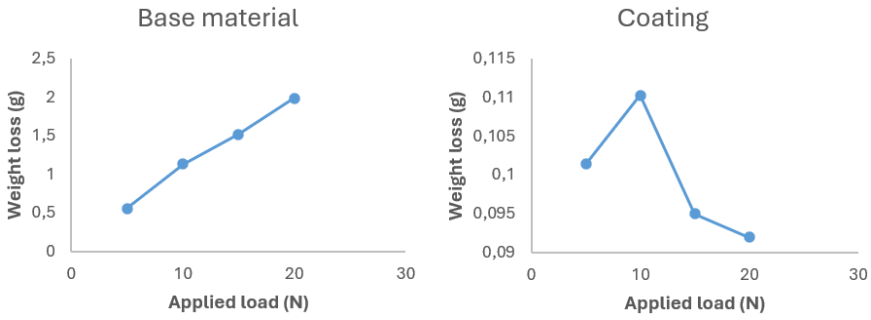

Figure 6. The optical microscope images and the SEM micrograph showing the coating

The nearly constant wear rate of the coated specimens across the load range demonstrates high tribological stability, indicating that the wear process is dominated by mild abrasive interaction rather than load-induced plasticity. The WC particles act as micro-barriers that absorb and distribute contact stress, preventing excessive deformation of the metallic binder. The hard Fe–Cr–C matrix, visible in Figure 4, also supports the reinforcement phase by maintaining cohesive strength and suppressing crack propagation around the carbide–matrix boundaries.

3.5. Analysis of Wear Mechanism Transition

Surface morphologies of the worn regions, shown in Figures 7 and 8, elucidate the transition of wear mechanisms due to WC reinforcement. The uncoated substrate (Figure 7) exhibited deep ploughing grooves and material delamination typical of a micro-cutting-dominated wear regime. In contrast, the coated specimens (Figure 8) displayed shallower scratches and isolated micro-pits, reflecting a micro-scratching or mild abrasion mechanism.

This shift in wear behavior can be attributed to the "shielding effect" of the hard WC particles, which act as protective protrusions on the surface, deflecting abrasive particles and reducing penetration depth. The Fe–Cr–Si matrix further stabilizes this behavior by accommodating minor deformation without fragmenting, maintaining coating integrity. Similar transformations in wear mode have been reported by Guo et al. [10] and da Silva et al. [9], affirming that optimized particle dispersion can redirect abrasive energy and extend service life under high-friction conditions.

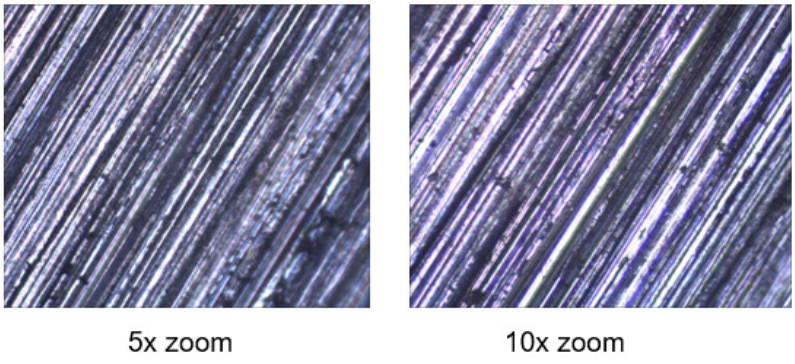

Figure 7. The worn surface morphology of the matrix after the abrasive wear test

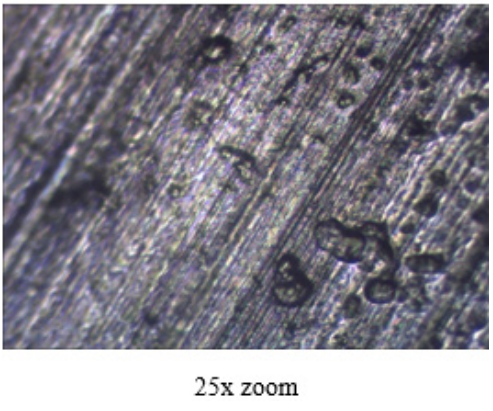

Figure 8. Surface morphology of the coating area after the abrasive wear test

Furthermore, the consistent wear resistance at elevated loads indicates that the coating's microstructural architecture effectively balances hardness and toughness a property often difficult to achieve in highly reinforced systems. The retention of WC morphology, as seen in Figures 3–5, plays a crucial role in ensuring that the reinforcement does not fracture prematurely, which would otherwise accelerate wear through particle pull-out.

3.6. Industrial Relevance and Optimization Perspectives

The mechanical and tribological performance demonstrated by the WC–Fe coating highlights its potential applicability in industries exposed to abrasive wear, such as mining tools, agricultural blades, drilling bits, cement mixers, and earth-moving machinery. The combination of high hardness, stable wear response, and metallurgical bonding offers a durable surface capable of replacing more expensive Co- or Ni-based overlays.

For future optimization, parameter refinement in hardfacing (e.g., current intensity, feed rate, and wire composition) could further tune carbide dissolution and distribution. Integrating post-treatment techniques such as laser remelting or microwave surface modification—shown in related studies [15, 17]—may enhance surface smoothness and reduce residual stress. Additionally, extending this coating system to gradient architectures or hybrid reinforcements (e.g., WC + TiC) could achieve tailored hardness profiles and improve multi-directional wear resistance, paving the way for next-generation MMC coatings in heavy-duty service applications.

4. CONCLUSION

This study demonstrated that tungsten carbide–reinforced Fe-based MMC coatings, deposited by the industrial hardfacing technique, provide a substantial enhancement in hardness, wear resistance, and surface integrity compared with uncoated structural steel. The findings can be summarized as follows:

Microstructural stability: WC particles were uniformly distributed within a dense Fe–C–Cr–Si matrix (Figures 3–4), ensuring strong metallurgical bonding and minimizing porosity.

Mechanical performance: The coating achieved a 40% increase in macrohardness (46.95 HRC) and a microhardness of 1553 $HV_{0.025}$, confirming the synergistic strengthening between WC and secondary carbides (Tables 2–3).

Tribological superiority: The coated specimens exhibited up to 22-

fold reduction in weight loss under abrasive loads (Tables 4–5, Figure 5), maintaining nearly constant wear behavior even under high stress.

Mechanism transition: The wear mode shifted from severe micro-cutting to mild micro-scratching, as visualized in Figures 6–7, owing to the protective effect of WC reinforcements and the tough supporting matrix.

Overall, the WC–Fe MMC coating represents a cost-effective, industrially scalable, and high-performance solution for extending component service life under severe wear conditions. The insights into microstructure–property relationships developed here can guide the design of next-generation MMC coatings for mechanical systems requiring both strength and tribological endurance.

Future research should focus on process–microstructure modeling, multi-reinforcement hybridization, and thermal fatigue evaluation to establish comprehensive design criteria for diverse industrial environments. Such advancements would accelerate the adoption of Fe-based MMC coatings as sustainable alternatives to conventional hardfacing materials in heavy-duty engineering applications.

REFERENCES

[1] Yuan, Y., & Li, Z. (2017). Microstructure and tribology behaviors of in-situ WC/Fe carbide coating fabricated by plasma transferred arc metallurgic reaction. Applied Surface Science, 423, 13-24.

[2] Mendez, P. F., Barnes, N., Bell, K., Borle, S. D., Gajapathi, S. S., Guest, S. D., ... & Wood, G. (2014). Welding processes for wear resistant overlays. Journal of Manufacturing Processes, 16(1), 4-25.

[3] Deschuyteneer, D., Petit, F., Gonon, M., & Cambier, F. (2015). Processing and characterization of laser clad NiCrBSi/WC composite coatings—Influence of microstructure on hardness and wear. Surface and Coatings Technology, 283, 162-171.

[4] Alidokht, S. A., Yue, S., & Chromik, R. R. (2019). Effect of WC morphology on dry sliding wear behavior of cold-sprayed Ni-WC composite coatings. Surface and Coatings Technology, 357, 849-863.

[5] Zhang, M., Li, M., Chi, J., Wang, S., Yang, S., Yang, J., & Wei, Y. (2019). Effect of Ti on microstructure characteristics, carbide precipitation mechanism and tribological behavior of different WC types reinforced Ni-based gradient coating. Surface and Coatings Technology, 374, 645-655.

[6] Mao, L., Cai, M., Liu, Q., & Han, L. (2021). Effects of spherical WC powders on the erosion behavior of WC-Ni hardfacing used for steel body drill bit. Surface and Coatings Technology, 409, 126893.

[7] Zhao, S., Xu, S., Yang, L., & Huang, Y. (2022). WC-Fe metal-matrix composite coatings fabricated by laser wire cladding. Journal of Materials Processing Technology, 301, 117438.

[8] Karimi, M. R., Wang, S. H., & Jelovica, J. (2023). Characterization of cold metal transfer and conventional short-circuit gas metal arc welding processes for depositing tungsten carbide-reinforced metal matrix composite overlays. The International Journal of Advanced Manufacturing Technology, 128(5), 2551-2570.

[9] da Silva, L. J., Pacheco, J. T., Moura, E. I. F., de Araújo, D. B., Reis, R. P., & D'Oliveira, A. S. C. M. (2025). Metal matrix composite coatings deposited by laser cladding: On the

effectiveness of WC reinforcement for wear resistance and its synergy with the matrix material (Ni Versus Co alloys). Coatings, 15(4), 468.

[10] Guo, X., Ma, M., Zhang, S., & Wei, Z. (2024). Microstructure and wear resistance of tungsten carbide particle reinforced titanium alloy coating by WAAM. Tribology International, 194, 109536.

[11] Singh, S., Keshri, A. K., & Mantry, S. (2024). Influence of residual stress on corrosion and mechanical properties of silicon carbide-reinforced nickel–tungsten coatings. Bulletin of Materials Science, 48(1), 11.

[12] Suresh, N., Balamurugan, L., & Jayabalakrishnan, D. (2023). Influence of SiC and WC reinforcements on the mechanical characteristics of AA6061 hybrid metal matrix composites. Proceedings of the Institution of Mechanical Engineers, Part E: Journal of Process Mechanical Engineering, 237(3), 955-970.

[13] Chen, X., Fang, C., Huang, X., Li, Z., Wei, H., Zhang, F., & Shan, Q. (2024). Effect of Thermal Gradient on Interfacial Microstructure and Mechanical Properties of WC Particle-Reinforced Steel Matrix Composites. Journal of Materials Engineering and Performance, 33(19), 10475-10484.

[14] Zhou, Z., Luo, C., Xiong, Y., Xiong, H., & Li, F. (2025). Effect of tungsten carbide additions on the microstructure, mechanical, and Tribological properties of M_2 high-speed steel matrix composites. Journal of Materials Engineering and Performance, 34(3), 2553-2566.

[15] Yuan, J., Huang, Y., Wang, L., Jia, C., Zhang, F., & Yang, L. (2023). Effect of the dissolution characteristic of tungsten carbide particles on microstructure and properties of $\text{Ni–WC/W}_2\text{C}$ reinforcement coating manufactured by TIG cladding. International Journal of Refractory Metals and Hard Materials, 110, 106047.

[16] Yang, Y., Peng, P., Liu, J. X., & Zhang, G. J. (2025). Multicomponent carbides reinforced tungsten matrix composites and their mechanical properties. Journal of the American Ceramic Society, 108(9), e20645.

[17] Pradeep, D. G., Nithin, H. S., Sharath, B. N., & Madhu, K. S.

(2024). Evaluation of dry sliding wear behavior of thermally sprayed and microwave post-processed TiO_2 reinforced tungsten carbide composite coating. Welding in the World, 68(2), 199-211.

[18] Zhang, G., Feng, A., Zhao, P., Pan, X., & Feng, H. (2023). Effect of energy density on the microstructure and wear resistance of nickel-based WC coatings by laser cladding of preset Zr702 alloy plates. Coatings, 13(5), 826.

[19] Govindarajan, V., Sivakumar, R., Patil, P. P., Kaliappan, S., Ch Anil Kumar, T., Kannan, M., & Ramesh, B. (2022). Effect of tungsten carbide addition on the microstructure and mechanical behavior of titanium matrix developed by powder metallurgy route. Advances in materials science and engineering, 2022(1), 2266951.

[20] Hu, J. J., Zhang, G. B., Xu, H. B., & Chen, Y. F. (2012). Microstructure characteristics and properties of 40Cr steel treated by high current pulsed electron beam. Materials Technology, 27(4), 300-303.

[21] Yin, P., Zang, H., Zhao, Y., Wu, C., Xu, X., Pan, D., & Jiang, W. (2020). Superior mechanical properties of 40Cr steel obtained by quenching and microstress relieving under electropulsing. Materials Science and Engineering: A, 772, 138782.

[22] Zhang, K., Ju, H., Xing, F., Wang, W., Li, Q., Yu, X., & Liu, W. (2023). Microstructure and properties of composite coatings by laser cladding Inconel 625 and reinforced WC particles on non-magnetic steel. Optics & Laser Technology, 163, 109321.

[23] Li, W., Di, R., Yuan, R., Song, H., & Lei, J. (2022). Microstructure, wear resistance and electrochemical properties of spherical/non-spherical WC reinforced Inconel 625 superalloy by laser melting deposition. Journal of Manufacturing Processes, 74, 413-422.

[24] Zhou, Z., Luo, C., Xiong, Y., Xiong, H., & Li, F. (2025). Effect of tungsten carbide additions on the microstructure, mechanical, and Tribological properties of M2 high-speed steel matrix composites. Journal of Materials Engineering and Performance, 34(3), 2553-2566.

Chapter 4

DATA ACQUISITION IN ENGINEERING

Ebubekir YAŞAR[1]

1 Mechanical Engineering Department, Tokat Gaziosmanpaşa University, 60250, Tokat, Türkiye

1. Introduction

Data is of great importance in almost every field of science. Knowledge is obtained through the systematic processing of data; therefore, data is one of the fundamental elements that determine the direction of scientific research. All disciplines utilize data and shape their work based on the results obtained from this data.

In engineering, data acquisition is defined as the process of measuring analog signals obtained from physical events (e.g., temperature, pressure, vibration, current, level, etc.) using sensors, conditioning them, converting them into digital format, and processing them in a computer environment (Doebelin & Manik, 2017). In other words, data acquisition is the process of collecting raw data from a source and transferring it to a digital environment for processing. In this process, data is not only collected but also stored, analyzed, visualized, and reported (Gültekin N, 2024).

Direct processing and analysis of analog signals is difficult; in contrast, digital signals are widely preferred in engineering applications due to their advantages such as ease of processing and reliability. The diversification and development of digital systems have enabled their use in different engineering disciplines. The superiority of digital data in terms of processing, storage, and transmission has significantly contributed to the development of data analysis and simulation-based applications in many scientific fields.

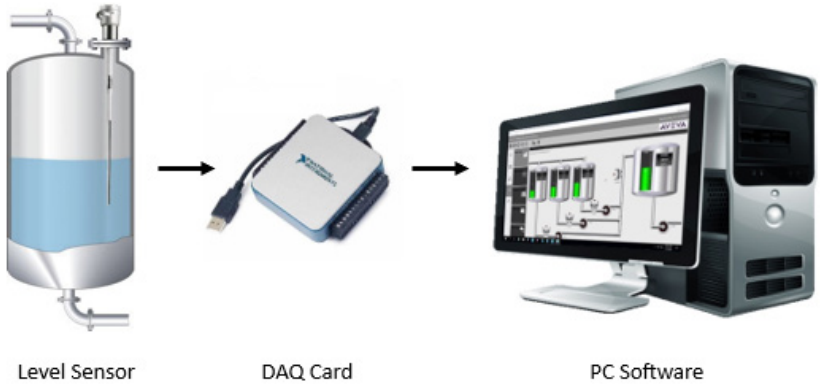

Figure 1. Data acquisition components

Almost every engineering study relies on data. Data plays a fundamental role in system design and problem identification (Daş, Pektezel, & Şimşek, 2025). Therefore, the data collection process requires meticulous attention. The higher the reliability of the collected data, the more accu-

rate the analyses based on that data will be. A typical data acquisition system consists of sensors, signal conditioning circuits, an analog-to-digital converter (ADC), and analysis software (Bentley, 2005). This study examines the fundamental characteristics of analog and digital data types, and particularly examines the components of digital data acquisition techniques in detail.

Data sources can vary across disciplines (Daş, Pektezel, Şimşek, & Akpınar, 2025). Sensors, IoT devices, operating systems, software, cameras, microphones, websites, and social media platforms are among the most common data sources. Sensors can generate analog or digital signals. Log files generated by system software and hardware, information extracted from websites, or data obtained from user feedback are also important data sources. This study focuses specifically on data obtained from sensors.

Why Data Acquisition is Necessary?

Data acquisition is a fundamental component of modern measurement systems (Şimşek, Yusuf, Ertuğrul, & Uğur, 2023). Advancing computer technologies have accelerated data collection, transmission, and storage processes, making it an effective part of measurement systems. Accurate data collection is crucial, particularly for quality control in industrial production, biomedical measurements in medicine, and scientific research (Doebelin & Manik, 2017).

Highly accurate measurements in engineering designs directly impact system reliability (Doebelin & Manik, 2017). Data acquisition shortens product development time in engineering and contributes to design optimization. Real-time data collection is essential for process monitoring, automation, and quality control in industrial applications (Bentley, 2005). This allows system performance analysis to reduce costs and increase efficiency (National Instruments, 2019). It also facilitates troubleshooting production errors, product updates, and error analysis (Gültekin, N., Ciniviz, M., 2024).

Data acquisition also plays a critical role in predictive maintenance. By monitoring machine vibrations, temperature changes, or current fluctuations, potential failures can be detected early (Doebelin & Manik, 2017). Furthermore, data acquisition systems are frequently used in universities and R&D centers to reliably acquire and record experimental data (Stallings, 2018).

2. Methodology

Signals cannot be transferred directly to a computer. They must undergo some processing before they can be stored in a computer. Figure 2 contains the necessary components. Every signal in nature is converted into a measurable signal by a suitable sensor. Signals must be converted to digital form before they can be transferred to a computer. To trust the converted signals, some processing is necessary. The signal is corrupted for various reasons and must be subjected to various processes, such as cleaning and amplification.

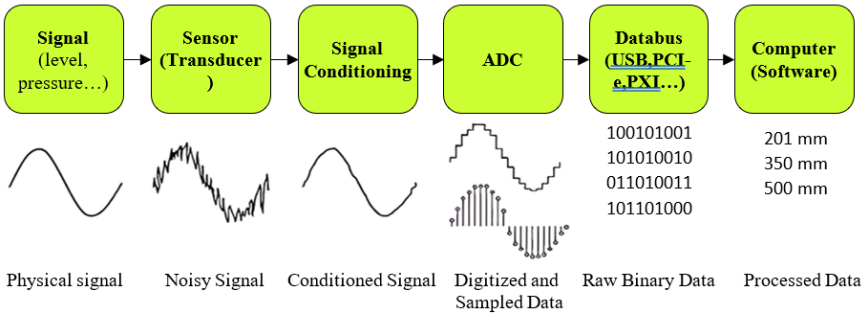

Figure 2. Data acquisition components block diagram

The data-carrying signal must be denoised and conditioned before being applied to the ADC (Gültekin, Gülcan, & Ciniviz, 2024). The signal is then converted to digital form. After digitization, the data's accuracy must be maintained, and the data must be standardized in appropriate file formats. The resulting data can be stored locally, on servers, or in the cloud. The stored data is processed using analysis software; during this process, statistical analysis, machine learning, visualization, and reporting methods are used to derive meaningful results from the data. In the following sections, all concepts and details necessary for understanding the methodology are explained in detail.

2.1. Signal

A signal is a physical quantity that can carry data and varies over time. It can occur in various media, such as electricity, electromagnetic fields, sound, or light. Signals are generally used for data transmission and communication; as such, they are physical representations of the information transmitted and are measurable. For example, the sound wave of a musical instrument or the electromagnetic wave carried by a particular radio channel are examples of signals.

While analog signals have an infinite number of intermediate values

between maximum and minimum values, digital signals consist of only two distinct values, usually 1 (high) and 0 (low) (Dueck, 2005; Proakis & Manolakis, 2007; Garg & Wang, 2005). The transition of digital signals from one state to another (e.g., from 0 to 1) is theoretically considered infinitely fast. Analog signals can take on an infinite number of values in any range of positive and negative values, while digital signals are defined by only two distinct positive values.

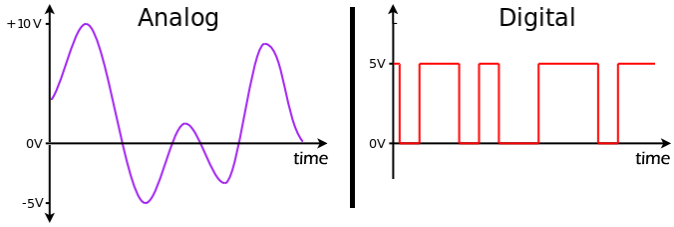

Figure 3. Analog and digital signal formats

Digital signals, like analog signals, carry data; however, in digital signals, the values are discrete. These signals are represented as a sequence of discrete values and are generally defined by a bit rate. Therefore, digital signals consist of a set of digital values obtained by sampling a continuously changing analog signal at specific time intervals.

2.2. Data

Data can be represented in analog or digital format. All numerical, verbal, visual, or auditory values obtained from various sources that are not meaningful on their own or interpreted are defined as "data." Although data is often confused with the concept of "information," information is the processed form of data. Data can be analyzed, transmitted, stored, and generally carried via signals in its raw form. Analog and digital signals represent data by converting physical variables such as temperature, speed, or pressure into electrical signals.

2.3. Analog Data

All physical quantities in nature are analog in nature (Bilgin, 2025). Analog data are a continuous, discrete set of values representing physical measurements. They are continuous in both amplitude and time; that is, they have a value at every instant of time. Therefore, even in the shortest time intervals, analog signals contain an infinite number of discrete data. Analog data is transmitted and stored in waveform.

2.4. Digital Data

Digital data is usually obtained by sampling analog signals and has discrete values in both time and amplitude (Khanna, 2009; Chitode, 2020). In digital data, each type of information (character, image, video, sound, speed, etc.) is represented by numbers. For example, an image is an object composed of colors; the digital equivalent of this image is created by representing each pixel with a specific numerical value. The way these values are arranged determines the image format (e.g., *.bmp, *.jpg, .png) and is a separate topic of study.

Digital data is expressed in the binary number system because the logic circuits used to process and store data can only operate at two different voltage levels (Di Paolo Emilio, 2015). Generally, a value of 1 corresponds to approximately 5 volts on the circuit side, and a value of 0 corresponds to 0 volts.

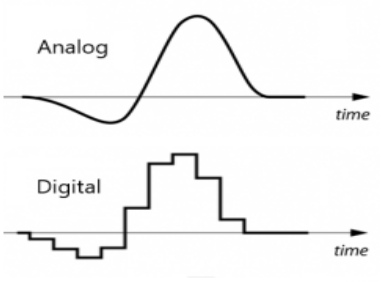

Figure 4. Analog data and its digital counterpart

2.5. Data Representation (Concept of Bit, Byte, and Word)

Digital systems use the binary number system. In the binary number system, each digit that makes up a number consists of only two digits: 1 and 0. Data in digital systems is processed, stored, and transmitted using this binary number system.

For example, the binary equivalent of the decimal number 15 is $(1111)_2$, while the binary equivalent of the decimal number 156 is $(10011100)_2$. Values in the binary number system are represented using specific data quantity definitions:

2.6. Bit

Bit is short for "Binary digit" (University of Edinburgh, n.d.). A bit can take only two different values: 1 and 0, or, in their verbal equivalents, true and false. A bit is the smallest unit of data that can be stored or represent-

ed in a computer.

A single bit can represent two opposite states. For example: Binary states such as yes–no, on–off, active–passive, male–female, retired–employed can be represented by a single bit.

A bit is also the name given to each digit in the binary number system. Bits combine to form larger data sets and can represent multiple characters or numbers.

For example, a system with a length of n bits can represent 2^n different values.

For 8 bits: $2^8 = 256$ different values are possible.

All data types used in scientific and engineering applications are represented and processed using the binary number system. Decimal numbers are converted to binary and stored and used in computer systems as follows.

	MSB			LSB
bit position	n-1	n-2	……. 1	0
binary(x = 1 or 0)	x	x	x	x
decimal	$x.2^{n-1}$	$x.2^{n-2}$	$x.2^1$	$x.2^0$

Of the abbreviations mentioned above, MSB stands for most significant bit, while LSB stands for least significant bit. In binary terms, MSB is the bit that has the greatest impact on the number and is the leftmost bit. For example, for the binary number 1011 1101, the most significant 4 bits on the left would be 1011. The least significant 4 bits would be 1101. For example, for decimal numbers, we can also understand the place values to the left and right of the midpoint of a number in the decimal numbering system. For example, if the ones digit of the number 1546 increases by 1, the number increases by 1, but if the thousands digit increases by 1, the number increases by 1000.

2.7. Byte

A byte is a group of data consisting of eight bits. The basic unit of information used in computer systems is the byte. A byte represents the number of bits required to encode a character on a computer (Buchholz, 1962; Bemer, 1959).

The eight-bit structure was initially used to define the 256 different characters in the ASCII (American Standard Code for Information Interchange) character table (Bemer, 1960; Bemer, 1961). Today, the byte is

used as the basic unit of representation not only for characters but also for numerical data, images, audio files, and other data types.

2.8. Scale (SI) Multipliers

In this system, multipliers are calculated based on powers of 10 and are primarily used by storage device manufacturers.

Name(Prefix)	Power of 10	Byte
1 Kilobyte (KB)	10^3	1.000 B
1 Megabyte (MB)	10^6	1.000.000 B
1 Gigabyte (GB)	10^9	1.000.000.000 B
1 Terabyte (TB)	10^{12}	1.000.000.000.000 B

Because computer architecture is based on binary, data quantities are sometimes defined as power of 2 (Bemer, 1960). Many popular operating systems, in particular, use these factors, but they use decimal factors as naming conventions.

Name(Prefix)	Power of 2	Byte
1 Kibibyte (KiB)	2^{10}	1.024 B
1 Mebibyte (MiB)	2^{20}	1.048.576 B
1 Gibibyte (GiB)	2^{30}	1.073.741.824 B
1 Tebibyte (TiB)	2^{40}	1.099.511.627.776 B

To clarify this distinction, the International Electrotechnical Commission (IEC) published the IEC 60027-2 standard in 1999, defining the terms “KiB, MiB, GiB” (Bemer, 1960).

Example Calculation

When a system has 4 GB of RAM, the binary equivalent of this value is approximately:

$4 \times 2^{30} = 4{,}294{,}967{,}296$ bytes.

Storage manufacturers generally use the decimal system (1 GB = 10^9 B), while operating systems use the binary system (1 GiB = 2^{30} B). Therefore, a “500 GB” hard drive appears to the operating system as approximately “465 GiB” due to this difference.

Accurately defining data amounts is crucial for both hardware-software compatibility and transparency in storage calculations. While a bit

is the smallest unit of information, a byte and its multiples form the basis of data storage, transmission, and processing.

2.9. Comparison of Analog and Digital Systems

When comparing analog and digital systems, the advantages of digital systems are clearly evident in many aspects. Chief among these is their ease of analysis. Digital systems are more accurate than analog systems due to their precise and consistent presentation of information. Digital systems are capable of processing large amounts of data quickly and accurately, and therefore have a wide range of applications. Digital systems are more immune to noise, meaning the transmitted information is less likely to be distorted. The advantage of analog systems is that they contain more values of real data and are more likely to be true to reality. Analog systems use continuous signals to represent information such as electrical voltages or sound waves. Analog systems are better suited to representing real-world phenomena such as sound and light, which are inherently continuous. No natural signal is discrete. Analog systems provide smooth and continuous transitions between different values, which can be important in media such as audio and video. Analog systems can be more complex than digital systems due to the need for additional circuitry to process and transmit signals. Both analog and digital systems can be used to process and transmit information. Both can be used together to overcome or take advantage of each other. For example, digital signal processing can be used to enhance analog signals (GeeksforGeeks, n.d.).

Table 1. Comparison of Analog and Digital Systems

Parameter	Analog	Digital
Analysis	Difficult	Easy
Signal	Continuous	Discrete
Accurate	Closer to the original	Fewer samples than the original.
Storage	Finite	Easy
Noise	Yes	Finite
Bandwidth	Low	High
Cost/data	Expensive	Cheap
Transmission/ Sharing	Orta	Easy
Data replication	Moderate – Difficult	Easy
Power	Consumes large power	Consumes negligible power

Uses	Usually for audio and video transmission	Usually for digital electronics
Memory	Stored as a wave signal	Stored in the binary bit as

2.10. Data Representation in Digital Systems

Because digital systems use numbers entirely, the data source is numbers. Therefore, to use other data types in digital systems, it is necessary to define and represent these data types. The numbers used in digital systems belong to the binary number base. Each digit that makes up the binary number system is called a bit and consists of the digits 1 and 0. The term byte refers to a fixed-length collection of bits (Mackenzie, 1980). Although fixed lengths such as 6, 7, and 8 were initially accepted, the fact that the extended ASCII (ISO-646) character table consists of a total of 256 (28) characters has established the acceptance that 8 bits constitute a byte. A byte is defined today in almost all computer science textbooks as a set of 8 bits.

In daily life, people use their own alphabets, special characters, and numbers for communication and correspondence. Control characters are also used, especially in digital systems. Control characters are special characters that control software and hardware components and correspond to a specific function. Many of these characters are invisible. They generally serve purposes such as data formatting and control, communication control, function modification, etc. (Mackenzie, 1980).

2.10.1. Characters

The ASCII (American Standard Code for Information Interchange) character definition table is one of the most widely used and fundamental character encodings for representing characters. ASCII uses a total of 7 bits to store each character code. This allows for 128 characters to be represented. The first 32 characters of ASCII are reserved for control characters. ASCII codes were initially developed with English as a support and were sufficient for this language.

Because the initial ASCII table of 128 characters did not include many world languages and common scientific symbols, Microsoft expanded it to define an additional 128 characters. New extended definitions, created in addition to the initial 7-bit ASCII definition table, total 8 bits and are available in different versions for different language needs. The rapid spread of computers worldwide and the computerized processing of data in all branches of science have led to the need to add symbols and abbreviations specific to those sciences to character sets. This has led to the need

for thousands of characters to be defined numerically. To this end, organizations such as the Unicode Consortium have created definition tables covering all letters, punctuation marks, and technical symbols. Character-numeric tables representing thousands of characters, including UTF and UCS, have been created, representing multiple types of characters. These essentially operate in a parallel system based on the ASCII table (Unicode Consortium, n.d.). The table shows the numerical equivalents of some characters.

Table 2. A part of ASCII table

Decimal Number	Character	Decimal Number	Character
65	A	97	a
66	B	98	b
67	C	99	c
36	$	47	/

Notice in the table above that the English letter order continues sequentially, one below the other. The numerical equivalents of uppercase and lowercase letters are different, and the numbers correspond to a numerical code.

2.10.2. Sounds

Sound is the continuous vibration of air particles and is an analog signal. Therefore, to process and store it using a computer, we need to convert sound to the binary number system. When converting sound to digital, it is created by converting amplitude values to numbers using an ADC at a specific sampling interval (frequency). These numerical values are saved in a file and converted into an audio file. For example, 44,100, 48,000, 96,000, or 192,000 separate samples can be taken from each second of an analog signal in a musical piece. The more samples taken, the more information is collected about the song's sounds, and the more detailed the tones are heard when the song is reproduced.

2.10.3. Images

Images are composed of dots called pixels. They are divided into two types: colored and colorless. In color images, each pixel contains 3 bytes (RGB) of color value. Images consist of red, green, and blue color values, each with a value between 0 and 255. Grayscale images, on the other hand, contain 1 byte of data per pixel. In black and white images, all sub-color values (R=G=B) are equal. Therefore, 8 bits of memory are sufficient.

2.10.4. Data Stream

A data stream is a data model in which data is generated and transmitted continuously, sequentially, and in real time. Unlike file-based data, data streams have no definite end; they flow continuously and are time-dependent (Babcock, Babu, Datar, Motwani, & Widom, 2002). They are used in digital systems, particularly in audio and video transmission, which have long bit rates.

Data streams have continuity. Data arrives uninterrupted from a specific source. For example, temperature and pressure measurements from IoT sensors (Golab & Özsu, 2003). Here, data is processed as soon as it is generated, which is critical, especially in fields such as finance, industry, and network security (Stonebraker, Çetintemel, & Zdonik, 2005). Data streams can be very large and cannot be stored and analyzed later using traditional batch processing methods. Instead, stream processing approaches are used (Marz & Warren, 2015). The time at which data is generated plays a significant role in the analysis. Therefore, time window techniques such as sliding windows are commonly used for analysis (Golab & Özsu, 2003).

2.10.5. Batch Processing

Batch processing is a data processing method in which data is collected and stored in advance, and then processed as a whole (batch). In this approach, data is processed on a scheduled basis rather than in real time (Dean & Ghemawat, 2004).

Here, the data to be processed is collected in advance and processed after completion (White, 2012). It is suitable for analyzing large data sets, but is inadequate in situations requiring low latency (Marz & Warren, 2015). In most cases, the time for processing data is not urgent. Therefore, it is suitable for applications that are tolerant to latency (Stonebraker, Çetintemel, & Zdonik, 2005). It is used in areas such as accounting reports, analysis of daily system logs, and big data mining (Babcock, Babu, Datar, Motwani, & Widom, 2002).

Apart from these, all types of data are converted into numerical values by sampling all their unique values at specific frequencies. Because the digital world offers advantages that allow for easy and effective analysis of data, different types of coding and representation have been created for many different purposes (Bemer, 1972).

2.11. File Formats

A file is a unit in a computer environment where data, information, or instructions are stored in a logically integrated manner. Files are stored in permanent memory for later access by users or operating systems (Silberschatz, Galvin, & Gagne, 2018). A file can contain different types of data, such as text, numbers, sound, images, video, or program code. One of the fundamental characteristics of files is that they are identified by a file name and extension (Stallings, 2018). The file extension consists of an abbreviation indicating the type of data (text, code, sound, etc.) the file contains.

The resulting data is combined and stored in the computer in specific formats. Data from the same process, combined and meaningful together, form digital data sets called files. In other words, a file format determines how the data is stored for a specific application (Tanenbaum & Bos, 2015). Not all applications can use formats other than the specific file formats they support. While some files can be read by some applications, others may not be able to edit them.

File formats are developed with the ability to transform raw data into action in mind. File formats act as bridges connecting raw data to information, determining how effectively data can be processed, stored, and analyzed. File formats define the rules for organizing data within a file according to specific standards and formats that are free from arbitrariness. This feature brings advantages such as the ability to share, reproduce, store, and use data globally.

Some file formats may not be supported by all software applications or devices. In this case, opening or working with these files may be impossible, or the ability to import certain data into a program may be restricted. When saving files, they should be saved in common and commonly used formats. Otherwise, differences in program versions can create disadvantages when using the file.

2.11.1. Text File Formats:

1) Text-Only Files

Data in character-only formats consists of only readable characters. These file formats include .TXT, .LOG, .INF, and CSV (White, 2012).

2) Rich Text Format Files

Rich text formats are created with non-textual additions such as formatting, graphics, tables, and images, along with text. The goal is to in-

crease the readability of pure text characters and to support their visualization and highlighting. These are used for many purposes today. Thus, new text formats have replaced pure text files, including .RTF, .DOC, .DOCX, .PDF, .WPD, .HTML, .ASC, .MSG, .LOG, .EML, .PAGES, .LTX, .PRT, and more.

2.11.2. Audio File Formats:

Audio file formats can include compressed and uncompressed audio formats. Common audio file extensions include .WAV, .AIF, .MP3, and .MID.

2.11.3. Image File Formats:

1) Raster Image Files

Raster graphics are the most common type of image file. They consist of a grid of pixels, with each pixel representing a distinct color in the image. Both web graphics and digital photographs are stored as raster graphics. While some raster image formats are uncompressed, most use image compression. Common raster image file extensions include .BMP, .TIF, .JPG, .GIF, .PNG, .PSD, .TGA, .RTL, and .QIF (Gonzalez & Woods, 2018).

2) Camera Raw Files

These are image files created by digital cameras. They consist of uncompressed and unprocessed data that stores the raw data captured by the camera's sensor. The RAW format varies depending on the camera type and manufacturer. Therefore, to open a camera raw file, the program must support both the file type and the specific camera model that captured the image. Common camera raw file extensions include .BAY, .RW2, .DNG, .CR2, .NEF, and .ARW.

3) Vector Graphics Files

Vector graphics consist of paths rather than individual pixels. These paths can be used to represent lines and shapes within an image. Because vector graphics store image data as paths, they can be enlarged without loss of quality, making them a good choice for logos and other types of artwork. Common vector image file extensions include .PS, .EPS, .AI, .CDR, .DRW, .WMF, and .SVG.

2.11.4. Video File Formats:

These files contain both moving images and audio. Video file formats store data using container formats and codecs. The container combines

audio and video into a single file, while the codec performs the compression and decompression of the data (Richardson, 2010). Common video file extensions include AVI, MP4, MKV, MOV, WMV, and FLV (Soares & Rodrigues, 2019; Vasudev, 2014).

2.11.5. Data Files:

Data files are organized data for specific purposes. Some are organized for computational purposes, some for presentation purposes, and some for easy access. From these files .DAT, .XLS, .XLSX, .PPT, .PPS, .PPTX,

3. ADC (Analog to Digital Converter)

An ADC is an electronic circuit that converts continuous signals into discrete digital values. It converts a continuous analog signal, in terms of both amplitude and time, into a discrete form, both in terms of time and amplitude. Because analog signals are continuous, they are defined at every instant of time. Therefore, the smallest analog signal segment contains an infinite number of discrete values. Since capturing, storing, and analyzing this infinite data is impossible in digital systems, this data is reduced in size. Analog signals are converted to digital signals by taking a certain number of instantaneous samples per unit of time and converting them to the nearest integer. The size of the reduced size varies depending on the type of data, but cannot be less than the frequency of the analog data. The ADC converts analog voltage inputs applied to the input to the corresponding integer values. When using an ADC, it is necessary to determine the analog signal limits applied to the input. These limits are VREF (+) for the peak value and VREF (-) for the minimum value.

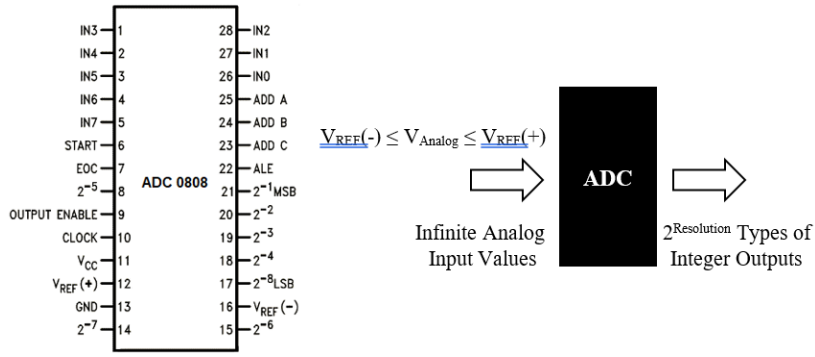

Figure 5. On the left, the pin functions of an old and functional 8-bit resolution 8-channel ADC (ADC 0808) are shown, and on the right, the block diagram showing the ADC operating logic.

For example, an ADC with 8-bit resolution will output 28-1=255 if the analog value applied to its input has a VREF(+) value. If it has a VREF(-) value, it will output 0. Therefore, an 8-bit ADC reduces the infinite analog value to 256 different values between 0 and 255. In other words, it separates the infinite input value into 256 different classes. The ADC assigns the value 0 to values starting from zero up to a certain threshold level. When the threshold level is reached, the value 1 is sent to the output. The output is incremented by 1 for each threshold level. The minimum change (A) at the input that will change the ADC output is found with the equation below.

$$A = \frac{\sum V_{REF}}{2^{Resolution}} \quad \text{(I)}$$

$$Output = \frac{(2^{Resolution}).V_{Analog}}{\sum V_{REF}} \quad \text{(II)}$$

In the first equation above, A represents the smallest analog voltage that changes the output. It is calculated as $\Sigma V_{REF} = V_{REF(+)} - V_{REF(-)}$. The VAnalog value represents the analog input value applied to the ADC input. The second equation above calculates the ADC output at any analog input. Below is a table showing some possible ADC outputs for an 8-bit ADC.

$V_{REF}(+) = 5V$
$V_{REF}(-) = 0V$
Resolution = 8 bit

Analog Input(V_{Analog})	**ADC Output (MSB … LSB)**
0 V	0000 0000 = (0)
2 V	0110 0110 = (102)
3.5 V	1011 0011 = (179)
5 V	1111 1111 = (255)

In the example above, we can use Equation 1 to find the value at which the ADC output will change by one for each voltage change at the input. This value is 5/255 = 0.0196 V. When the ADC input changes by at least this value, the output will change by 1. If the ADC resolution is 12 bits, this amount will be 0.00122 V. As can be seen, as resolution increases, the ADC's sensitivity also increases.

ADC outputs are integers. Therefore, the data obtained does not have the same precision as the decimal point. The difference between the closest values is 1. It can be seen that the digitizing process causes some loss

of information due to the quantization of the analog signal, and the amplitude of the signal is represented by the nearest series of fixed levels. A continuous signal is also quantized in time, and information is available only at the fixed times at which samples are acquired. An analog-to-digital converter performs two main steps on an analog signal:

- Sampling, or discretization of time
- Quantization, or discretization of amplitude

Time discretization means that the ADC measures the amplitude of the analog signal in fixed time steps. Quantization arises from the fact that digital numbers are represented by bits. A digital number can only take a finite number of values, defined by the number of bits. For example, an 8-bit ADC can only output 28 = 256 different values. Quantization can be viewed as the process of "rounding" the analog amplitude to obtain a digital value. This "rounding" usually introduces some quantization error in the amplitude. Quantization errors lead to an increase in the noise floor on the digital side. In general, the more bits an ADC converter has, the less quantization noise the ADC produces.

The quality of a digital signal depends on the number of samples per unit of time and the sampling depth (resolution). To reduce quantization errors, it is important to ensure that a sufficient number of digitizing levels are available to represent the signal amplitude at an acceptable level and that enough samples are taken to represent the time course. The rate at which samples should be taken depends on how rapidly the analog signal is changing. According to the Nyquist theorem, the sampling rate should be at least twice the signal frequency. Otherwise, a sample rate that is too low will not accurately represent the original signal; it will be distorted or aliased when reproduced.

When an analog signal is sampled (converted to digital), the original signal is attempted to be recovered from the resulting signal. If the sampling rate is lower than the frequency of the analog signal, the analog signal cannot be accurately sampled to its true value. Aliasing refers to the phenomenon where a signal reconstructed from samples of the original signal contains low-frequency components not present in the original. To avoid this, the sampling frequency should be at least doubled.

3.1. Sampling Rate

Sampling rate is defined as the number of samples taken from the analog signal per unit time (at a specific frequency). Its unit is bps (bits per second) or sps (samples per second). The more samples taken from a sig-

nal per unit of time, the more similar the digital signal becomes to an analog signal. It's also important to remember that each sample taken will occupy memory space. Each sample taken is converted into an integer equal to the resolution of the ADC. The width of this integer in bits is a measure of the ADC's resolution. As the ADC's resolution increases, it separates the infinite values applied to the ADC input into classes equal to two resolutions. Quantization errors decrease as resolution increases. In the figure below, the initial sampling is done six times, producing a total data size of 6 x 8 = 48 bits for an ADC with 8-bit resolution.

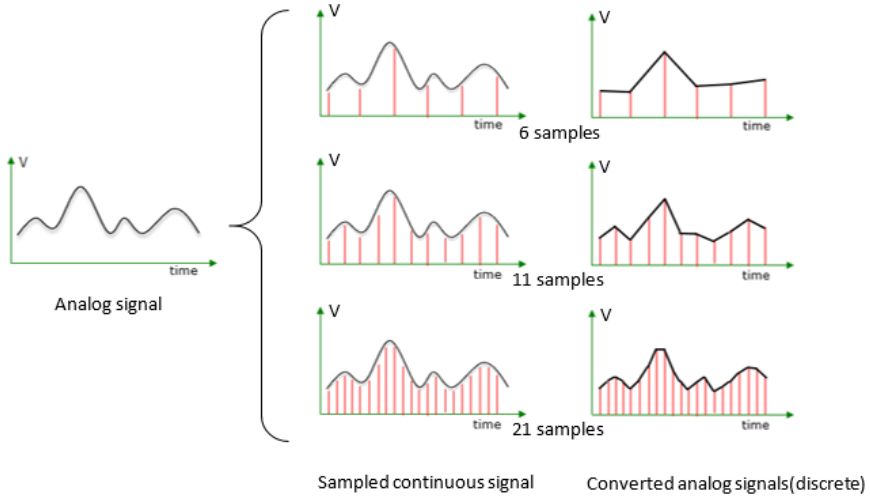

Figure 6. Sampling rate effect on the conversation

It can be seen from the figure that as the sampling rate increases, the resulting signal becomes more similar to the original signal. For example, taking six samples per unit time from an analog signal means reducing the infinite analog values in that range to six. Data loss is an accepted condition. Otherwise, we will certainly lose out on the advantages of the digital world. When using an ADC, an appropriate sampling rate should be selected based on the application. As mentioned under "Aliasing," a sampling rate at frequencies lower than the frequency of the analog signal will result in incorrect sampling of the actual signal.

3.2. Resolution

Resolution refers to the smallest change in the analog input signal that can be detected by the ADC. In other words, the resolution of an ADC is the number of bits it uses to digitize the input samples. Its unit is the bit. It determines how many different classes the infinite analog data applied

to the input can be divided into. The number of discrete digital levels that can be generated for an n-bit ADC is 2n. Therefore, a 10-bit ADC has 210 = 1024 levels. As the number of classifications increases, i.e., the resolution increases, the conversion process will achieve a more accurate translation. In other words, resolution determines the minimum change in the analog input voltage that causes the output to change by one. Resolution is crucial for applications such as audio, medical imaging, and scientific instrumentation. Typically, ADCs have resolutions of 7, 8, 10, 12, 16, and 24 bits. For a fabricated ADC, the resolution parameter is fixed and cannot be changed.

Table 3: Resolution effect on conversation

Resolution versus step size for ADC ($\sum V_{REF}$ = 5V)		
n-bit	Number of steps (2^n)	Step size
8	256	5V/256 = 19,53 mV
10	1024	5V/1024 = 4,88 mV
12	4096	5V/4096 = 1,2 mV
16	65.536	5V/65.536 = 0,076 mV

The table shows the smallest analog input voltage values that will cause output changes due to different resolution values for an ADC with a reference voltage range of 5V. As resolution increases, the ADC will produce a separate output for smaller analog voltage changes at its input, increasing the number of output types.

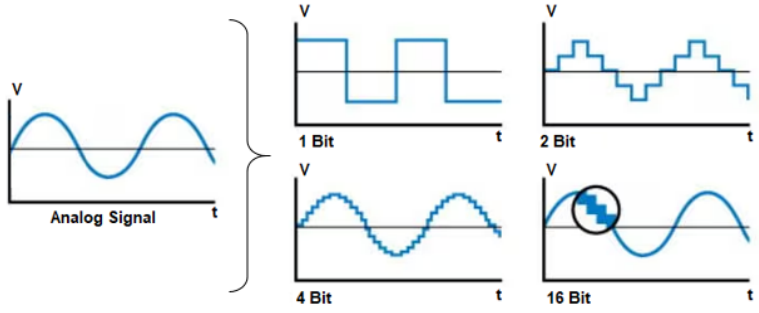

Figure 7. Representation of analog signal at different resolutions

For an ADC, resolution is a key parameter for approximating the true analog value. For example, in the figure above, for an ADC with a 1-bit resolution, the ADC only produces 2^1=2 different values for an infinite analog value applied to the ADC input. When the resolution increases by one bit, to 2 bits, the ADC produces 4 different values. Representing

infinite values in two ranges with more bits, that is, with a wider variety of numbers, results in a more realistic data conversion. For an ADC, resolution and sampling rate together determine the amount of data produced by the ADC.

Example:

How much data can a 12-bit ADC with a 1Ksps sampling rate produce in 3 minutes? 1 Ksps = 1000 sps

1000 sps = 1000 x 12 (= 12,000) bps

1 min = 60 sec

Data generated in 1 minute = 12,000 x 60 = 720,000 bits

Total data generated in 3 minutes = 720,000 x 3 = 2,160,000 bits

2,160,000 bits = 270,000 Bytes

3.3. Quantization

The infinite variety of analog values applied to the ADC input are clustered into the closest possible value ranges, resulting in similar values. This creates a difference between the actual value and the new value. Thus, when a continuous analog signal is approximated with discrete digital values, quantization errors occur during analog-to-digital conversion. In an ADC converter, each voltage sample is rounded (quantized) to the nearest usable value and then converted to its corresponding binary code. When the digital code is converted back to analog via the DAC, any rounding errors are reproduced. In practice and theory, this conversion, from analog to digital, will never be 100% accurate; that is, a limited amount of information will be lost forever during the conversion process. This means that when the digital representation is converted back to analog, the result will not be the same as the original waveform (Jalilinia, 2025).

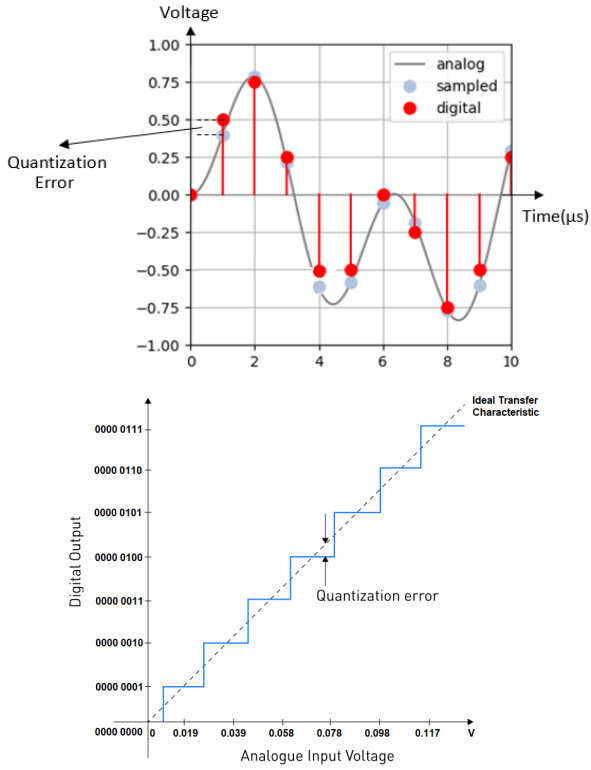

Figure 8. A section of the characteristic diagram of an 8-bit ADC with Time and Amplitude Discretization on the left and 0-5 volt reference values on the right.

This resulting error is a sawtooth pattern error voltage that manifests as white noise added to the analog input signal. This error is also called quantization noise (Qn). When the number of bits (n) used for the conversion is small, the quantization error is generally larger because fewer quantization levels are required to accurately represent the continuous signal. As the number of bits increases, the quantization error becomes smaller, resulting in a more accurate representation of the original analog signal. Practically, it is possible to reduce the error to values small enough to be negligible in many applications.

3.4. Accuracy

Accuracy refers to how close the ADC output is to the true value of the input signal. Linearity encompasses several factors, including offset error, gain error, and noise.

- *Offset Error:* This refers to the difference between the actual input

signal and the ADC output when the input is zero.

- *Gain Error:* The deviation from the expected output scale.
- *Non-Linearity:* How well the ADC output follows the expected linear relationship with the input.

3.5. Conversion Time

Conversion time is the time it takes for the ADC to convert the captured analog input into a digital number. This parameter is related to the sampling rate. This means that as the sampling rate increases, the conversion time decreases. There is an inverse relationship between these two parameters.

3.6. Aliasing Error

When sampling high-frequency signals, a phenomenon called aliasing occurs. This is when a new waveform with a lower frequency, not present in the input (original) signal, is generated at the ADC output. This is because as the input signal frequency approaches a sampling frequency, fewer samples can be taken to faithfully represent the input signal. According to the Nyquist sampling theorem, in an ideal sampled data system, at least two data bandwidth samples per cycle are required to reproduce the sampled data without losing information. Therefore, the first consideration when determining the system sampling rate is aliasing error, that is, errors resulting from information loss due to insufficient samples per signal frequency cycle. The figure below illustrates aliasing error resulting from an insufficient number of samples per data bandwidth cycle.

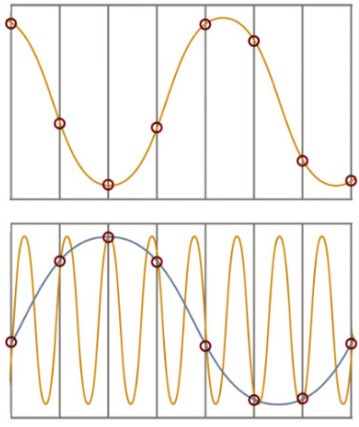

Figure 9. Aliasing occurs as a result of a much lower sampling frequency

3.7. Analog Input Channels

Many data acquisition applications require multiple analog inputs for an ADC. This allows multiple analog inputs to be converted to digital in any desired order via a single converter. Therefore, a single ADC chip can have 2, 4, 8, or 16 channels. Multi-channel ADCs can convert only one channel to digital at a time.

4. DAQ Card Data Transfer

Data converted to digital by the ADC requires a suitable data bus to be transferred to memory. To avoid bottlenecks, the data transfer rate must be equal to or greater than the sampling rate. Data transfer rate is the number of bits or bytes per second as data travels between two points. You can think of it as similar to the flow rate used in water flow. The abbreviations mbps (Mega bit per second) or mBps (Mega Byte per second) are used to express the data transferred per second.

Data traffic, on the other hand, is the volume of data flowing over the bandwidth. It is used to describe the current data flow.

4.1. Bandwidth

The term bandwidth is used to describe the capacity of a data communication medium. As bandwidth increases, data transfer speed also increases.

4.2. Bus

The buses used in DAQ (Data Acquisition) cards determine how the card connects to a computer or embedded system. These buses can vary depending on speed, bandwidth, compatibility, and usage.

4.3. Buses Used in DAQ Cards

1. PCI (Peripheral Component Interconnect)

This is an older-generation internal computer bus that transfers parallel data. Although it offers higher speeds, it has now been superseded by PCIe (Horowitz & Hill, 2015; National Instruments, 2019).

2. PCI Express (PCIe)

This is the serial and faster version of PCI. It is the most widely used standard in desktop DAQ cards today. Bandwidth varies depending on the channel multiplier (Brooks, 2003; National Instruments, n.d.-b).

3. USB (Universal Serial Bus)

This is the most commonly used connection in external and portable DAQ devices. It offers plug-and-play functionality and various speed standards (USB 2.0, 3.0, 3.1+). It can also meet the need for external power for connected devices (Axelson, 2015; National Instruments, n.d.).

4. PXI / PXIe (PCI eXtensions for Instrumentation)

This modular standard is designed for test and measurement systems. Based on PCI/PCIe, it provides high speed and synchronization. Designed for DAQ systems, it is designed for professional use (Choi, 2014; National Instruments, 2019). PXI enclosures are available for PXI cards. They have their own dedicated connection sockets.

5. Ethernet (LAN)

Used in industrial applications and remote measurements. It provides high bandwidth with Gigabit and 10G Ethernet speeds (Siemens AG, 2018; Beckhoff Automation, n.d.).

6. CompactDAQ (cDAQ) / CompactRIO

NI's USB or Ethernet-based modular DAQ solutions. It is preferred in embedded systems and flexible measurement applications (National Instruments, n.d.-a).

Table 4. DAQ Card Buses Comparison Table

Data Buses	**Speed / Bandwidth**
PCI	133 MB/s
PCI Express (PCIe)	x1: 250 MB/s, x16: 4 GB/s
USB	USB 2.0: 60 MB/s; USB 3.0+: 625 MB/s
PXI / PXIe	12/24 GB/s
Ethernet (LAN)	10/100/1000 Mbps, 10 Gbps+
CompactDAQ / cRIO	USB veya Ethernet based, modular
FireWire (IEEE 1394)	400–800 Mb/s(old)

7. FireWire (IEEE 1394)

Historically used for high-speed data transfer, it has been largely superseded today by USB 3.0 and Ethernet technologies (IEEE 1394 Trade Association, 2002).

Figure 10. DAQ card types.

5. Signal Enhancement in Data Acquisition

Most sensors used in data acquisition (DAQ) cannot directly produce signals suitable for the measurement system. Signal enhancement is critical for making the raw signals received from sensors stronger, cleaner, more reliable, and compatible with the measurement system (Bilgin & Nishimura, 2003). This allows the DAQ card and computer to reliably process the actual physical data.

Signal enhancement in data acquisition is necessary for the following reasons. Weak signal levels are often encountered in measurement systems, as some sensor outputs such as thermocouples produce signals in the millivolt range and therefore require amplification to reach measurable levels suitable for analog-to-digital conversion; the ADC must be properly adapted to the operating levels it requires, while high voltage applications demand adequate noise immunity for stable operation (Horowitz & Hill, 2015). In addition, industrial environments commonly expose measurement systems to electromagnetic interference (EMI, RFI), which can distort the acquired signal, so filter circuits are generally implemented to remove such unwanted noise and ensure signal integrity (Kester, 2005). Another important issue is the mismatch between the measurement range of the DAQ card and the sensor output, which may lead to inaccurate or clipped readings if not properly scaled or conditioned (National Instruments, 2019). Finally, electrical isolation and protection are vital because sudden high-voltage pulses or transients can damage sensitive DAQ circuitry, making isolation components an essential safeguard in data acquisition system design (Bentley, 2005).

What is done?

Filtering: Low-pass, high-pass, or band-pass filters are used to reduce noise (Kester, 2005).

Amplification: This amplifies weak sensor outputs to a measurable level, typically using instrumentation amplifiers (Horowitz & Hill, 2015).

Isolation: Galvanic isolation is applied to protect against high voltages and ground faults (Bentley, 2005).

Linearization: The outputs of nonlinear sensors (e.g., thermistors) are corrected with appropriate mathematical models (National Instruments, 2019).

Offset Adjustment: Zero-point drifts are eliminated before measurement.

Digital Processing: Digital filters (FIR, IIR), moving averages, and FFT-based analysis are used to reduce noise (Smith, 1997).

5.1. Filters

A filter is a circuit that can pass (or amplify) certain frequencies and attenuate others. Thus, the filter suppresses unwanted signals by considering the frequency difference. In other words, signal filters are basic circuit elements that improve signal quality by suppressing unwanted frequency components or passing specific frequency ranges. These filters, divided into two main classes: analog and digital, are widely used in data acquisition, communication, audio processing, and control systems.

Low-pass filters pass low-frequency components while suppressing high-frequency noise; high-pass filters do the opposite. Band-pass and band-stop filters, on the other hand, selectively pass or block specific frequency ranges. Digital filters, implemented with digital signal processing (DSP) algorithms, offer more flexible design possibilities and achieve high accuracy in tasks such as noise reduction and signal separation (Smith, 2003; Oppenheim & Schafer, 2010). In modern applications, fast Fourier transform (FFT) and adaptive algorithms are also effectively used in filter design (Proakis & Manolakis, 2007).

Figure 11. Effect of filter on noisy signal

5.2. Signal Amplification

Signal amplification is the process of increasing the amplitude of a weak electrical signal, making it more usable in measurement, transmission, or processing systems (Bilgin, 2023). This process is critical for increasing the signal's immunity to noise and improving data accuracy, especially when sensor outputs are low (Horowitz & Hill, 2015). Amplification is typically achieved through transistors or operational amplifiers (op-amps). These circuit elements merely increase the amplitude of the input signal while preserving its shape. Furthermore, amplifiers are categorized according to the frequency characteristics of the signal—for example, audio, radio frequency, or power amplifiers—and are optimized for specific applications (Sedra & Smith, 2020). In modern systems, signal amplification is also integrated with methods such as digital preprocessing and adaptive filtering, enabling higher sensitivity and accuracy (Franco, 2014).

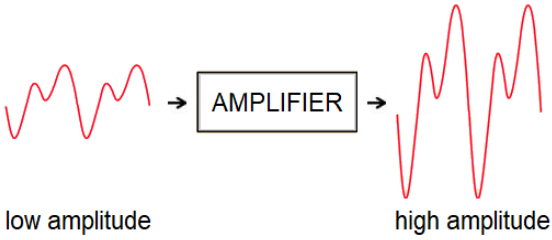

Figure 12. Amplifier effect on low signal

5.3. Signal Linearization

Signal linearization is the process of converting nonlinear responses occurring in measurement systems or sensor outputs into a linear relationship using a specific mathematical model or electronic circuit. This method is used to increase measurement accuracy and system stability, particularly in situations where sensor output characteristics are not proportional to the input variable (Kester, 2009). Linearization can be achieved through hardware (analog circuits, diode compensation) or software (polynomial, piecewise linear, artificial neural network-based) methods (Fraden, 2016). Currently, software linearization methods are widely preferred in microcontroller-based systems due to their low cost and high flexibility. Furthermore, the easier processing of linearized signals significantly improves system performance during filtering and calibration processes (Rangan, Sarma, & Mani, 2015).

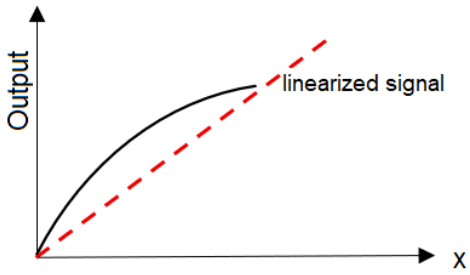

Figure 13. The effect of signal linearization on a nonlinear signal

6. Conclusions and Recommendations

Data acquisition systems are one of the most critical components underlying modern engineering applications. By converting physical quantities obtained from sensors into digital form, engineers can more accurately analyze system behavior and manage optimization processes more effectively. The advanced data acquisition cards used today, with their high sampling rates, wide resolution ranges, multi-channel architectures, and real-time data processing capabilities, have become indispensable in both research and industrial engineering applications. The study clearly demonstrates the impact of resolution and sampling rates on conversion quality.

Different bus architectures such as USB, PXI, and PCIe offer significant advantages in terms of flexibility and performance, depending on system requirements. Furthermore, the proper application of signal conditioning, noise reduction, and synchronization techniques is critical for measurement accuracy and system reliability.

In the future, data acquisition systems are expected to become more integrated with AI-supported predictive analysis, IoT-based remote monitoring, and cloud-based data management. In this context, data acquisition in engineering will not only involve measurements; It will be one of the most important building blocks of decision-making processes, optimization and autonomous systems.

REFERENCES

Axelson, J. (2015). USB complete: The developer's guide (5th ed.). Lakeview Research.

Babcock, B., Babu, S., Datar, M., Motwani, R., & Widom, J. (2002). Models and issues in data stream systems. Proceedings of the 21st ACM SIGMOD-SIGACT-SIGART Symposium on Principles of Database Systems, 1–16. https://doi.org/10.1145/543613.543615

Beckhoff Automation. (n.d.). EtherCAT technology overview. Beckhoff Automation. Retrieved from https://www.beckhoff.com/

Bentley, J. P. (2005). Principles of measurement systems (4th ed.). Pearson Education.

Bemer, Robert William (1959), "A proposal for a generalized card code of 256 characters", Communications of the ACM, 2 (9): 19–23, doi:10.1145/368424.368435.

Bemer, R.W., (1960), "ESCape-A Proposal for Character Code Compatibility," Comm. ACM, Vol. 3, No. 2.

Bemer, R.W., (1961) "Survey of Modern Programming Techniques," The Computer Bulletin.

Bilgin, S. (2023) "The effect of using activated carbon obtained from sewage sludge as a fuel additive on engine performance and emissions", Thernal Science, 27 (4) pp. 3313-3322.

Bilgin, S., Nishimura, M. (2003) "Implementation of a WIP modeling system at LSI logic", 2003 IEEE International Symposium on Semiconductor Manufacturing Conference Proceedings. pp. 293-296.

Bilgin, S. (2025, February). Strategic directions for Turkey according to the Global Energy Outlook 2024 report. In Proceedings of the 4th International Palestra Scientific Research Congress (pp. 177–178). Azerbaijan.

Brooks, D. (2003). Signal integrity issues and printed circuit board design. Prentice Hall.

Buchholz W.(1962), Planning a Computer System Project Stretch, McGraw-Hill Book Company Inc.

Chitode, J.S., (2020) Communication Systems I, Technical Publication. ISBN 9789333223997.

Choi, J. (2014). PXI-based modular instruments for measurement and automation. International Journal of Instrumentation Science, 3(2), 25–31.

Daş, M., Pektezel, O., Şimşek, M., Akpınar, E. (2025) "Thermodynamic and artificial intelligence-based performance analysis of parabolic vacuum tube solar collector assisted greenhouse drying system", Case Studies in Thermal Engineering, 75 (0).

Daş, M., Pektezel, O., Şimşek, M. (2025) "Solar energy for greenhouse drying: Performance evaluation of parabolic trough solar collector with two-axis tracking system", Solar Energy, 299 (1).

Dean, J., & Ghemawat, S. (2004). MapReduce: Simplified data processing on

large clusters. Proceedings of the 6th Symposium on Operating System Design and Implementation (OSDI), 137–150.

Di Paolo Emilio, M. (2015). Data Acquisition Systems: From Fundamentals to Applied Design. Germany: Springer New York.

Doebelin, E. O., & Manik, D. N. (2017). Measurement systems: Application and design (6th ed.). McGraw-Hill Education.

Robert K. Dueck. (2005). Digital Design with CPLD Applications and VHDL. Thomson/Delmar Learning. ISBN 1401840302.

Dijital ve Analog Sistem Arasındaki Fark https://www.geeksforgeeks.org/difference-between-digital-and-analog-system/

Franco, S. (2014). Design with operational amplifiers and analog integrated circuits (4th ed.). McGraw-Hill Education.

Fraden, J. (2016). Handbook of modern sensors: Physics, designs, and applications (5th ed.). Springer.

Vijay K. Garg, Yih-Chen Wang. (2005). Introduction To Digital Communication And Communication Networks, The Electrical Engineering Handbook, Academic Press, Pages 949-950, ISBN 9780121709600.

Gonzalez, R. C., & Woods, R. E. (2018). Digital image processing (4th ed.). Pearson.

Golab, L., & Özsu, M. T. (2003). Issues in data stream management. ACM SIGMOD Record, 32(2), 5–14. https://doi.org/10.1145/776985.776986.

Gültekin, N. (2024) "Experimental study of the effects of diesel, bioethanol, and hydrogen on combustion, emissions, mechanical vibration, and noise in a CI engine with different valve lift", International Journal of Hydrogen Energy, 93 (1) pp. 1011-1021.

Gültekin, N., Ciniviz, M. (2024) "Experimental investigation of the effects of energy ratio and combustion chamber design on engine performance and emissions in a hydrogen-diesel dual-fuel CRDI engine", Atmospheric Pollution Research, 15 (9) pp. 1-12.

Gültekin, N., Gülcan, H.E., Ciniviz, M. (2024) "The impact of hydrogen injection pressure and timing on exhaust, mechanical vibration, and noise emissions in a CI engine fueled with hydrogen-diesel", International Journal of Hydrogen Energy, 78 (1) pp. 871-878.

Horowitz, P., & Hill, W. (2015). The art of electronics (3rd ed.). Cambridge University Press.

https://home.unicode.org/

https://www.inf.ed.ac.uk/teaching/courses/inf2c/lectures/CS02_notes.pdf

IEEE 1394 Trade Association. (2002). IEEE 1394: High performance serial bus standard. IEEE Standards Association.

Jalilinia K, (2025) Analog To Digital Conversion – Performance Criteria, https://www.electronics-lab.com/article/analog-to-digital-conversion-performance-criteria/

Kester, W. (2005). Practical design techniques for sensor signal conditioning.

Analog Devices, Inc.

Kester, W. (2009). Practical design techniques for sensor signal conditioning. Analog Devices.

Vinod Kumar Khanna (2009). Digital Signal Processing. S. Chand. p. 3. ISBN 9788121930956.

Charles E. Mackenzie, (1980), Coded Character Sets, History and Development, Addison-Wesley.

Marz, N., & Warren, J. (2015). Big data: Principles and best practices of scalable real-time data systems. Manning Publications.

National Instruments. (2019). Fundamentals of data acquisition. National Instruments. Retrieved from https://www.ni.com/

National Instruments. (2019). Comparing DAQ bus technologies: PCI, PCIe, PXI, and PXIe. National Instruments. Retrieved from https://www.ni.com/

National Instruments. (n.d.). DAQ bus technologies overview. National Instruments. Retrieved from https://www.ni.com/

National Instruments. (n.d.). CompactDAQ and CompactRIO manuals. National Instruments. Retrieved from https://www.ni.com/

Oppenheim, A. V., & Schafer, R. W. (2010). Discrete-time signal processing (3rd ed.). Prentice Hall.

Proakis, John G.; Manolakis, Dimitris G. (2007). Digital Signal Processing. Pearson Prentice Hall. ISBN 9780131873742.

Rangan, C. S., Sarma, G. R., & Mani, V. S. (2015). Instrumentation devices and systems (2nd ed.). Tata McGraw-Hill Education.

Richardson, I. E. G. (2010). The H.264 advanced video compression standard (2nd ed.). Wiley.

Sedra, A. S., & Smith, K. C. (2020). Microelectronic circuits (8th ed.). Oxford University Press.

Siemens AG. (2018). Industrial Ethernet handbook. Siemens AG. Retrieved from https://new.siemens.com/

Silberschatz, A., Galvin, P. B., & Gagne, G. (2018). Operating system concepts (10th ed.). Wiley.

Smith, S. W. (1997). The scientist and engineer's guide to digital signal processing. California Technical Publishing.

Smith, S. W. (2003). The scientist and engineer's guide to digital signal processing. California Technical Publishing.

Soares, L. D., & Rodrigues, R. F. (2019). Multimedia file formats and standards: A survey. IEEE Multimedia, 26(1), 76–85. https://doi.org/10.1109/MMUL.2018.2873538

Stallings, W. (2018). Computer organization and architecture: Designing for performance (11th ed.). Pearson.

Stallings, W. (2018). Operating systems: Internals and design principles (9th ed.). Pearson.

Stonebraker, M., Çetintemel, U., & Zdonik, S. (2005). The 8 requirements of real-time stream processing. ACM SIGMOD Record, 34(4), 42–47. https://doi.org/10.1145/1107499.1107504.

Şimşek, M., Yusuf, B., Ertuğrul, D., Uğur, M. (2023) «The Study of the Friction Properties of AA6082 and AA7075 Material Journal Bearings Coated with Micro Arc Oxidation», Journal of Materials Engineering and Performance, 32 (5) pp. 2307-2318.

Tanenbaum, A. S., & Bos, H. (2015). Modern operating systems (4th ed.). Pearson.

Vasudev, B. (2014). Modern video compression: Understanding H.264 and H.265. Springer.

White, T. (2012). Hadoop: The definitive guide (3rd ed.). O'Reilly Media.